Andean retroarc-basin dune fields and Pampean Sand Sea (Argentina): Provenance and drainage changes driven by tectonics and climate

Eduardo Garzanti, Tomas Capaldi, Alfonsina Tripaldi, Marcelo Zárate, Mara Limonta, Giovanni Vezzoli

ABSTRACT. We here review in terms of tectono-magmatic setting and Quaternary landscape dynamics what is known about the provenance of Argentine dune fields and their fluvial feeder systems draining the Andean Cordillera. The detrital signatures of these eolian sediments were previously investigated based on either framework petrography and heavy minerals or detrital-zircon geochronology, and their peculiar volcaniclastic nature was long recognized. Compositional variability, however, was only broadly evaluated, and quantitative provenance analysis based on a systematic multimethod approach across the entire region was not carried out so far. For this reason, here we integrate original and previously obtained petrographic, heavy-mineral, and detrital-zircon geochronology data to present the first comprehensive provenance study of dune fields stretching for 1000 km across central Argentina from the Andean piedmont to the Atlantic Ocean.

In dune fields along the Andean retroarc basin, sediment composition defines a steady northward decrease in volcanic detritus. This reflects active magmatism in the Southern Volcanic Zone and Payenia province (38°-34°S), in contrast with the ~600-km-long Pliocene-Quaternary magmatic gap in the Pampean flat-slab segment (33°-27°S), where sediment is derived from deeper-seated tectono-stratigraphic levels of the continental arc and uplifted blocks of retroarc-basin basement. In distal Pampean lowlands extending across the bulge and backbulge depozones, instead, sand dunes display notably homogeneous compositional signatures, indicating that detritus was mostly generated north of 34°S and transported by a paleo-Desaguadero trunk river that formed during southward-progressing diachronous uplift of the Sierras Pampeanas since the late Miocene. In contrast with huge African and Arabian deserts that contain multiply recycled quartzose to pure quartzose sand, even very fragile volcanic clasts, plagioclase feldspar, and unstable ferromagnesian minerals are widespread, testifying to largely first-cycle volcanic provenance and only minor effects of mechanical breakdown and chemical weathering in the Pampean Sand Sea.

During the Late Pleistocene, after a first southward shift of the Desaguadero trunk river possibly induced by increased water and sediment discharge at the end of the penultimate glacial maximum, tectonic uplift eventually outpaced stream power during the last glacial period. Paleo-rivers were thus forced to shift farther southwards, leading to the formation of an integrated paleo-Desaguadero+Colorado drainage system. During the latest Pleistocene-early Holocene, such a large trunk river fostered the rapid progradation of a wide delta and littoral sand transport all along the shores of the Buenos Aires Province. Climate change and repeated waxing and waning of glaciers through the Quaternary have left a prominent mark on sediment distribution, dominated by fluvial processes during periods of high fluvial discharge but alternating with arid phases characterized by limited transport capacity and vegetation cover, extensive wind deflation of floodplains, and sand accumulation in the dune fields.

Figure 1 Click here to access/download;Figure;Figure 1 ArgenDunes.jpg

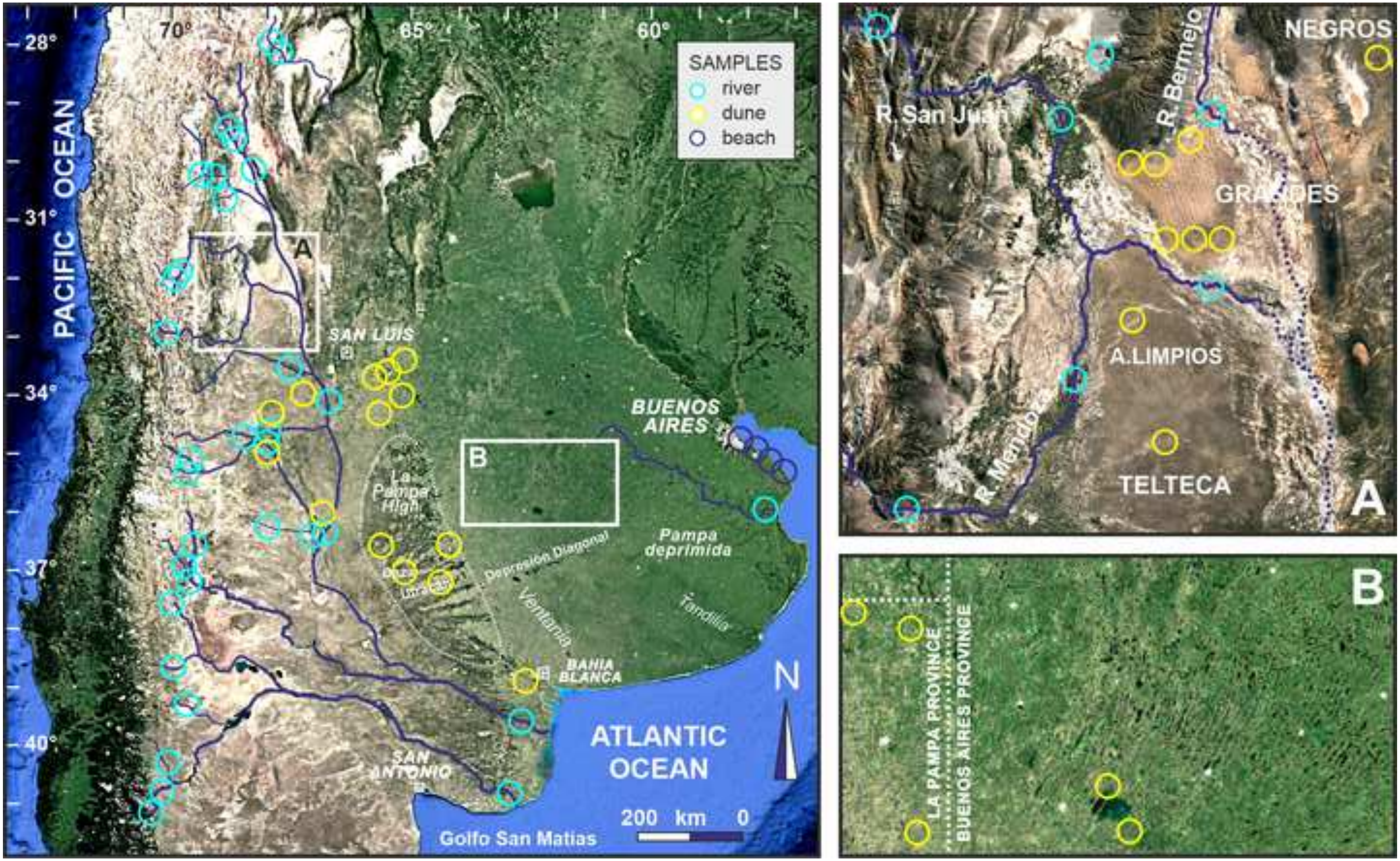

Figure 2 Click here to access/download;Figure;Figure 2 ArgenDunes Medanos.jpg

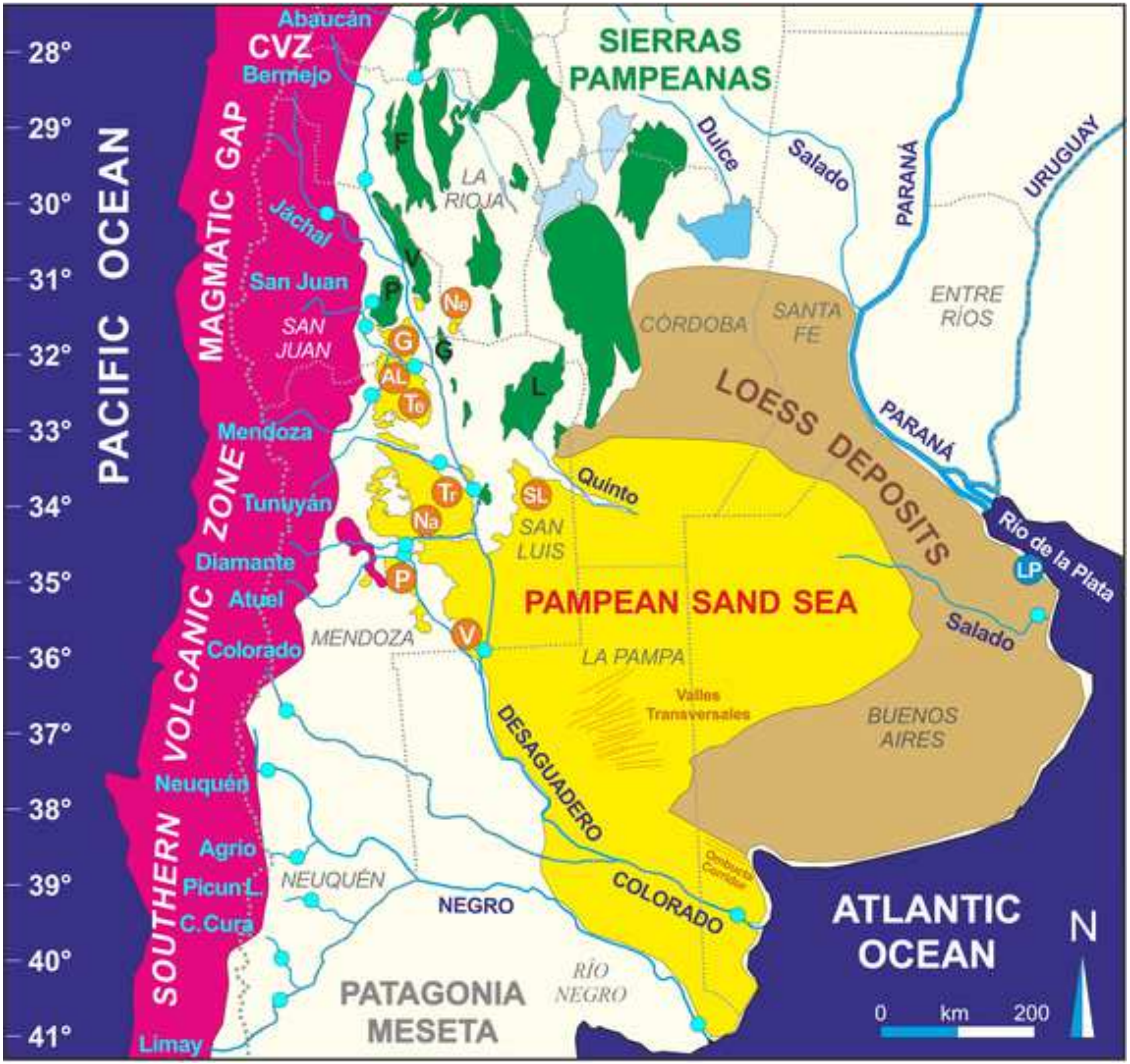

Figure 3

Click here to access/download;Figure;Figure 3 ArgenDunes Rain&Wind.jpg

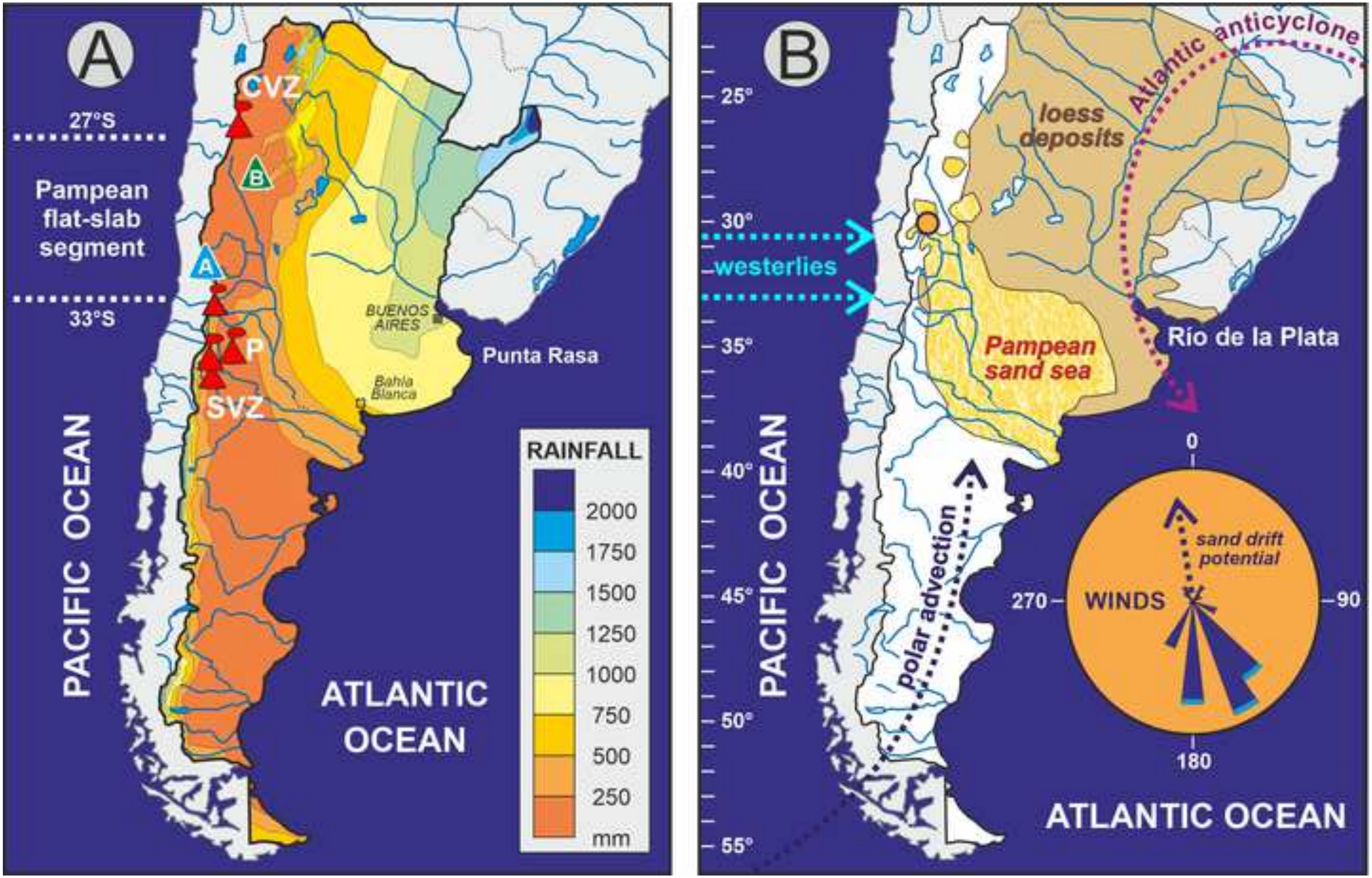

Figure 4

Click here to access/download;Figure;Figure 4 ArgenDunes Foto PT.jpg

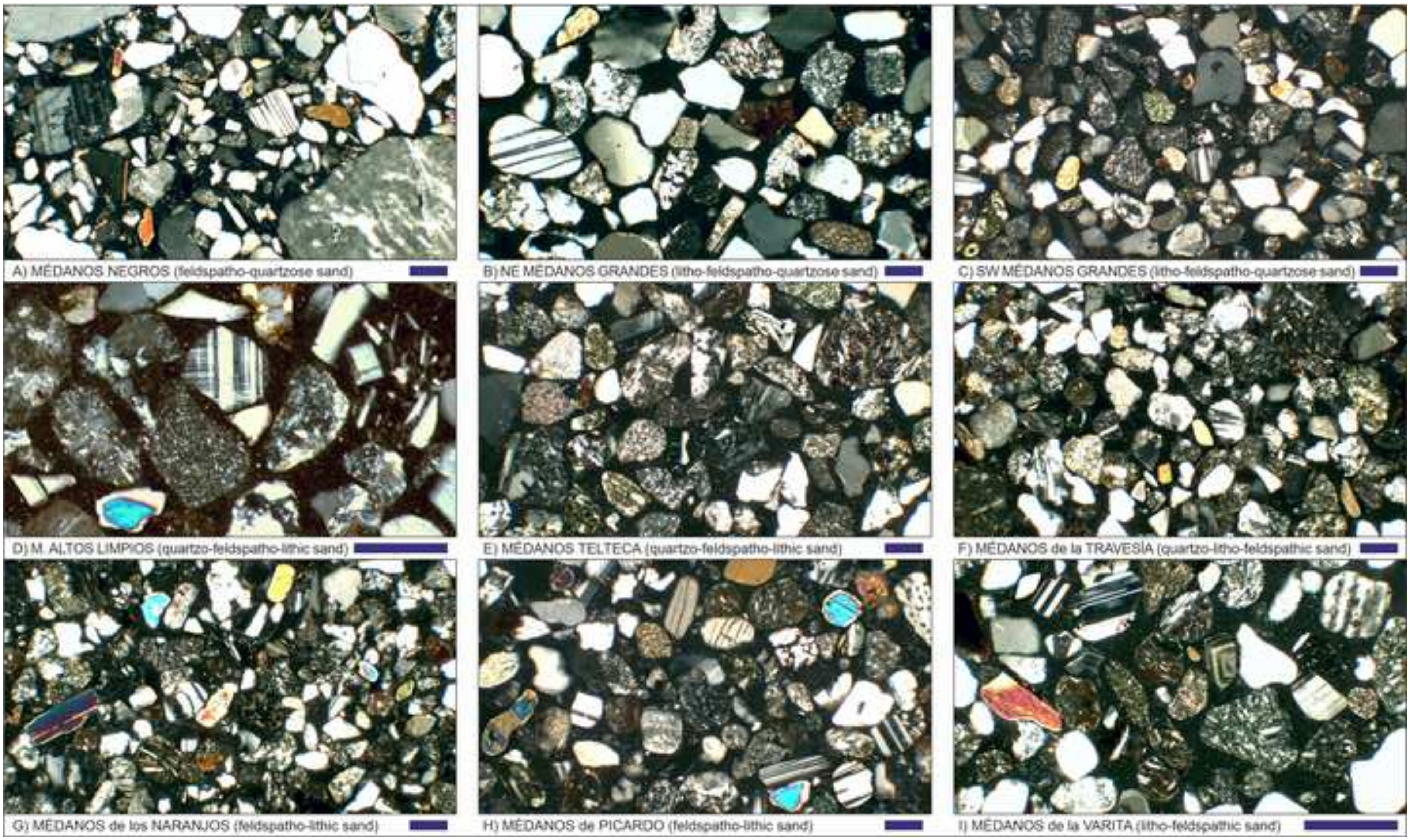

Figure 5

Click here to access/download;Figure;Figure 5 ArgenDunes Plots PTHM.jpg

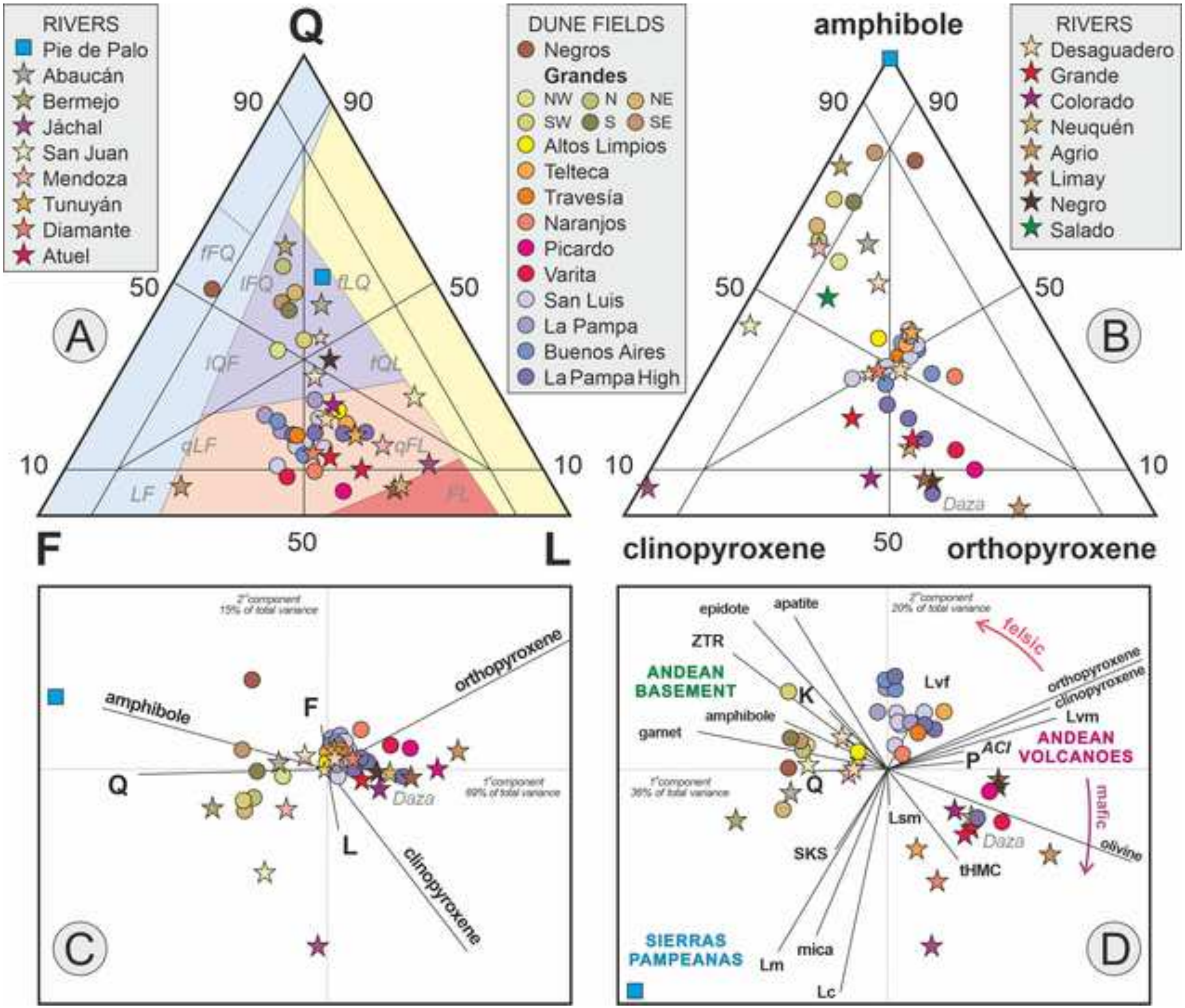

Figure 6

Click here to access/download;Figure;Figure 6 ArgenDunes Torte QFL & HM.jpg

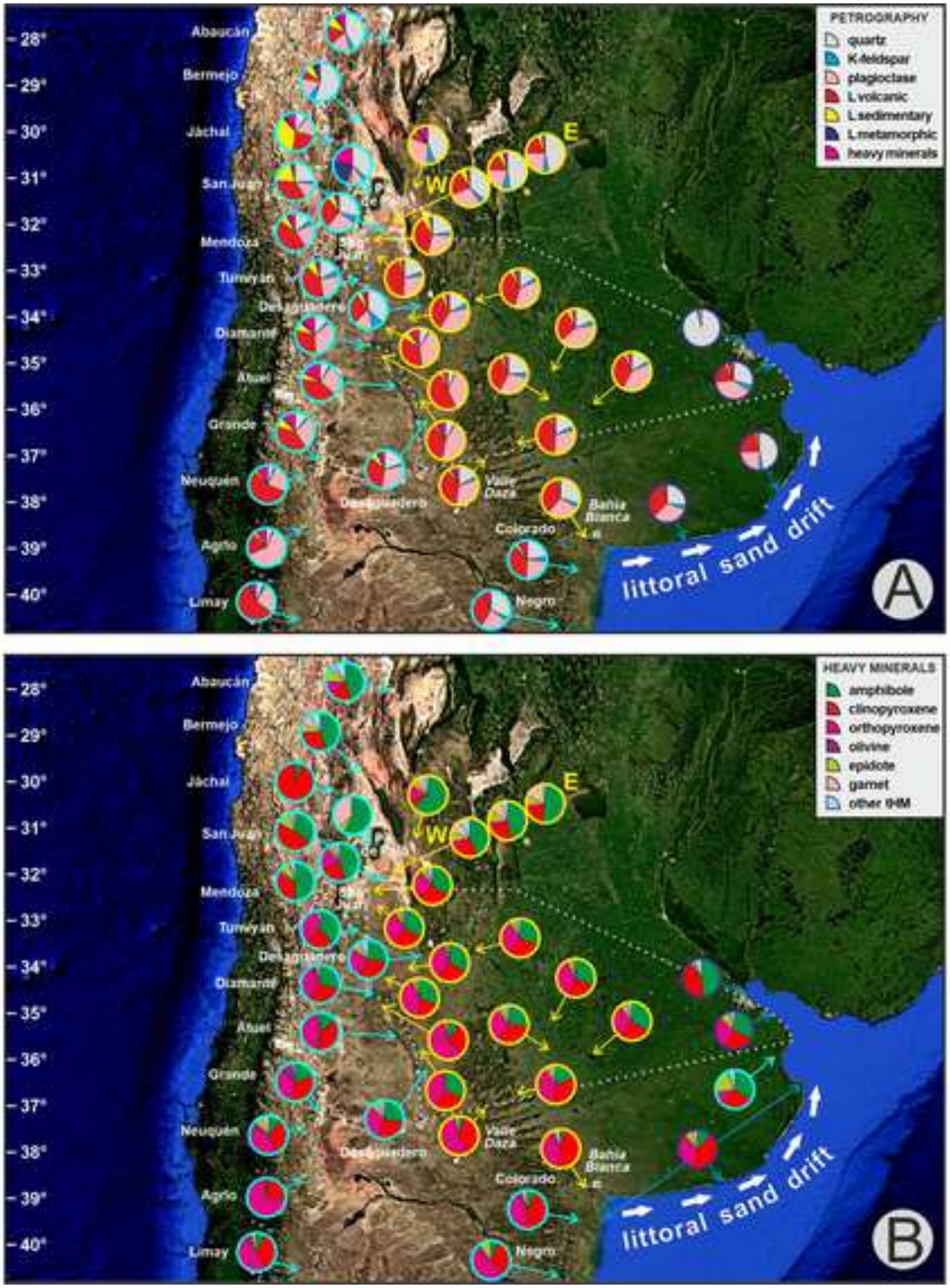

Figure 7

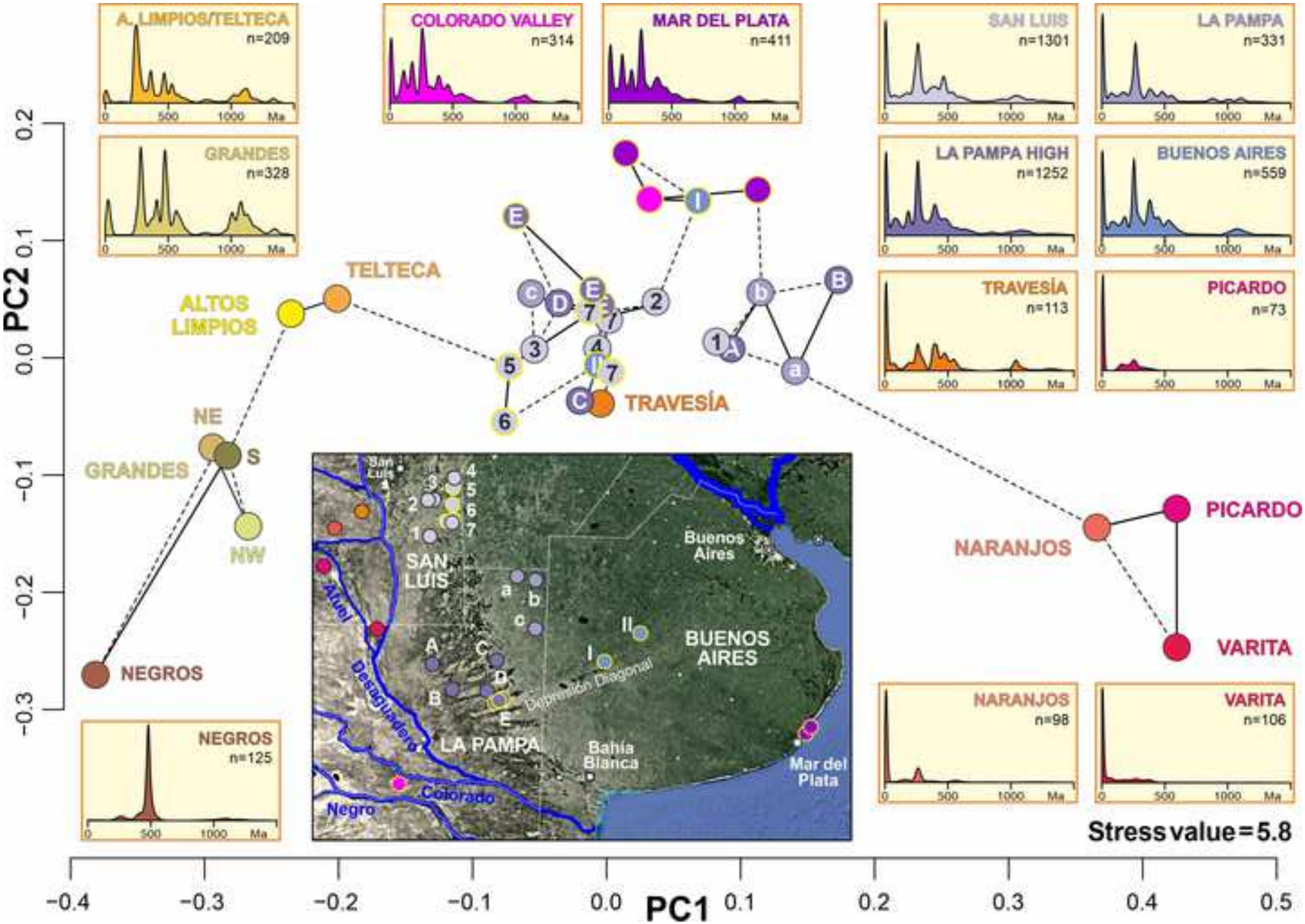

A. LIMPIOS/TELTECA
n=209
COLORADO VALLEY
n=314
MAR DEL PLATA
n=411
SAN LUIS
n=1301
LA PAMPA
n=331
GRANDES
n=328
LA PAMPA HIGH
n=1252
BUENOS AIRES
n=559
TRAVESÍA
n=113
PICARDO
n=73
NARANJOS
n=98
VARITA
n=106
NEGROS
n=125
TELTECA
ALTOS LIMPIOS
NE
S
NW
GRANDES
NEGROS
TRAVESÍA
NARANJOS
PICARDO
VARITA
San Luis
SAN LUIS
LA PAMPA
Buenos Aires
BUENOS AIRES
Bahía Blanca
Mar del Plata
Depresión Diagonal
Atuel
Desaguadero
Colorado
Negro
Stress value=5.8
PC1
PC2

Figure 8

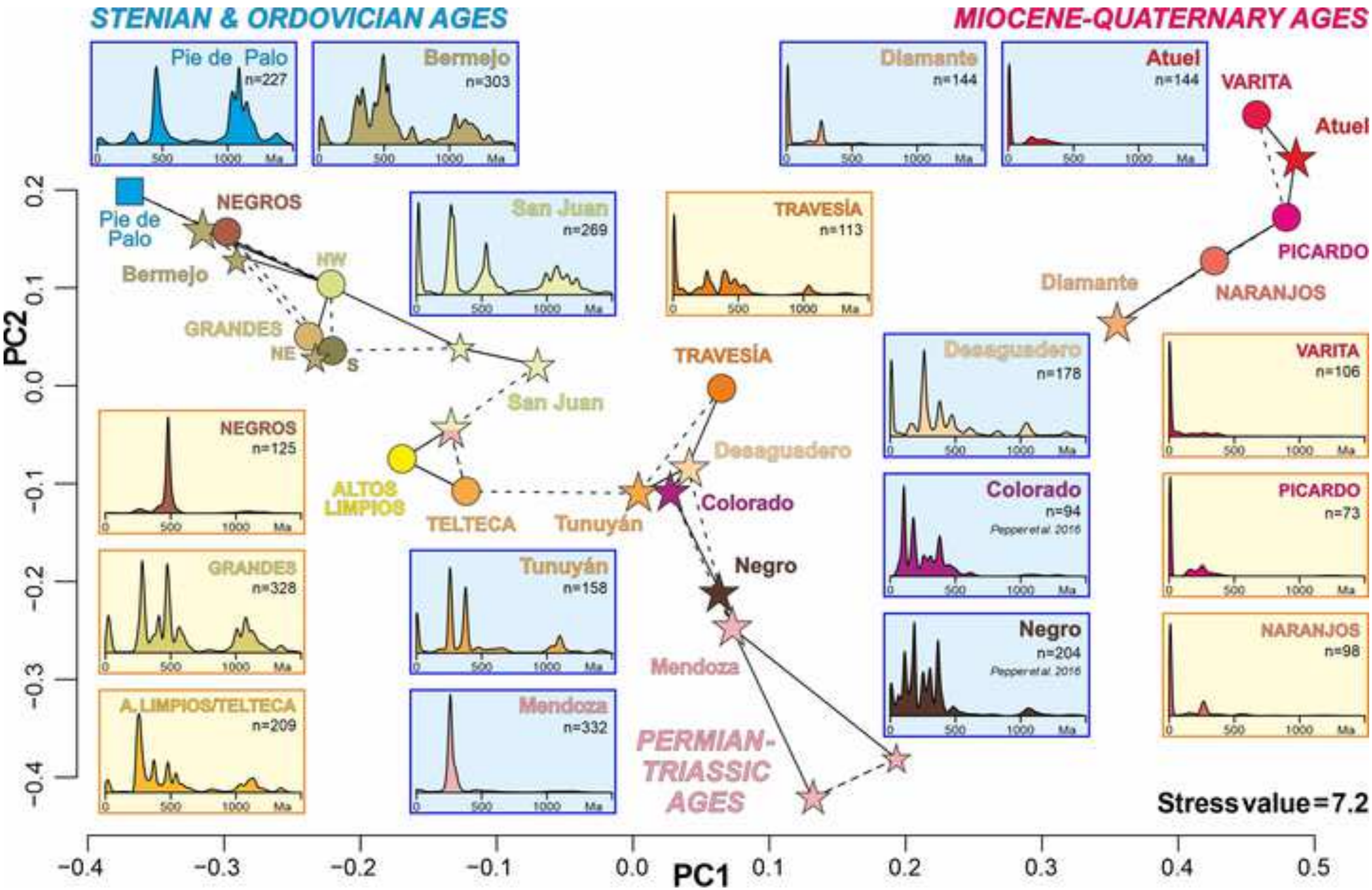

STENIAN & ORDOVICIAN AGES
MIOCENE-QUATERNARY AGES
PERMIAN-TRIASSIC AGES
Pie de Palo n=227
Bermejo n=303
Diamante n=144
Atuel n=144
San Juan n=269
TRAVESÍA n=113
Desaguadero n=178
VARITA n=106
NEGROS n=125
GRANDES n=328
A. LIMPIOS/TELTECA n=209
Tunuyán n=158
Mendoza n=332
Colorado n=94 Pepper et al. 2016
PICARDO n=73
Negro n=204 Pepper et al. 2016
NARANJOS n=98
Pie de Palo
NEGROS
Bermejo
NW
GRANDES
NE
S
San Juan
ALTOS LIMPIOS
TELTECA
Tunuyán
TRAVESÍA
Desaguadero
Colorado
Negro
Mendoza
VARITA
Atuel
PICARDO
NARANJOS
Diamante
Stress value=7.2
PC1
PC2

Figure 9

Click here to access/download;Figure;Figure 9 Argendunes MDS DZ Pampa.jpg

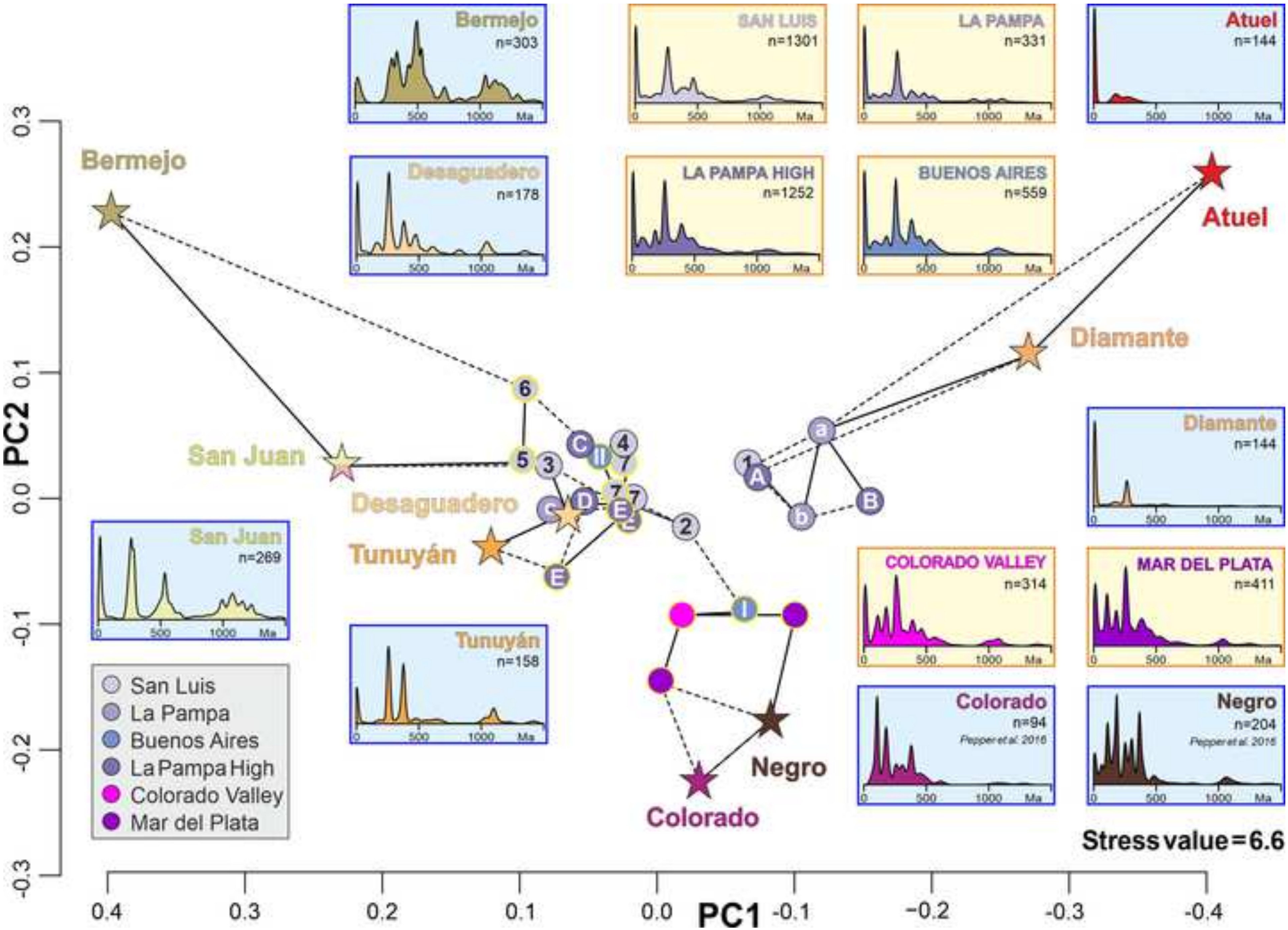

Figure 10

Click here to access/download;Figure;Figure 10 ArgenDunes Youngest DZ age.jpg

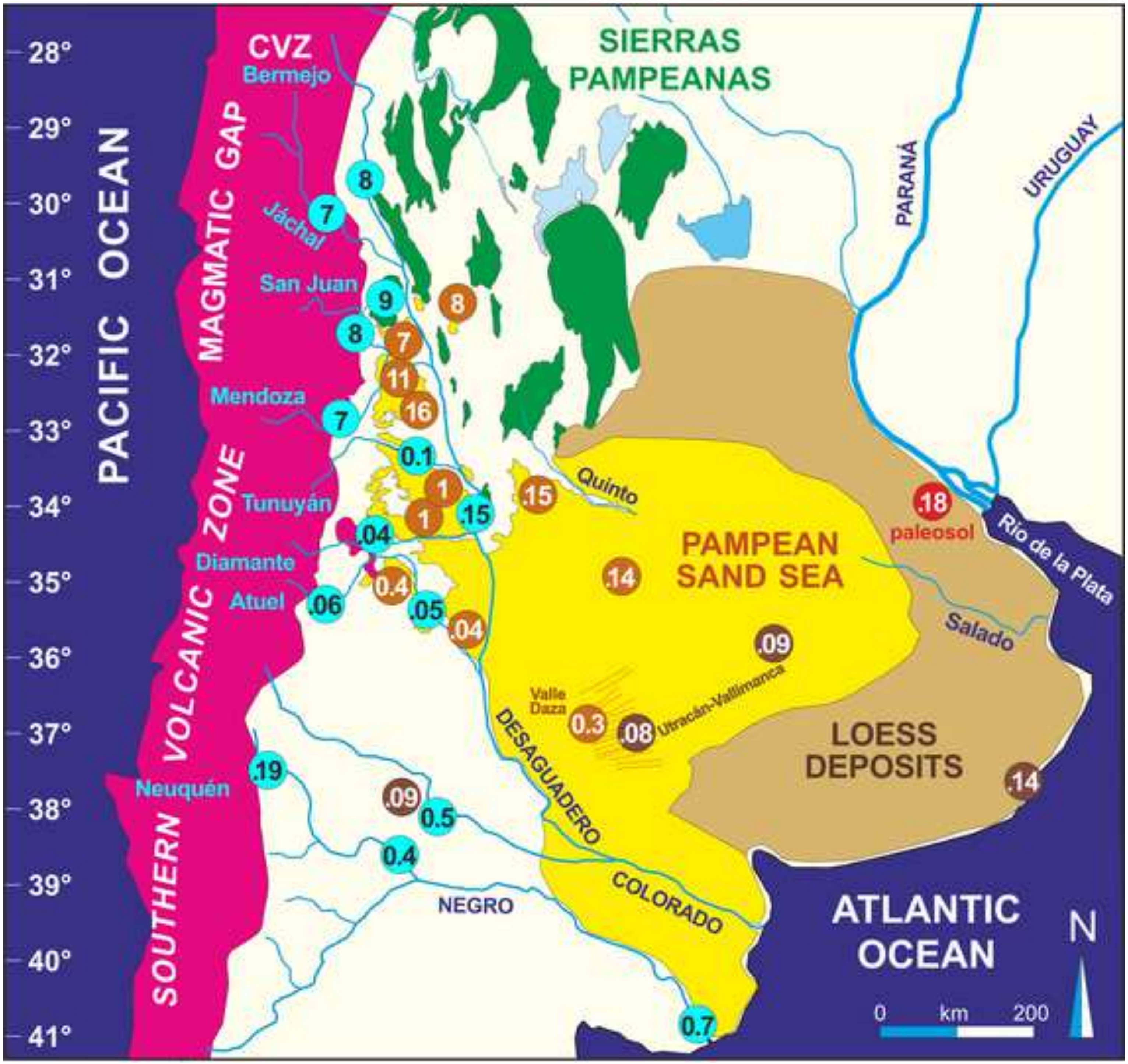

Figure 11 Click here to access/download;Figure;Figure 11 ArgenDunes Drainages.jpg

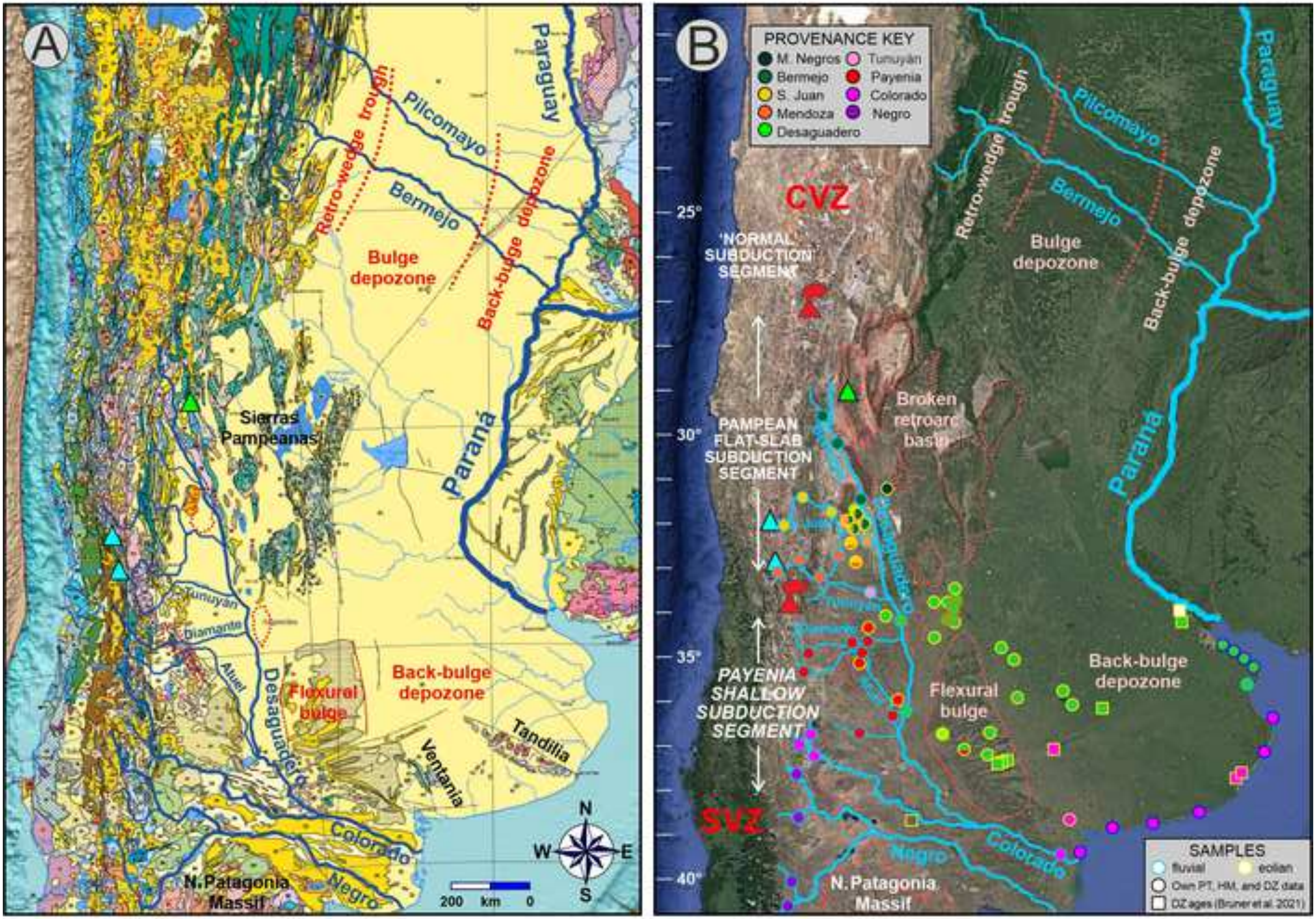

Table 1

DUNES	Sample	GSZ	Q	KF	P	Lvf	Lvm	Lc	Lsm	Lm	total	mica	tHMC	ZTR	Ap	Ttn	Ep	Grt	SKS	Amp	Cpx	Opx	Ol	total	ACI
M. Negros	E5899	130	49	8	35	2	4	0	2	0.3	100.0	3%	7.3	2	1	0	5	7	1	64	6	14	0	100.0	51
M. Grandes (NE)	E5890	200	48	5	23	5	11	2	4	2	100.0	0%	1.9	2	0	0	10	21	0.5	41	22	3	0	100.0	50
M. Grandes (SE)	E5887	140	46	5	26	6	13	0.3	2	1	100.0	0%	2.6	2	1	0	6	10	0	63	11	6	0	100.0	48
M. Grandes (N)	E5891	150	54	7	20	4	11	0.8	3	0	100.0	0.3%	2.4	1	1	1	7	16	0.5	43	24	5	0	100.0	68
M. Grandes (S)	E5888	115	45	7	24	5	12	0.6	6	2	100.0	0%	1.9	3	1	2	14	6	0	50	17	7	0	100.0	54
M. Grandes (NW)	E5892	120	36	4	33	8	14	0.6	4	1	100.0	0.3%	3.0	5	2	0	5	10	0	43	25	10	0	100.0	66
M. Grandes (SW)	E5889	100	38	6	25	10	13	0.6	7	0	100.0	0%	1.8	6	2	1	11	13	0	45	17	3	0	100.0	62
M. Altos Limpios	E5893	135	23	4	29	11	26	1	6	0.8	100.0	0%	2.0	1	1	1	4	3	0	34	29	26	0	100.0	74
M. Telteca	E5894	160	20	4	28	12	33	0	3	0.3	100.0	0%	2.7	1	0.5	0.5	4	2	0	33	26	31	1	100.0	80
M. de la Travesía	E5895	110	18	5	39	5	30	0	4	0.3	100.0	0%	3.2	1	0.5	0	2	1	0	33	29	33	0.5	100.0	78
M. de los Naranjos	E5898	125	9	1	42	4	36	0.6	6	0	100.0	0.3%	7.2	1	0.5	0	3	1	0	28	21	44	0	100.0	81
M. de Picardo	E5896	180	5	0.3	40	0	52	0	3	0	100.0	0%	5.8	0	0	0	2	1	0	9	28	58	1	100.0	92
M. de la Varita	E5897	155	8	1	48	3	37	0	2	1	100.0	0%	10.2	0	0	0	0.5	0	0	14	30	55	0.5	100.0	85
San Luis	E6036	87	14	3	36	9	31	0	5	0.8	100.0	0.5%	3.7	2	1	0	3	3	0	31	26	33	1	100.0	74
San Luis	E6037	84	11	2	48	6	31	0	3	0	100.0	1%	4.5	2	3	0	4	1	0	35	23	30	0.5	100.0	75
San Luis	E6038	100	21	4	33	15	25	0	2	0.5	100.0	0%	3.6	3	0.5	0	2	2	0	27	39	26	0.5	100.0	79
San Luis	E6039	85	16	5	37	8	28	0	6	0.6	100.0	0%	4.7	1	1	0	4	3	0	29	31	30	0.5	100.0	75
San Luis	E6040	110	15	3	41	7	33	0	2	0	100.0	0%	3.6	2	0.5	0	3	2	0	33	25	34	1	100.0	77
Buenos Aires	E6041	88	13	3	41	10	31	0	3	0	100.0	0%	3.3	2	0.5	0	5	1	0	35	25	31	0	100.0	68
Buenos Aires	E6042	95	20	3	42	9	25	0	1	0	100.0	0%	3.6	0.5	2	0	6	2	0	33	26	30	0	100.0	72
La Pampa	E6043	125	25	4	32	6	31	0	2	0.3	100.0	0.3%	2.5	1	1	0	3	3	0	25	34	32	0	100.0	84
La Pampa	E6044	130	22	4	42	8	20	0	4	0	100.0	0%	3.0	0.5	0	0	4	1	0	29	25	40	0	100.0	81
La Pampa	E6045	90	18	3	41	8	24	0	5	0	100.0	0%	3.8	1	1	0	5	2	0	33	25	34	0	100.0	80
Utracan	E6046	115	17	5	38	8	31	0	1	0	100.0	0%	3.9	1	1	0	5	1	0	19	33	39	0	100.0	74
Daza	E6047	140	18	3	36	12	27	0	3	1	100.0	0%	5.9	0	0	0	0	3	0	4	38	53	0.5	100.0	85
NW La Pampa High	E6048	160	18	3	27	13	37	0	2	0.3	100.0	0%	3.3	1	0.5	0	3	3	0	21	35	34	1	100.0	76
Cantera Toay	E6049	150	18	3	30	10	36	0	2	0.3	100.0	0%	2.1	0.5	0.5	0	4	4	0	15	32	43	1	100.0	74
RIVERS																									
Abaucán	S5521	125	46	4	19	10	8	3	7	2	100.0	1%	3.9	6	2	1	12	3	0	45	19	12	0	100.0	65
Berrmejo	S5902	115	58	5	19	2	6	1	6	1	100.0	3%	1.9	5	3	0	7	9	1	56	16	2	0	100.0	43
Jáchal	S5525	600	11	0.3	21	6	20	2	38	2	100.0	0.5%	8.4	0	0	0	0	0	0	6	93	1	0	100.0	64
Pie de Palo	S5933	120	52	5	16	0.8	0.8	2	0.8	23	100.0	8%	15.8	1	0	1	6	34	1	57	0	0	0	100.0	11
San Juan	S5909	240	26	2	14	20	17	1	20	1	100.0	0.3%	0.7	2	2	0	11	3	0	35	47	3	0	100.0	76
Mendoza	S5906	260	15	4	23	21	26	3	4	2	100.0	0%	1.1	2	2	0	10	0.8	0	50	29	6	0.4	100.0	85
lower San Juan	S5932	124	30	6	27	11	19	1	6	0.6	100.0	0%	1.9	2	1	0	4	3	0	45	24	20	0	100.0	72
Tunuyán	S5910	320	17	6	26	10	32	2	7	0.8	100.0	0.3%	2.1	0.5	0	0	0.5	1	0.5	38	26	33	0.5	100.0	80
upper Desaguadero	S5444	200	38	10	17	21	7	1	4	0.7	100.0	0.3%	1.5	4	1	0.5	6	3	0	26	33	26	1	100.0	76
Diamante	S5443	118	13	2	41	8	27	3	4	2	100.0	1%	8.1	0.5	1	0	0.5	2	0	28	33	31	4	100.0	82
Atuel	S5912	130	10	2	32	9	40	4	3	0	100.0	0.8%	4.4	0	0.5	0	1	0.5	0	15	38	45	0.5	100.0	91
Desaguadero	S5915	160	21	2	33	15	21	1	5	1	100.0	0.3%	3.9	2	1	0.5	6	3	0	27	28	32	0	100.0	79
Salado (B. Aires)	S5368	6	n.d.	n.d.	n.d.	n.d.	n.d.	n.d.	n.d.	n.d.		n.d.	1.5	0.5	5	0	21	1.4	0	34	28	11	0	100.0	45
Grande	S5440	150	13	2	37	2	40	3	3.4	0	100.0	0.3%	5.7	0.5	0	0	0	0.5	0	20	45	31	2	100.0	89
Colorado	S5438	125	12	2	33	5	39	6	3	0.3	100.0	0.3%	6.6	0.5	1	0	0	2	0	19	34	33	11	100.0	93
Neuquén	S5437	200	6	0.8	28	6	57	1	1	0	100.0	1%	3.3	0	0	0	7	6	0	12	32	38	6	100.0	66
Agrio	S5436	450	6	0.7	69	4	17	0.5	3	0	100.0	0%	8.5	0	0	0	0	0	0	1	25	72	2	100.0	n.d.
Limay	S5433	110	6	2	28	5	58	0	0.7	0.6	100.0	0.1%	2.8	0.5	0	0	4	0.2	0	7	35	47	6	100.0	57

	HIMALAYAN-TYPE OROGENS	ANDEAN-TYPE OROGENS	APENNINIC-TYPE OROGENS
Main basin	FORELAND BASIN	RETROARC BASIN	FOREDEEP
Basement	Subducting lower plate	Overriding upper plate	Subducting lower plate
Subsidence cause	Plate subduction + load	Tectonic load	Slab retreat
Long-term rate	≤ 300 m/ Ma	~ 100 m/ Ma	> 1000 m/ Ma
Main depozone	Pro-wedge trough	Retro-wedge trough	Wedge top
Typical condition	Overfilled	Strongly overfilled	Strongly underfilled
Drainage	Axial fluvial (e.g., Ganga)	Transverse fluvial (e.g., Amazon)	Axial (turbidite)

Declaration of interests

☒The authors declare that they have no known competing financial interests or personal relationships that could have appeared to influence the work reported in this paper.

☐The authors declare the following financial interests/personal relationships which may be considered as potential competing interests:

Andean retroarc-basin dune fields and Pampean Sand Sea (Argentina): Provenance and drainage changes driven by tectonics and climate

Eduardo Garzanti[1*], Tomas Capaldi[2], Alfonsina Tripaldi[3], Marcelo Zárate[4], Mara Limonta[1], Giovanni Vezzoli[1]

[1] Laboratory for Provenance Studies, Department of Earth and Environmental Sciences, Università di Milano-Bicocca, 20126 Milano, Italy

[2] Department of Geosciences, University of Nevada, Las Vegas, NV, 89154, USA.

[3] Instituto de Geociencias Básicas, Aplicadas y Ambientales de Buenos Aires (IGEBA - CONICET), Department of Geology, University of Buenos Aires, Intendente Güiralde 2160, Ciudad Universitaria, Buenos Aires C1428EHA, Argentina

[4] Instituto de Ciencias de la Tierra y Ambientales de La Pampa (Consejo Nacional de Investigaciones Científicas y Técnicas (INCITAP - CONICET), University of La Pampa, Avenida Uruguay 151, 6300 Santa Rosa, La Pampa, Argentina

Emails: eduardo.garzanti@unimib.it (Garzanti), tomas.capaldi@unlv.edu (Capaldi), alfo@gl.fcen.uba.ar (Tripaldi), mzarate@exactas.unlpam.edu.ar (Zárate), mara.limonta@unimib.it (Limonta), giovanni.vezzoli@unimib.it (Vezzoli)

* Corresponding author

Keywords: Sedimentary petrology; Heavy minerals; Detrital zircon geochronology; Desaguadero and Colorado rivers; Broken retroarc basin; Pampean dune fields; Quaternary climate; Landscape changes; Argentina.

ABSTRACT. We here review in terms of tectono-magmatic setting and Quaternary landscape dynamics what is known about the provenance of Argentine dune fields and their fluvial feeder systems draining the Andean Cordillera. The detrital signatures of these eolian sediments were previously investigated based on either framework petrography and heavy minerals or detrital-zircon geochronology, and their peculiar volcaniclastic nature was long recognized. Compositional variability, however, was only broadly evaluated, and quantitative provenance analysis based on a systematic multimethod approach across the entire region was not carried out so far. For this reason, here we integrate original and previously obtained petrographic, heavy-mineral, and detrital-zircon

geochronology data to present the first comprehensive provenance study of dune fields stretching for 1000 km across central Argentina from the Andean piedmont to the Atlantic Ocean.

In dune fields along the Andean retroarc basin, sediment composition defines a steady northward decrease in volcanic detritus. This reflects active magmatism in the Southern Volcanic Zone and Payenia province (38°-34°S), in contrast with the ~600-km-long Pliocene-Quaternary magmatic gap in the Pampean flat-slab segment (33°-27°S), where sediment is derived from deeper-seated tectono-stratigraphic levels of the continental arc and uplifted blocks of retroarc-basin basement. In distal Pampean lowlands extending across the bulge and backbulge depozones, instead, sand dunes display notably homogeneous compositional signatures, indicating that detritus was mostly generated north of 34°S and transported by a paleo-Desaguadero trunk river that formed during southward-progressing diachronous uplift of the Sierras Pampeanas since the late Miocene. In contrast with huge African and Arabian deserts that contain multiply recycled quartzose to pure quartzose sand, even very fragile volcanic clasts, plagioclase feldspar, and unstable ferromagnesian minerals are widespread, testifying to largely first-cycle volcanic provenance and only minor effects of mechanical breakdown and chemical weathering in the Pampean Sand Sea.

During the Late Pleistocene, after a first southward shift of the Desaguadero trunk river possibly induced by increased water and sediment discharge at the end of the penultimate glacial maximum, tectonic uplift eventually outpaced stream power during the last glacial period. Paleo-rivers were thus forced to shift farther southwards, leading to the formation of an integrated paleo-Desaguadero+Colorado drainage system. During the latest Pleistocene-early Holocene, such a large trunk river fostered the rapid progradation of a wide delta and littoral sand transport all along the shores of the Buenos Aires Province. Climate change and repeated waxing and waning of glaciers through the Quaternary have left a prominent mark on sediment distribution, dominated by fluvial processes during periods of high fluvial discharge but alternating with arid phases characterized by limited transport capacity and vegetation cover, extensive wind deflation of floodplains, and sand accumulation in the dune fields.

¿Qué poemas nuevos fuiste a buscar? / Una voz antigua de viento y de sal
Te requiebra el alma y la está llevando / Y te vas hacia allá como en sueños
Félix Luna, Alfonsina y el mar

1. Introduction

During the Quaternary, inland dune fields formed all along the eastern side of the Andean orogen from the subequatorial Orinoco and Amazonian basins to Patagonia (Tripaldi and Zárate, 2016). In central Argentina, a vast region covered by Pleistocene-Holocene eolian sediments offers a key to reconstruct the complex climatic, geologic, and geomorphologic history of the region (Fig. 1; Iriondo and Garcia, 1993; Zárate and Tripaldi, 2012). These Andean and Pampean eolian sand and loess deposits are not only important archives of hydrological change associated with distal seasonal effects of the South American Monsoon (Clapperton, 1993; Iriondo and Kröhling, 1995; Zárate, 2003; Tripaldi and Forman, 2016) but also represent the parent material of soils in an intensely cultivated region strongly sensitive to climatic variability (Imbellone and Teruggi, 1993). Much attention has been consequently devoted to soil genesis, conservation, and erosion (Kemp et al., 2006; Mendez and Buschiazzo, 2010; Rubio et al., 2019).

Argentine dune fields occur along the Andean retroarc basin as far south as ~38°S and extend eastwards across the bulge depozone and Pampean lowlands representing the backbulge depozone (Fig. 2; DeCelles, 2012; Folguera and Zárate, 2019). During Pleistocene glacial/interglacial cycles, sediment production was greatly enhanced in the most elevated tract of the Andes corresponding to the Pampean segment of the Nazca-South America plate boundary (Zárate and Blasi, 1993), where very-shallow-angle subduction is associated with a lack of magmatic activity. In contrast, in the Payenia segment to the south, intense Neogene-Quaternary magmatism took place in the Southern Volcanic Zone of the Cordillera and in the retroarc region (Hickey et al., 1986; Cembrano and Lara, 2009; Ramos and Folguera, 2011). As an effect of nearly flat subduction, both the Andes mountains and uplifted basement blocks of the Sierras Pampeanas in the retroarc region are characterized by high structural and topographic relief, reaching elevations up to 7000 and 6000 m a.s.l. (above sea level), respectively (Ramos and Folguera, 2009; Fig. 3A). High sediment-production in the highlands is thus coupled with low long-term sediment-storage capacity in the broken retroarc basin (Dickinson, 1978; Garzanti et al., 2021a), where during arid stages detritus is temporarily stored and extensively reworked by wind owing to limited transport efficiency of river systems (Capaldi et al., 2019).

Investigating the interplay between the geological agents that controlled landscape change during the late Quaternary is the principal aim of this article, which reviews what is currently known about the linked fluvial-eolian processes across this vast area and illustrates the first multimethod provenance study of Andean dune fields and the Pampean Sand Sea. The geology of the region is first outlined in the wider context of the Central and Southern Andes of Argentina, before reviewing the climate-related history of the dune fields and their potential fluvial feeder systems. The results of previous mineralogical and provenance research are summarized next. Numerous studies of Argentine dune fields have been devoted to understanding the relationships among sedimentation, climate, and tectonics (e.g., Malagnino, 1989; Zárate and Blasi,1993; Forman et al., 2014; Tripaldi et al., 2018a) and the origin of dune sands has been examined based on framework petrography and heavy minerals (e.g., Teruggi, 1957; Etchichury and Tófalo, 2004; Szelagowski et al., 2004; Tripaldi et al., 2010) or detrital-zircon geochronology (Capaldi et al., 2019; Bruner et al., 2022). These studies have documented the peculiarly quartz-poor composition of dune sand in this region, dominated by volcanic rock fragments, plagioclase, and ferromagnesian silicates shed from magmatic rocks of the adjacent Andean Cordillera and thus so different from quartzose to pure quartzose sands of vast African and Arabian deserts. A systematic provenance analysis based on a multimethod approach, however, has not been carried out so far.

For this reason, we here present new results from integrated bulk-petrography, heavy-mineral, and detrital-zircon U–Pb geochronology analyses of eolian-dune sands collected over a 1000-km-long stretch including the Andean retroarc basin of the La Rioja, San Juan, Mendoza, and Neuquén Provinces of Argentina, as well as the bulge and backbulge depozones in Pampean lowlands of the

San Luis, La Pampa, and Buenos Aires Provinces (Fig. 2). A set of statistical techniques is applied to this multi-proxy dataset to adequately illustrate the compositional variability of eolian sand across the Pampean Sand Sea, reveal meaningful mineralogical patterns, identify and wherever possible quantify the original sediment sources, and gain insight into sand dispersal pathways and landscape changes through time. Compositional signatures of river sands generated in the Andes between 28°S and 41°S are compared to eolian sands to assess and disentangle tectonic and climatic control on the sediment-routing system. This large dataset is eventually employed to discuss sediment-generation processes and depositional style, as well as Quaternary drainage evolution across the bulge and backbulge depozones as controlled by the interplay between tectonic activity and climate change.

2. Geology

The Andes have undergone a complex geological evolution, traditionally subdivided into five main orogenic cycles: i) Pampean (Neoproterozoic-early Cambrian); ii) Famatinian (Cambrian to Devonian); iii) Gondwanide (Carboniferous to Middle Triassic); iv) Patagonide (Jurassic-Cretaceous); and v) Andean (Cenozoic) (Ramos, 1988; Ramos and Alemán, 2000). The Pampean and Famatinian cycles resulted in the successive collision and assembly of diverse terranes against the Neoproterozoic margin of Gondwana. The Cuyania terrane (present Precordillera and Sierra de Pie de Palo; Rapela et al., 2016), derived from Laurentia and containing a carbonate platform, was accreted during the middle Ordovician Ocloyic orogeny (Astini and Dávila, 2004). The Chilenia terrane, a Grenvillian basement block, was accreted to the Cuyania margin during the late Devonian Chanic orogeny (Charrier et al., 2015). East-dipping subduction was renewed to the west of Chilenia in the late Paleozoic to Triassic, when arc rocks including granites and rhyolites were generated along the continental margin (Gondwanide orogeny; Pankhurst et al., 2006; Capaldi et al., 2021). In the Mesozoic, the Paleozoic basement was affected by extension and the frontal part of the arc-trench system was destroyed by tectonic erosion, as indicated by the proximity between the extinct Jurassic arc and the Chilean trench (Kay et al., 2005; Stern, 2020).

2.1. The Andean Cordillera

Between 27°S and 38°S, three major tectonic domains are identified in the Andes from west to east: the Cordillera Principal, the Cordillera Frontal, and the Precordillera.

The Cordillera Principal magmatic arc consists of Oligo-Miocene to Holocene volcanic rocks and fluvial volcaniclastic sandstones overlying a deformed 12-15 km-thick succession of Jurassic to Paleogene sedimentary rocks (Giambiagi et al., 2003). Tectonic and magmatic processes differed significantly in time and space along the Andean active margin. North of ~35°S, andesite and basalt interfingered eastwards with carbonate and clastic sediments of the Aconcagua platform. South of ~35°S, instead, the magmatic arc remained stationary along the main axis of the Cordillera Principal, and the Jurassic-Cretaceous Neuquén retroarc basin developed in the east (Mpodozis and Ramos, 1989; Horton and Fuentes, 2016).

The Cordillera Frontal represents a tectonic culmination composed of lower Paleozoic low-grade metasedimentary rocks intruded by granitoids. The unconformably overlying cover sequence consists of up to 2-4 km-thick basalt, andesite, volcaniclastic breccia, and rhyolitic ignimbrites more common in the upper part (Permian-Triassic Choiyoi igneous complex; Kleiman and Japas, 2009; Martínez and Giambiagi, 2010). Thick continental volcanic and volcaniclastic units of Neogene age unconformably follow (Heredia et al., 2002).

The Precordillera (28°-33°S) includes a ~3 km-thick succession of Cambro-Ordovician marine carbonates with red beds, evaporites, quartz-rich sandstones and mudrocks at the base and graptolitic shale at the top (Keller, 1999). Silurian-Devonian shelfal siliciclastic rocks and orogenic turbidites are exposed in the central part of the Precordillera (Astini et al., 1995), where they are overlain with angular unconformity by Carboniferous-Permian continental and glaciomarine sediments passing westwards to fossiliferous marine deposits. Lower Paleozoic rocks underwent low-grade metamorphism in the west during the late Devonian Chanic orogeny (von Gosen 1995; Giambiagi et al., 2011). During the Mesozoic, the Precordillera remained as a structural high. Triassic lacustrine sediments with plant remains occur in the west, whereas no Jurassic and Cretaceous strata are recorded (Ramos and Kay, 1991). Cenozoic fluvial, lacustrine, and eolian sediments and sedimentary rocks together with mainly Miocene volcanic rocks are exposed in the east and are preserved in footwall blocks of major thrust faults with preferential erosion forming intermontane valleys between thrust-generated ranges (Peralta, 2003; Capaldi et al., 2017).

2.2. The Sierras Pampeanas and the broken retroarc basin

The Sierras Pampeanas are a series of mainly eastward-tilted blocks bounded by steeply dipping and N-S-striking reverse faults that started to be uplifted within the retroarc region in the late Miocene, after a long period of peneplanation and limited burial (Jordan et al., 1989; Goddard and Carrapa, 2018; Goddard et al., 2018). The geological history documented by these blocks includes the intrusion of granitoid batholiths above an eastward-dipping subduction zone during the Famatinian cycle (Ramos et al., 1986; Capaldi et al., 2021). Minor Devonian to Carboniferous plutonism was followed by accumulation of up to 5 km-thick Carboniferous-Triassic fluvial clastic sediments (Dahlquist et al., 2021). Subsequent Mesozoic rifting associated with alkaline volcanism and reactivation of Paleozoic structures led to deposition of Mesozoic clastic sediments to the west and around the Sierra de San Luis (Bense et al., 2017). Upper Paleogene deposits are also locally exposed at the piedmont of the sierras and an extensive apron of upper Miocene silty sandstones underlies the upper Quaternary eolian mantle in the central part of the La Pampa province (Chiesa et al., 2011).

The Sierra de Pie de Palo, adjacent to the Precordillera, consists of 1.0-1.2 Ga (Grenvillian/Sunsas) amphibolite-facies gneiss and schist with local migmatite and granulite, overlain by upper Neoproterozoic schist, quartzite, amphibolite, and marble (Rapela et al., 2010; Mulcahy et al., 2011). To the southeast, the Sierra de San Luis exposes Neoproterozoic to lower Paleozoic granitoid and metamorphic rocks, including schist, migmatite, gneiss, and phyllite (Llambías et al., 1998). Farther south, Neoproterozoic-lower Paleozoic metamorphic and igneous rocks of the Sierras Pampeanas and the Choiyoi Permian-Triassic igneous complex crop out in the very-low-elevation Sierra de Lonco Vaca and Chadileuvú Block (Folguera and Zárate, 2018).

2.3. Time structure of Andean source rocks

The rapid development of detrital-geochronology techniques has added a new dimension to provenance analysis, allowing the definition of a "time structure" of source rocks that represents an essential complement to the information on their lithological structure obtained by traditional petrographic and mineralogical methods (Garzanti, 2016). Although the age spectra of detrital zircons reflect past events of crustal growth, durable zircon can survive even multiple sedimentary cycles. The ages of recycled zircons, therefore, do not refer to their siliciclastic parent rocks but to the igneous or metamorphic rocks in which they originally crystallized (i.e., the protosource, Pell et al., 1997; Andersen et al., 2018).

Several age components characterize detrital zircons in Andean sediments. Calymmian-Ectasian (~1.4 Ga) Laurentia-derived ages are diagnostic of a Cuyania terrane protosource (Ramos, 2009), whereas Stenian (1.2-1.0 Ma) Pampia basement ages are sourced from numerous metamorphic basement units across the western Sierras Pampeanas and are ubiquitous in most Ordovician to Permian strata of the Precordillera (Ramos, 2004, 2009; Bahlburg et al., 2009; Rapela et al., 2016). Cryogenian-Ediacaran (720-550 Ma) ages can be recycled from metasedimentary rocks of the eastern Sierras Pampeanas (Puncoviscana Formation; Rapela et al., 2007) or from Carboniferous to Permian strata of the Precordillera fold-thrust belt (Fosdick et al., 2015; Capaldi et al., 2017). Ediacaran-Cambrian (Pampean; 555-515 Ma) to Cambrian-Ordovician (Famatinian; 495-460 Ma) arc rocks are exposed in the western Sierras Pampeanas (Rapela et al., 2018). Carboniferous-Permian (340–280 Ma) arc rocks and Permian–Triassic (280–240 Ma) Choiyoi igneous rocks are exposed in the Cordillera Principal, Cordillera Frontal, and adjacent regions (Mpodozis and Kay, 1992; Rocha-Campos et al., 2006), but zircon with these ages can also be recycled from Triassic strata of the Sierras Pampeanas, from Jurassic to Cretaceous strata of the high Andes, and from Neogene deposits throughout the Frontal Cordillera and Precordillera (Fosdick et al., 2015; 2017; Mackaman-Lofland et al., 2019). Jurassic (175–145 Ma) Cretaceous (120-80 Ma), and Upper Cretaceous to Eocene (75-30 Ma) intrusions are presently found in Chile throughout the Coastal Cordillera and the Principal

Cordillera (Haschke et al., 2006), but zircon with these ages can also be recycled from Mesozoic and Neogene retroarc-basin deposits along the eastern flank of the Andes (Balgord and Carrapa, 2016; Horton et al., 2016). Finally, young zircons of Neogene-Quaternary ages (< 25 Ma) are derived from Andean volcanic rocks broadly distributed from the hinterland Principal Cordillera to the Payenia volcanic field (Stern, 2004; Ramos and Folguera, 2011), or recycled from Neogene Andean retroarc-basin sediments.

3. Geomorphology

3.1. Climate

Central Argentina has temperate climate. Winter months (June-August) are mild, with an average temperature of 10°C. Spring and autumn have mild days and cool nights, with average temperatures of 14-16°C. In summer (December-February), mean temperatures rise to 20°C but are cooler in the southeastern Buenos Aires Province owing to maritime influence. Mean maximum temperatures during the humid summer season may exceed 35°C.

Precipitation is generated by wet air masses from the Atlantic Ocean, giving rise to humid- subhumid conditions on the northeastern Pampas (mean annual rainfall up to more than 1000 mm), rapidly changing to semiarid–arid along the Andean piedmont (mean annual rainfall as low as 90 mm; Garreaud et al., 2009) (Fig. 3A). Most precipitation (>70%) is delivered during the spring and summer (October to March) and reflects influence of the South American Monsoon (Silva and Kousky, 2012; Espinoza et al., 2020). The precipitation flux is associated with the pressure gradient between a thermal-orographic dynamic Chaco Low located east of the Andes and the subtropical South Atlantic Anticyclone (Compagnucci et al., 2002; Barros et al., 2008). This pressure gradient increases during the austral summer when solar insolation is maximum, resulting in northeasterly flow and net import of moisture from the Atlantic Ocean. Significant moisture is also derived from the low-level meridional Chaco Jet, which reaches wind speeds >15 m/s at ~1.5 km above ground level and pushes air masses from tropical jungles and humid lowlands of Bolivia and Brazil southwards along the eastern margin of the Andes (Salio et al., 2002; Marengo et al., 2004). The vegetation cover, strongly modified by agricultural activities, varies from grassland in the northeast, to savannah-like plain with grasses and scattered trees, and to xerophytic woodland and shrubs in the southwest (Cabrera, 1994). The subtropical Andean Cordillera, with mean peak elevation 4000 m a.s.l., acts as an effective barrier for the direct import of moisture from the Pacific Ocean, even though middle tropospheric Rossby Wave trains associated with strong El Niño events may enhance convective precipitation in western Argentina with advected sources from the Atlantic Ocean and the western Amazon Basin (Grimm, 2003; Barros et al., 2015; Kayano et al., 2020).

Wind conditions are controlled by subtropical high-pressure cells (Pacific and Atlantic anticyclones), the intensity of the quasi-stationary low in the Gran Chaco, and the prevailing westerlies at middle latitudes. Southerly winds predominate along the Andes piedmont and the western Pampas, whereas northeasterly winds prevail through the year across the eastern Pampas (Fig. 3B). In winter, westerlies predominate in northern Patagonia and the southern Pampas. Dry föhn-like *Zonda* winds, generated from polar maritime air warmed while descending across the eastern flank of the Andes, are dominant along the downslope Andean piedmont and particularly strong where the cordillera is highest. Cold *Pampero* winds are bursts of cold polar air from the south that blow mostly in winter over the eastern pampas, accounting for net northward sand transport (Prohaska, 1976).

3.2. Landscapes and rivers

Central Argentina encompasses the Andean piedmont to the west of the Desaguadero axial drainage, the Pampean plain in the east, and the northern Patagonia plateau to the south of the Río Colorado (*río*, river in Spanish). The Andean piedmont, decreasing gradually in elevation from 900 to 700 m a.s.l. at the mountain front to ~200 m a.s.l., is traversed by several major tributaries of the Río Desaguadero, whose fluvial discharge largely depends on winter snowfall in the high Cordillera generated by humid air masses from the Pacific anticyclonic cell.

The Desaguadero includes the Bermejo headwater branch and takes the names Salado downstream of the Río San Juan confluence, Chadileuvú downstream of the Río Atuel confluence, and finally Curacó (total length ~1500 km, catchment area ~300,000 km^2; Fig. 2). This trunk-river system mostly drains the tract of the Andes corresponding to the Pampean flat-slab-subduction segment, where Paleozoic to Miocene rocks have been tectonically uplifted to elevations up to 6962 m a.s.l. at the summit of the Aconcagua massif (Farías et al., 2008; Ramos and Folguera, 2009). Here in the north, the Cordillera Principal drains mostly toward Chile, and a limited amount of detritus from Mesozoic and Cenozoic arc rocks is fed into the retroarc basin mixed with detritus from the bimodal (basal mafic and upper felsic) rocks of the Permian-Triassic Choiyoi igneous complex.

The Bermejo River flows along Neogene strike-slip and reverse faults bordering the uplifted basement blocks of the western Sierras Pampeanas, which reach 6097 a.s.l. in the Sierra de Famatina (Fig. 3). The Desaguadero trunk river continues southwards among broad floodplains and evaporitic lakes but, in the present dry climate and after profound anthropic intervention and dam construction, sediment transport has virtually ceased. Water flow reaches as far as the Colorado River only occasionally (e.g., during the 1983 El Niño event).

Among major tributaries, the San Juan River is sourced from the > 6000-m-high Cordillera de la Ramada and drains the igneous rocks of the Cordillera Frontal and the sedimentary to low-grade metasedimentary rocks of the Precordillera. The Mendoza River is sourced from the Aconcagua massif in the Cordillera Principal and cuts across the Cordillera Frontal and the southern tip of the Precordillera to reach the retroarc basin, where it flows northwards along the western border of the Médanos de Telteca to join the San Juan River south of the Médanos Grandes (*médano*, sand dune in Spanish; Fig. 1A).

The Tunuyán, Diamante, and Atuel drainage basins include the Cenozoic volcanic rocks of the Cordillera Principal and the active Southern Volcanic Zone, the Jurassic-Cretaceous retroarc strata of the Malargüe fold-thrust belt, and Devonian-Carboniferous strata with overlying Permian-Triassic Choiyoi igneous rocks uplifted in the San Rafael Block (Kleiman and Japas, 2009).

In the south, the Colorado River (length ~1100 km, catchment area ~70,000 km^2; Fig. 2) is formed by the confluence between the Grande and Barrancas tributaries. Sourced in the Cordillera Principal, it drains the northern Neuquén Basin and basaltic lavas of the Quaternary Payenia volcanic province

(Ramos and Folguera, 2011). Farther south, the Negro River (length ~1200 km, catchment area ~130,000 km^2) is formed by the confluence between the Limay and Neuquén tributaries. Sourced in the Cordillera Principal, it drains the Agrio fold-thust belt (Valcarce et al., 2006) and the southern Neuquén basin, where an Upper Triassic to Paleogene continental and marine sedimentary succession is exposed (Howell et al., 2005; Balgord and Carrapa, 2016; Di Giulio et al., 2017).

The Atlantic coast north of the Negro and Colorado river mouths includes several tidal channels, salt marshes, and tidal flats representing the remnants of a ~200 km-wide deltaic complex formed in the late Pleistocene-early Holocene (Colorado Delta; Spalletti and Isla, 2003). To the north, the ~660 km-long mesotidal to microtidal coast of the Buenos Aires Province between Bahía Blanca and Punta Rasa (Fig. 3A) includes wide dissipative sandy beaches and backshore dunes fed by littoral sand drift (Isla, 2014). Farther north lies the hook-shaped Samborombón Bay, where only mud is supplied by very-low-gradient distributary channels draining a flat wetland underlain by Quaternary loess and shell ridges. The major stream flowing into the bay is the Salado River, draining a large part of the Buenos Aires Province but characterized by inefficient runoff because of its very low topographic gradient (Iriondo and Kröhling, 2007). The low-relief southern coast of the microtidal Río de la Plata Estuary is lined by ultra-dissipative beaches with multiple rippled bars exposed during low tide. Only a minor part of the sandy bedload carried by the Paraná River reaches the estuary, and beaches overwhelmingly consist of very-fine-grained sand fed from local reworking of loess deposits (Garzanti et al., 2021b).

3.3. Dune fields

The central region of Argentina, between ~31°S and ~39°S, is largely covered by an eolian blanket displaying a variety of morphologies (barchan-barchanoid, linear, parabolic, transverse and lunette dunes, deflation basins, sand sheets) and extending over an area of ~700,000 km^2 from the foot of the Andes to the Atlantic coast (Zárate and Tripaldi, 2012). One of the first attempts to frame these eolian landscapes as an integrated eolian system — grading from sand in the Andean piedmont and western Pampas to loess and loess-like deposits in the eastern and northern Pampas — was made by Iriondo

(1990), who formally distinguished the Pampean Sand Sea in the west from the loess belt in the east (Fig. 2). The origin of the western dune fields has been investigated by several more recent studies (e.g., Tripaldi and Forman, 2007, 2016; Tripaldi et al., 2018; Capaldi et al., 2019), which revealed geomorphological and sedimentological complexities controlled by both local tectonic and regional climatic factors. A variety of eolian landforms, spanning the past ~150 ka, were identified in dune fields and sand sheets that occupy the central and western parts of the sand sea, along with loess mantles, dunes, and blowouts characterizing the eastern Pampean lowlands (Tripaldi and Zárate, 2016). The earliest Quaternary evidence for activity in the Pampean Sand Sea is an eolian sand in the southern Santa Fe Province, which yielded a minimum limiting OSL (optically stimulated luminescence) age of ~146 ka and is overlain by loess and loess-like deposits dated by OSL as ~69 ka and ~63 to 23 ka, capped in turn by a paleosol (Kemp et al., 2004). Loess and loess-like deposits, intercalated with fluvial sediments and paleosols, accumulated along the eastern piedmont of the Sierras Pampeanas in the north between 115 and 10 ka (Frechen et al., 2009). Across Pampean lowlands from the Andean piedmont to the Atlantic Ocean, eolian activity continued during the last Pleistocene glaciation and episodically through most of the Holocene (Zárate et al., 2009; Kruck et al., 2011; Tripaldi et al., 2011; Tripaldi and Forman, 2016). A most recent episode of pervasive eolian reactivation took place in the 1930s in the western Pampas, triggered by a severe drought with 30-60% deficit in precipitation and amplified by rapid expansion of wheat cultivation with poor soil-conservation practices in a fragile environment (Tripaldi et al., 2013).

The Andean retroarc basin is characterized by a series of upper Quaternary dune fields and associated eolian sand sheets and fluvial-eolian interaction plains, at present mostly vegetated and stabilized (Fig. 2). From north to south, these include the Médanos (M.) Negros to the east of the Bermejo River, M. Grandes between the Bermejo and San Juan rivers, M. Altos Limpios-Telteca south of the San Juan River and west of the northward-flowing Mendoza River, M. de la Travesía and M. de los Naranjos between the Tunuyán and Diamante rivers, and M. de Picardo and M. de la Varita to the south and east of the Atuel River (Krömer, 1996; Tripaldi and Forman, 2007; Tripaldi, 2010). Most dunes show NW-SE and NNW/SSE-trending crests, but some are oriented NNE-SSW. Cross patterns and dune superposition are common in these dune fields, suggesting successive phases of dune growth, stabilization, and reactivation under the predominant action of paleowinds from the western and the southern quadrant, and subordinately from the NE (González Díaz and Fauqué 1993; Krömer 1996; Tripaldi, 2002, 2010).

The Médanos Negros (Fig. 1), covering an area of ~1000 km^2 and associated with a saline ephemeral lake (Salinas de Mascasín), are bounded to the north and east by alluvial deposits and to the west by the Sierra de Valle Fértil and Sierra de Guayaguas, where Proterozoic–lower Paleozoic plutonic and metamorphic rocks capped by Triassic–Cretaceous strata are exposed. This dune field receives ~370 mm of precipitation, strongly concentrated in the summer when maximum temperature reaches 32°C, resulting in a dense vegetation cover of shrubs and trees casting shadows on the dunes that thus appear dark (hence the name *Negros*, black). Wind data show a strong northeasterly component with resultant drift potential to the south. A regular pattern of W/E-trending transverse dune ridges showing steeper faces to the south, with ~50 m of relief and spaced ~2–4 km apart, are locally incised by drainage and covered by coarse colluvium. Superposed on this undulating topography are 5–10 m-high, NW/SE-trending transverse dunes facing to the SW/SSW and extending westwards and southwards with sinuous crests commonly modified by coppice dunes. Linear dunes 3–5 m-high, 20–30 m-wide, and 100 m-long grown on salt-lake deposits commonly occur in the northeast (Tripaldi and Forman, 2007).

The Médanos Grandes cover an area of 732 km^2 and are bounded to the north by the up to 3100-m-high Sierra de Pie de Palo. This much drier dune field records a mean annual precipitation of only 91 mm, concentrated between October and March when temperatures may exceed 40°C. Wind data show a strong southerly to southwesterly component, with resultant drift potential to the NNW (Fig. 3B). Transport of windblown sand is hindered by scattered trees, shrubs, and grasses (Pastran, 2012). Up to 50-m high and > 5 km-long parallel dune ridges are spaced between 250 m and ≥ 1.5 km and are oriented NNW/SSE in the northwest (Fig. 1A). Transverse dunes show steeper faces to the NNE in the north but to the SSW in the south, indicating opposite wind directions. Superposed are NW/SE-trending smaller linear dunes, forming a complex assemblage of landforms at a variety of scales that suggest multiple episodes of eolian deposition/reactivation. Blowout dunes ≤ 1 km in diameter with asymmetric ≤ 50-m-deep hollows indicating southeasterly paleowinds occur in the central area. The dune field is surrounded by a lower-relief rolling surface mainly formed by N/S- to NW/SE-trending linear dunes subsequently modified by coppice dunes (Tripaldi and Forman, 2007, 2016).

High-relief (50 m) parallel ridges of dominantly longitudinal dunes and asymmetric transverse dunes also occur in the Altos Limpios-Telteca dune field occupying the northern part of the Mendoza Province. In the San Rafael plain of the southern Mendoza Province, eolian sand covers an area > 25,000 km^2 with dunes of diverse size partially stabilized by vegetation and intersected by ephemeral lacustrine or fluvial deposits, especially along the Diamante and Atuel river courses. The Naranjos and Picardo dune fields are dominated by transverse dunes and megadunes with NE/SW-trending crests and steep faces toward the W/NW. Superposed smaller dunes display NW/SE-trending crests facing to the SW. Transverse, longitudinal, and large parabolic dunes, in relative age order, characterize the Travesía and Varita dune fields (Tripaldi, 2010).

The San Luis paleo-dune field in the southern half of the San Luis Province represents the northwestern part of the Pampean Sand Sea, mantled by well vegetated and stabilized eolian sand showing different degrees of deflation and reworking in the form of blowouts and small parabolic dunes. Annual precipitation (~700 mm) and mean temperature (17°C) support a Savannah-type vegetation with surface soils. Wind data show dispersed components from the NE to SE, with resultant drift potential to the NNW (Tripaldi and Forman 2007, 2016).

The Central Pampean dune field occupies a ~600-km-wide distal eastern area in the La Pampa and Buenos Aires Provinces (Fig. 1B; Iriondo and Kröhling, 1995). Parallel ridges up to 50-m-high of dominantly longitudinal (*seif*) dunes with NW/SE to NNW/SSE-trending crests associated with asymmetric transverse dunes indicate two interacting wind systems. In the SE, the sand sea is characterized by 100–130 km-long and 2–3 km-wide, low-relief linear dunes with flooded interdune strips. Linear dunes with N/NE-trending crests, suggesting predominantly westerly to southwesterly paleowinds and associated with large parabolic dunes in the south (Malagnino, 1989), grade eastwards to very fine sand-sheet and loess deposits of the Pampa deprimida (Fig. 2; Zárate and Blasi, 1993).

3.4. The La Pampa High and the Valles Transversales

As part of the retroarc basin, a low relief (~300 m a.s.l.) structural high stands out in the plain of the La Pampa Province between 35°and 39°S, at a distance of ~400 km from the Andean front (Fig. 1). Delimited by faults along both sides, this relief is known as La Pampa High or Central Block and is interpreted as a flexural uplift generated during a post-Miocene compressional phase (Folguera and Zárate, 2011, 2018; Nivière et al., 2013). A series of six major depressions, 60–100 km-long with general SW-NE trend, 1–2 km-wide, and 80–100 m-deep cut across the structural high and are known as "Valles Transversales" (Malagnino, 1989; Calmels, 1996) (Fig. 2). These landforms have been interpreted as paleo-vallyes carved into upper Miocene deposits by major rivers with large catchments, and their westward-sloping western part has been ascribed to flexural tilting after fluvial abandonment (Nivière et al., 2013). The southernmost valley, extending as far as the Atlantic coast at Bahía Blanca and representing the eastern continuation of a dry Colorado paleo-valley with similar width, is widely interpreted as a former course of the Colorado River (e.g., Perillo et al., 2001; Spalletti and Isla, 2003). The northern valleys were instead considered as formerly occupied by the Desaguadero River (Malagnino, 1988). The main Utracán-Vallimanca alignment, directed northeastwards across the La Pampa and Buenos Aires Provinces along the Depresión Diagonal north of the Ventania and Tandilia ranges (Fig. 1), was also considered as a former valley of a major river (Frenguelli, 1956; Martínez, 1987). An alternative view is that the Valles Transversales never represented river courses but were created entirely by wind erosion, because these corridors of wind transport lack any evidence of Pleistocene fluvial sediments (Tripaldi et al., 2018a).

In the Valles Transversales, wind-dominated activity is documented throughout the last ~30 ka (Mehl et al, 2018), blowouts may locally expose the Sierras Pampeanas basement, and the only fluvial sediments were deposited by local ephemeral creeks in the latest Pleistocene-Holocene. A series of elongated dune corridors are formed by up to 40-m-high, complex parabolic megadunes with 3–13 km-long, SW/NE-oriented trailing arms, superposed by barchanoid ridges and blowout dunes. The position of dune noses and orientation of dune arms indicate a mean transport direction toward 68°N, in accordance with regional southwesterly winds (Tripaldi et al, 2018a).

4. Overview of previous provenance research

In his pioneering study, Teruggi (1957) documented the peculiar volcaniclastic origin of eolian sediments in central Argentina, testified by abundant and commonly zoned plagioclase (labradorite and andesine with minor oligoclase and albite), mafic to felsic volcanic rock fragments, and low quartz (2-30%) and K-feldspar. Heavy-mineral suites (mostly accounting for 0.7-1.5% and up to 6% of bulk sediment) were described as dominated by Ti-rich magnetite, amphiboles (fresh green or green-brown hornblende and minor oxyhornblende) and pyroxenes (weakly pleochroic hypersthene and mostly dark green augite), with minor epidote-group minerals, garnet, rare zircon, tourmaline and rutile, and no apatite. Volcanic glass shards were reported to increase markedly in the silt fraction of loess deposits, with montmorillonite as the dominant clay mineral. Provenance largely from Andean pyroclastic rocks was thus inferred, with negligible local contribution from quartzites and other metamorphic or sedimentary rocks of the Ventania and Tandilia ranges (Fig. 1).

Pampean eolian deposits have long been considered as fed by major rivers draining the Andes (Iriondo, 1990), where large valley glaciers developed during the last Pleistocene glaciation (Clapperton, 1993). Huge amounts of water were released during final melting of the Cordilleran ice sheet, when sediment-laden rivers flowed eastwards in much wider valleys than today. Zárate and Blasi (1993) suggested that detritus generated in the northern Patagonian Andes and northern extra-Andean Patagonia was deposited in the floodplain of the Colorado and Negro rivers, deflated by southwesterly winds, and eventually accumulated in the southern part of the La Pampa and Buenos Aires Provinces. Iriondo (1994) favoured the Bermejo-Desaguadero-Atuel river system as the main supplier of sand to the Pampean Sand Sea to the north.

Etchichury and Tófalo (2004) traced the petrographic and heavy-mineral signatures of fluvial and eolian sediments across a vast lowland area in central to northern Argentina. Sediments in the northern Santa Fe, Corrientes, and Entre Rios Provinces — dominated by rounded quartz derived from source rocks in Brazil and Uruguay with minor staurolite, kyanite, dravitic tourmaline, sillimanite, andalusite, and Fe-Ti-Cr opaque oxides — were sharply distinguished from the quartz-poor deposits of the southern San Luis, La Pampa, and Buenos Aires Provinces, rich instead in volcanic rock fragments, pyroxene, hornblende, and basaltic hornblende. Within the Buenos Aires Province, they identified a central zone broadly corresponding to the Depresión Diagonal (Fig. 1), characterized by higher heavy-mineral concentration. Plagioclase and blue-green hornblende were observed to be more common in the San Luis and Córdoba Provinces closer to basement exposures of the Sierras Pampeanas.

Szelagowski et al. (2004) carried out a provenance study of upper Pleistocene to recent dunes developed along the Valles Transversales and concluded that fine to medium sand containing abundant feldspars and commonly altered volcanic rock fragments together with variable amounts of heavy minerals (augite, hypersthene, both magmatic and metamorphic amphibole, plus sporadic olivine, garnet, epidote, zircon, tourmaline, Cr-spinel, apatite, or staurolite) was supplied by the Desaguadero River as well as by local rock outcrops of Permian-Triassic Choiyoy magmatic rocks and the Payenia volcanic field. Repeated episodes of reworking and erosion were inferred from the observed abundance of rounded detrital grains.

The petrographic and geochemical study by Tripaldi et al. (2010) investigated sand provenance in the M. Negros, M. Grandes and San Luis dune fields, and the relationships with Pampean loess. The mainly litho-quartzo-feldspathic M. Negros sands were considered, also based on mafic trace-element composition, to be chiefly derived from ultramafic-mafic lithologies of the Sierra Pampeanas. The mainly quartzo-feldspatho-lithic M. Grandes sands, containing both volcanic and metamorphic rock fragments and characterized by felsic trace-element composition, were inferred to be supplied from metamorphic and igneous rocks of the Sierras Pampeanas and pre-Quaternary volcanic rocks, plus direct input from Andean explosive volcanism. The mainly feldspatho-quartzo-lithic San Luis sands — containing fresh pumice and glass shards and displaying felsic trace-element composition — were held to be derived from Andean volcanic sources and local metamorphic and igneous rocks. The observed broad petrographic and geochemical similarities led Tripaldi et al. (2010) to suggest a common source for eolian sand and Pampean loess, the latter considered to be chiefly generated by eolian abrasion in western Pampean dune fields. A further petrographic and geochemical study on eolian dunes of the San Luis Province by Forman et al. (2014) highlighted the homogeneous composition of Holocene sands and their similarity as Upper Pleistocene sands, suggesting that the former may have been largely recycled from the latter.

Tripaldi et al. (2017) determined the feldspatho-lithic to quartzo-feldspatho-lithic volcaniclastic composition of eolian sand close to the Colorado River in the southern Mendoza Province. Tripaldi et al. (2018b) reported the abundance of volcanic rock fragments (felsic, intermediate, and mafic types with minor vitric or pyroclastic grains), associated with mostly monocrystalline quartz and feldspars in the central part of the Buenos Aires Province. They noted that grains are more rounded than in dunes of the San Luis and La Pampa Provinces, quartz and K-feldspar being mostly subangular to subrounded whereas lithic fragments and plagioclase are mainly rounded to well rounded. Sand was held to be dominantly derived from the Andean Cordillera *via* the Desaguadero trunk river and then multiply reworked by winds in the lowlands.

Based on U-Pb ages of detrital zircons, Capaldi et al. (2019) outlined the progressive mixing of fluvial sources in the M. Grandes to M. Altos Limpios/Telteca dune fields, testified by the northward-increasing abundance of zircon grains older than 380 Ma. Mixing-model calculations indicated that zircon contribution from the Bermejo River decreases southwards from 64% to 18% while supply from the Mendoza River increases from 14% to 56%, the rest being chiefly accounted for by the San Juan River. Bruner et al. (2022) also used U-Pb ages of detrital zircons as provenance tracers across the Pampean Sand Sea, from the Río Desaguadero to the Atlantic Ocean. The results of these two detrital-geochronology studies complement our newly obtained dataset and will be discussed in section 7 below.

5. Methods

In this study, we carried out framework-petrography and heavy-mineral analyses of 27 samples of eolian-dune sands, 13 collected in July 2017 and August 2018 in the Andean retroarc basin (six in the Médanos Grandes and one each in the Negros, Altos Limpios, Telteca, Travesía, Naranjos, Picardo, and Varita dune fields) and 14 previously collected in the Pampean Sand Sea (five in the San Luis Province, three at the northeastern corner of the La Pampa Province, four close to or within the La Pampa High, and two in the Buenos Aires Province) (Fig. 1). Newly studied eolian-dune samples cover an area of ~250,000 km^2, extending from ~31°20'S to ~37°20'S and from ~68°W to ~62°20'W. To assess the provenance of eolian sand in diverse dune fields, the obtained results are compared with detrital modes of 40 sand samples collected from active bars of rivers draining the Andes between Tinogasta (~28°S) and Lake Nahuel Huapi (41°S) and 14 coastal sediments of the Buenos Aires Province including Ombucta corridor dune sand, Río Salado silt, and Río de la Plata beach sands (Fig. 2), all analysed with the same methodological approach (Garzanti et al. (2021a, 2021b). Furthermore, 24 selected samples were analysed for U-Pb detrital zircon geochronology: 17 eolian dunes (including twelve from the Pampean Sand Sea and one each from the Negros, Travesía, Naranjos, Picardo, and Varita dune fields) and 7 river bars (including the Desaguadero and its tributaries Tunuyán, Diamante, and Atuel). Full information on sampling sites is provided in Appendix Table A1 and in the Google Earth™ file *ArgenDunes.kmz*.

5.1. Framework petrography and heavy minerals

An aliquot of each sand sample was impregnated with araldite epoxy and cut into a standard thin section. Petrographic analyses were carried out by counting 450 points on each thin section by the Gazzi-Dickinson method (Ingersoll et al. 1984). Sand classification was based on the relative abundance of the three main framework components quartz (Q), feldspars (F), and lithic fragments

(L), considered if exceeding 10%QFL. According to standard use, the less abundant component goes first, the more abundant last (e.g., a sand is named quartzo-litho-feldspathic if F > L > Q > 10%QFL). Fifteen fields are thus defined in the QFL plot (Garzanti, 2019a). Rock fragments were classified based on mineralogy, texture, and metamorphic rank according to Garzanti and Vezzoli (2003). Median grain size was determined in thin section by ranking and visual comparison with in-house standards of sieved $\phi/4$ classes.

Heavy-mineral analyses were carried out on bulk samples for clean and well sorted dune samples and on the > 15 µm fraction obtained by wet sieving for the M. Negros and Pampean dune samples containing up to 20% of fine silt (< 15 µm). The weight percentage of the discarded fine and coarse tails of the size distribution is indicated in Appendix Table A3. From a split aliquot of each sample, the dense-mineral fraction was separated by centrifuging in Na-metatungstate (density 2.90 g/cm^3) and recovered by partial freezing with liquid nitrogen. To minimize overestimation of smaller grains, ≥ 200 transparent heavy minerals were point-counted at suitable regular spacing on each grain mount (Garzanti and Andò, 2019).

Transparent heavy-mineral assemblages, called for brevity “tHM suites” throughout the text, are defined as the spectrum of detrital extrabasinal minerals with density >2.90 g/cm^3 identifiable under a transmitted-light microscope; opaque or altered grains, carbonates, and slow-settling phyllosilicates are excluded. According to the concentration of transparent heavy minerals (tHMC index, expressed as a percentage of total sediment), tHM suites are described as “poor” (tHMC < 1), “moderately poor” (1 ≤ tHMC < 2), “moderately rich” (2 ≤ tHMC < 5), “rich” (5 ≤ tHMC < 10), or “very-rich” (10 ≤ tHMC < 20). Mineralogical parameters used in this article include the Cpx/Px (clinopyroxene/pyroxene) ratio. The ZTR index (sum of zircon, tourmaline, and rutile over total tHM; Hubert 1962) expresses the durability of the tHM suite through multiple sedimentary cycles (Garzanti, 2017). The Amphibole Colour Index [ACI = (1/3 green + 2/3 green/brown + brown amphibole)/total amphibole x 100; Andò et al., 2014] varies from 0 in detritus from low-grade metamorphic rocks yielding exclusively blue/green amphibole to 100 in detritus from granulite-facies or volcanic rocks yielding exclusively brown amphibole or oxyhornblende. Significant minerals are listed in order of abundance (high to low) throughout the text. The complete petrographic and heavy-mineral datasets are provided in Appendix Tables A2 and A3.

5.2. U–Pb geochronology

From each of the 24 selected samples, non-magnetic heavy-mineral fractions obtained with standard techniques (water table, dense liquids, magnetic separator) were poured onto double sided tape (2.54 cm) on epoxy resin mounts. At least 120 zircon grains were chosen randomly, targeting non-broken, inclusion-free grains. Zircon U-Pb ages were determined by laser ablation-inductively coupled plasma-mass spectrometry (LA-ICP-MS). Full analytical information is provided in Appendix B. Zircon U-Pb ages and 2σ errors are reported for analyses with < 10% $^{206}Pb/^{238}U$ discordance, < 20% discordance, and < 5% reverse discordance. Reported values for grains < 850 Ma are $^{206}Pb/^{238}U$ ages with $^{206}Pb/^{238}U$ vs. $^{207}Pb/^{235}U$ discordance, whereas values for grains > 850 Ma are $^{207}Pb/^{206}Pb$ ages with $^{206}Pb/^{238}U$ vs. $^{207}Pb/^{206}Pb$ discordance. Filters for Miocene zircons (< 23 Ma) were expanded to incorporate ages with < 20% $^{206}Pb/^{238}U$ discordance and < 50% $^{206}Pb/^{238}U$ discordance, to prevent biasing due to exclusion of young grains with higher ^{207}Pb and associated calculated $^{207}Pb/^{235}U$ ages that are systematically older than measured $^{206}Pb/^{238}U$ ages. Overall, 2890 concordant ages were obtained. The compilation of 10,339 U-Pb zircon ages presented in Appendices B1 and B2 contains new as well as previously published analyses from Pepper et al., (2016), Capaldi et al. (2017, 2019, 2020) and Bruner et al. (2022) on 76 samples overall (36 eolian and 40 fluvial sediments).

5.3. Statistical analysis and graphical displays

Preliminary provenance inferences were made by comparing detrital modes of river and dune sands with similarity analysis. Similarity metrics is a mathematical technique used to compare objects, measure numerical distances between them, and identify objects belonging to the same cluster. The similarity between detrital modes of a sediment sample and various reference compositions can be simply assessed by the coefficient of determination R^2 obtained by the regression method (Vezzoli and

Garzanti, 2009).

The relative contribution of each potential source (provenance budget) was evaluated mathematically with forward mixing models based on integrated petrographic and heavy-mineral data (Weltje, 1997; Garzanti et al., 2012). Terrigenous sediments (dunes in this case) are mixtures of numerous detrital components supplied in various proportions by different potential end-member sources (rivers in this case). The forward mixing model calculates a row vector of compositional data as a non-negative linear combination between a matrix of fixed end-member compositions and a row vector of coefficients representing the proportional contribution of each end member to the observation. The robustness of the calculations is guaranteed only if the end-member signatures of each potential source are well distinct and precisely assessed with little variability dependent on grain size, weathering, or hydraulic sorting. Additional information on the method and its limitations is contained in Appendix A and Resentini et al. (2017).

Statistical techniques used to illustrate our datasets include the compositional biplot (Gabriel, 1971; Aitchison and Greenacre, 2002) and multidimensional scaling (MDS; Vermeesch, 2013; Vermeesch and Garzanti, 2015). The compositional biplot (drawn using CoDaPack software by Comas-Cufí and Thió-Henestrosa, 2011) allows us to discriminate among multivariate observations (points) while shedding light on the mutual relationships among multiple variables (rays). The length of each ray is proportional to the variance of the corresponding variable: if the angle between two rays is 0° or 180°, then the corresponding variables are perfectly correlated or anticorrelated. MDS analysis produces a map of points in which the distance among samples is approximately proportional to the Kolmogorov-Smirnov dissimilarity of their compositional or chronological signatures. Closest and second-closest neighbours are linked by solid and dashed lines, respectively, and the goodness of fit is evaluated using the “stress” value of the configuration (20 = poor; 10 = fair; 5 = good; Kruskal, 1964). The *provenance* package of Vermeesch et al. (2016) was used to plot MDS maps and U-Pb age distributions as kernel density estimates (KDE).

6. Sand petrography and heavy minerals

This section provides a summary of data previously obtained on sand composition in the Desaguadero, Colorado and Negro rivers, in their diverse tributaries draining the Andes, and in coastal sediments of the Buenos Aires Province (Garzanti et al., 2021a, 2021b). The mineralogy of eolian sand in diverse Argentine dune fields is next illustrated in detail. Finally, the diverse environmental factors that may have altered the original provenance signals are critically examined. Key compositional parameters are provided in Table 1.

6.1. River sands

Sediments generated in the Andes and fed into the retroarc basin are largely derived from subduction-related mesosilicic volcanic rocks of the Cordillera. They consequently share broadly similar composition, characterized by volcanic rock fragments, plagioclase, and moderately rich to rich tHM suites including clinopyroxene, orthopyroxene, and amphibole in different proportions (Fig. 4). Despite several similarities, however, sediments carried by major river systems can be confidently discriminated. Sand ranges from litho-feldspatho-quartzose in the north, where sedimentary lithics are common (Bermejo River), to quartzo-feldspatho-lithic in the center (e.g., Jáchal, San Juan, Mendoza, and Tunuyán rivers), and to feldspatho-lithic volcaniclastic in the south (e.g., Atuel, Barrancas, Neuquén, and Limay River) (Fig. 5A). The abundance of quartz, K-feldspar, and sedimentary to low-rank metasedimentary rock fragments reaches maximum in correspondence with the Pampean flat-slab segment where volcanism is inactive, whereas volcanic detritus from the Cordillera Principal and Payenia lavas becomes overwhelming southwards.

Trends displayed by tHM suites are even sharper, changing from amphibole $\gg$ pyroxene in the north, to amphibole $\approx$ clinopyroxene $\approx$ orthopyroxene in the middle, and to orthopyroxene $\geq$ clinopyroxene $\gg$ amphibole in the south (Fig. 5B). Amphibole is dominantly of volcanic origin (brown titanian pargasite, magnesio-hornblende, and oxyhornblende; Deruelle, 1982; Pinto et al., 2018), although blue-green hornblende from basement rocks of the Sierras Pampeanas is nearly as abundant as magmatic amphibole in Bermejo river sand. Clinopyroxene composition straddles the augite/diopside boundary and orthopyroxene composition the bronzite/hypersthene boundary (Borromeo et al., 2022).

Amphibole accounts for nearly half of the tHM suite in Abaucán, Bermejo, San Juan, and Mendoza river sands, decreases in Tunuyán sand, represents a fifth of the tHM suite at most in Atuel sand and Colorado catchment, and a tenth of the tHM suite in the Negro catchment. The southward decreasing amphibole content in sand of southern rivers mirrors the distribution of hornblende-bearing andesites in the Southern Volcanic Zone, which are abundant between 33°S and 34°S and scarce between 36° and 41°S (Hickey et al., 1986). Conversely, orthopyroxene increases southwards, being minor in the Bermejo and San Juan catchments and representing about a tenth of the tHM suite in the Abaucán and Mendoza catchments, a third to half of the tHM suite in the Tunuyán, Atuel, and Colorado catchments, and up to more than half of the tHM suite in the Negro catchment. Clinopyroxene percentages are much lower in Bermejo sand than in San Juan sand, highly variable in Jáchal and Mendoza sands, increase progressively southwards from Tunuyán sand to Atuel and Colorado sand, to finally decrease in the Negro catchment. Olivine, negligible in the north, increases southwards from the Diamante to the Negro catchments (Table 1).

Sand shed from the Sierra de Pie de Palo has highly distinct feldspatho-litho-quartzose composition with abundant high-rank metapelite, metapsammite, and amphibolite rock fragments, common muscovite and biotite, and very rich tHM suites dominated by mostly blue-green hornblende and garnet, with minor epidote and rare kyanite (Table 1).

Along the Desaguadero mainstem, sand composition becomes feldspatho-litho-quartzose downstream of the Tunuyán confluence, and eventually quartzo-feldspatho-lithic upstream of the Atuel confluence (Fig. 5). The moderately poor to moderately rich tHM suite contains subequal amounts of clinopyroxene, orthopyroxene, and amphibole (mainly green-brown hornblende) with minor epidote, garnet, and zircon.

6.2. Coastal sediments

Because of limited long-term sediment-storage capacity of the retroarc basin, masses of volcaniclastic detritus have been transferred through time by rivers from the Andean magmatic arc to the Atlantic passive margin, thus creating a long-recognized mismatch between the tectonic setting of the source and the tectonic setting of the sink (Potter, 1984). The Negro River carries to the Atlantic Ocean feldspatho-quartzo-lithic sand with abundant plagioclase and volcanic rock fragments, which is dispersed by longshore currents both north and south of the mouth. The moderately rich tHM suite contains mostly orthopyroxene and clinopyroxene, with epidote and minor olivine and amphibole (Fig. 5).

The Colorado River carries quartzo-feldspatho-lithic volcaniclastic sand with a similar tHM suite but notably higher Cpx/Px ratio and minor garnet. The same signature characterizes eolian dune sand of the Ombucta corridor (Fig. 2) and beaches of the Buenos Aires Province as far north as Mar del Plata city, where the Tandilia range intersects the coast and sand is enriched in quartz derived locally from erosion of coastal cliffs (Fig. 6A). Farther north, fine silt carried by the Salado River to muddy Samboronbón Bay yields a moderately poor tHM suite notably richer in amphibole. A similarly amphibole-rich tHM suite characterizes beaches of the Río de la Plata Estuary east of Buenos Aires, which consist of very fine-grained litho-quartzo-feldspathic volcaniclastic sand. At the western edge of Buenos Aires city, instead, pure quartzose beach sand is supplied by the Paraná River, although the extremely poor tHM suite is still dominated by Andean-derived amphibole and clinopyroxene (Fig. 6B).

6.3. Eolian dunes

The Médanos Negros contain plagioclase-rich feldspatho-quartzose sand (Fig. 4A) with a rich tHM suite dominated by amphibole (mostly green-brown and subordinately blue-green hornblende with minor oxyhornblende), associated with orthopyroxene and minor garnet, clinopyroxene, and epidote (Fig. 5). The Médanos Grandes consist of litho-feldpatho-quartzose volcaniclastic sand in the central and eastern parts (Fig. 4B), and of less quartz-rich sand (Q ≈ F ≈ L) along the western edge of the dune field, where felsic volcanic rock fragments are more common (Fig. 4C). The tHM suites range from moderately rich in the north to mainly moderately poor in the south and include amphibole (mainly green-brown hornblende) with subordinate clinopyroxene, garnet, epidote, and minor orthopyroxene. In the M. Grandes, epidote and especially garnet (which reaches maximum in the northwest) are notably more abundant, and the Cpx/Px ratio much higher, than in any other dune field (Table 1; Fig. 6B). Amphibole tends to relatively increase southwards (with the ACI slightly decreasing both eastwards and southwards), whereas ZTR minerals and apatite relatively increase westwards.

Farther south, eolian sand ranges from quartzo-feldspatho-lithic in the Altos Limpios-Telteca dune field (Figs. 4D and 4E) to quartzo-litho-feldspathic in the Travesía dune field (Fig. 4F). Both felsic and mafic volcanic rock fragments occur and moderately rich tHM suites contain subequal amounts of amphibole, clinopyroxene, and orthopyroxene (Fig. 5B). Relative to the Médanos Grandes, pyroxene (especially orthopyroxene) increases at the expense of amphibole, garnet, and epidote (Table 1). ZTR minerals are rare, and a few olivine grains occur.

Quartz decreases further in feldspatho-lithic Naranjos and Picardo dunes (Figs. 4G and 4H) or litho-feldspathic Varita dunes (Fig. 4I), where volcanic rock fragments are mostly intermediate to mafic. The rich tHM suites mainly consist of orthopyroxene and subordinate clinopyroxene (Fig. 5B). Amphibole is common in Naranjos dunes north of the Diamante River but minor south of the Atuel River. Orthopyroxene and the ACI are higher in the south and reach highest values in Picardo dunes.

In the Pampean Sand Sea, from the San Luis to the Buenos Aires Province, dune sand displays notably homogeneous quartzo-litho-feldspathic to quartzo-feldspatho-lithic composition, with mainly microlitic to lathwork volcanic and subordinate sedimentary to very-low-rank metasedimentary and metavolcanic rock fragments (Fig. 5A). The tHM suites are moderately rich with subequal amounts of amphibole, clinopyroxene, and orthopyroxene. Epidote is minor, garnet and zircon very minor, and tourmaline and olivine rare. Staurolite, kyanite, and sillimanite are lacking. Amphibole decreases southwards toward the La Pampa High and the tHM suite of the Valle Daza dune dominantly consists of orthopyroxene and clinopyroxene, with minor amphibole and garnet, and rare olivine (Table 1).

6.4. Evaluating environmental bias

Detrital modes depend on the mineralogy of source rocks but may also reflect textural control or physical and chemical processes in the sedimentary environment. Before performing forward-mixing calculations or using statistical tools for provenance analysis, the dataset must be inspected carefully to assess the importance of grain-size effects, wind-sorting, weathering and mechanical abrasion, and thus identify possibly anomalous sample compositions.

Major grain-size-dependent intersample variability is not expected for the studied dune samples, which display remarkably consistent texture (mean diameter 3.0 ± 0.4ϕ). Around the La Pampa High, dunes are slightly coarser than in the Central Pampean dune field in the north (2.8 ± 0.2ϕ *versus* 3.4 ± 0.2ϕ), plausibly as an effect of deflation by southwesterly winds (Tripaldi et al., 2018a). Also, the F/L ratio tends to increase with decreasing grain size, but a similar trend is not observed in other dune fields. No significant grain-size control on tHM suites was detected.

A parameter most useful to check for hydrodynamic concentration of denser minerals during erosion, transport, or deposition is the weighted average density (g/cm^3) of terrigenous grains (SRD index of Garzanti and Andò, 2007), which for each sample should be equal to the weighted average density of source rocks in the absence of environmental bias (Garzanti et al., 2009). This index is remarkably constant among samples collected in the Médanos Grandes to the north (SRD 2.68 ± 0.01) and increases consistently in Travesía and Pampean dunes (SRD 2.71 ± 0.01), in two dunes collected in the Valles Transversales (both SRD 2.73), and in the Naranjos, Picardo, and Varita dunes to the south (SRD 2.75 ± 0.01). These values faithfully reflect southward increasing detritus from denser intermediate to mafic volcanic rocks at the expense of detritus from less dense sedimentary and very-low-grade metasedimentary rocks. Major hydraulic-sorting-dependent variability can thus be safely excluded. Minor effects of wind deflation, locally causing subtle enrichment in ultradense opaque Fe-Ti-Cr oxides and garnet, with corresponding depletion in less dense and platier amphibole grains, may be suggested for a few Pampean dunes (samples E6038, E6043, and E6049 in Table 1).

Mineralogical modifications caused by chemical weathering can be considered as minimal, because of dominantly physical erosion in the Cordillera and arid climatic conditions in the Andean piedmont.

Selective mechanical breakdown may have affected only the softest grains (Garzanti et al., 2015, 2017). These include calcareous rock fragments, which are less abundant in eolian sands (0.6 ± 0.4% of total grains in the M. Grandes and M. Altos Limpios dunes, undetected elsewhere) than in river sands (1−1.5% in the Bermejo, Jáchal, and Pie de Palo catchments; 1.5−2% in the Tunuyán, Diamante, and Atuel catchments; 2−3% in the San Juan catchment, 3−4% in the Mendoza catchment, and 4−5% in the Colorado catchment). The large majority of clasts range from angular to subrounded at most (Fig. 4), testifying to a minor role played by mechanical abrasion. This is best highlighted by the widespread preservation even of most fragile fragments such as fresh pumice and glass shards (Teruggi, 1957; Tripaldi et al., 2010), which challenges the long-held idea that high-energy ballistic impacts in wind-dominated environments lead to extensive breakdown of feldspars and rock fragments, and consequent quartz enrichment and "maturation" (as in Dutta et al., 1993, or in Muhs, 2004).

7. U-Pb ages and provenance of zircon grains

The results discussed in this section are based on new geochronological data on 7 river sands and 17 eolian-dune sands, as well as on literature data on 33 fluvial and 19 eolian sediments (Pepper et al., 2016; Capaldi et al., 2017, 2019, 2020; Bruner et al., 2022). Selected and composite age spectra are presented in Figs. 7, 8, and 9; the full dataset is provided in Appendix B.

7.1. River sands

River sands display marked differences in the U-Pb age spectra of detrital zircons, especially between northern catchments (i.e., Bermejo, Pie de Palo, San Juan), where Stenian ages typically represent ~20% of total ages and Pliocene-Quaternary zircons are lacking, and southern catchments, where Stenian ages invariably account for < 10% of total ages and Miocene to Quaternary zircons invariably occur and are locally dominant (Fig. 8).

The bimodal age spectrum of zircon grains in the stream draining the Pie de Palo basement block of the Sierras Pampeanas displays major Stenian and subordinate Ordovician peaks. The multimodal spectrum of Bermejo sand includes major Ediacaran-Ordovician (33% of total ages) and Carboniferous-Triassic (23%) clusters, plus some Cenozoic ages (6%). The spectrum of San Juan river sand is similarly multimodal but with a reversed proportion of Ediacaran-Ordovician (19%) and Carboniferous-Triassic (31%) clusters, and more common Cenozoic ages (12%). A simpler spectrum characterizes Mendoza river sand, where 77% of zircon ages are Carboniferous to Triassic indicating major contribution from felsic igneous rocks of the Choiyoi igneous complex (Fig. 8).

To the south, Quaternary zircon grains derived from the active Southern Volcanic Zone (7%) appear in Tunuyán river sand, characterized by Stenian, Devonian (~380 Ma), and Permian-Triassic age peaks. Quaternary ages increase progressively southwards in Diamante (9%) and Atuel (12-13%) river sands, also characterized by abundant Miocene ages (33% and 43% respectively) and minor Permian and Jurassic clusters.

Desaguadero river sand is characterized by a polymodal spectrum with a main Permian-Triassic peak (290-237 Ma; 25% of total ages) and Stenian (8%), Ordovician (7%), Devonian (12%), and Miocene (12%) clusters; ages younger than 4 Ma are lacking. Only a few Miocene to Quaternary zircons (≤ 6%) occur in Colorado river sand, which is characterized by a polymodal spectrum with common Cretaceous (6-26%), Jurassic (6-21%), Permian (7-24%), and Devonian ages (10-14%); older ages are mainly Cambrian-Ordovician (6-14%) (Pepper et al., 2016; Bruner et al., 2022). Age spectra are similar in sand of the Negro River and of its Neuquén and Limay branches farther south, where Miocene to Quaternary zircons (mostly ≤ 5%) are less common than Cretaceous (6-15%), Jurassic (12-19%), Permian (7-21%), and Devonian grains (≤15%); older ages are mainly Stenian (4-9%) (Pepper et al., 2016; Bruner et al., 2022).

7.2. Retroarc-basin dune fields

In northern retroarc-basin dune fields, most zircons yield Proterozoic to Paleozoic ages, and Pliocene-Quaternary zircons are lacking. U-Pb age spectra are radically different in southern dune fields, where most zircon ages are younger than 15 Ma (Fig. 7).

In the Médanos Negros, 68% of Cambro-Ordovician ages indicate that most zircon grains are ultimately derived from Famatinian arc rocks of the western Sierras Pampeanas. In the Médanos Grandes, half of zircon grains yielded Paleozoic and the other half largely Stenian ages, indicating mixed protosources including mostly Famatinian arc rocks and Pampia basement of the Sierras Pampeanas (Fig. 8). The proportion of Permian-Triassic zircon grains ultimately derived from Choiyoi igneous rocks largely exposed in the Cordillera Frontal is significant, and greater in the northeastern and southern parts of the dune field. No zircon age < 7 Ma was obtained.

Stenian and Cambro-Ordovician ages decrease progressively southwards in the Altos Limpios-Telteca dune field and Permian-Triassic ages correspondingly increase further, indicating increasing zircon contribution from Choiyoi igneous rocks at the expense of supply from the Sierras Pampeanas (Fig. 8). Farther south, the proportion of Miocene zircons increases in the Travesía dune field (15%), where a few Pliocene-Quaternary grains occur (5%) and become prevalent in the Naranjos dune field (54%), where only 14% of ages are older than the Permian indicating predominant supply from recent Andean volcanic rocks south of 33°S. Younger and younger ages become overwhelming in the Picardo (41% Miocene, 1% Pliocene, and 15% Pleistocene) and Varita dune fields (20% Miocene, 7% Pliocene, and 37% Pleistocene), with only 11-12% of grains older than the Permian.

7.3. Pampean Sand Sea

In Pampean lowlands, U-Pb age spectra of detrital zircon are broadly homogeneous, polymodal, and characterized by Pliocene-Quaternary (7 ± 4%), Miocene (11 ± 4%), Jurassic-Cretaceous (10 ± 3%), Permian-Triassic (22 ± 3%), Devonian (8 ± 3%), Cambro-Ordovician (8 ± 3%), and minor Stenian clusters (5 ± 2%) (Figs. 7 and 9).

Eolian sediments in the middle Colorado Valley and near the Atlantic coast north of Mar del Plata city yielded notably more Jurassic-Cretaceous zircon ages (22 ± 3%) and somewhat less Miocene-Quaternary ages (11 ± 5% overall; Bruner et al., 2022). Eolian sediments collected near the Paraná River in the north display a rapid northward decrease in ages younger than the Cambrian (dropping from 62% to 9% in a few tens of km), and an abundance of ages ranging from Cambrian to Stenian (rising to 60%, half of which Ediacaran) and from Orosirian to Rhyacian (up to 22%; Bruner et al., 2022).

7.4. Distribution pattern of "zero-age" zircons

U-Pb dating of very young zircons is challenging because of low levels of radiogenic Pb that approach instrument detection capability (Kirkland et al., 2020). The very young ages obtained in this study may have large uncertainties and should thus be considered with real caution. Zircon grains yielding a U-Pb age < 1 Ma were found in Tunuyán (8 grains, 3 of which as young as ~100 ka), Diamante (14 grains, 11 of which younger than 100 ka), and Atuel river sands (12 grains overall in two samples, 6 of which younger than 100 ka) (Fig. 10). Among retroarc-basin dune fields, the youngest zircon grain in the Travesía, Naranjos, and Picardo samples resulted to be 1.2, 1.1, and 0.4 Ma old, respectively. The Varita sample yielded the largest percentage of < 1 Ma zircons by far (30 grains, 5 of which younger than 100 ka). In the Pampean Sand Sea, ages < 1 Ma are recurrent (132 out of 4504 grains from this study and Bruner et al., 2022, with no systematic difference observed between sand dunes and loess deposits). The youngest grains yielded ages of 140-150 ka in dunes and loess from the center-north and of 80-90 ka in loess from the southern Utracán-Vallimanca region and middle Colorado Valley (Fig. 10).

The occurrence of several zircon grains yielding U-Pb ages very close to zero in both fluvial and eolian sediments collected in the southern part of the studied region, where volcanism is active, solidly confirms the validity of the zircon-chronostratigraphy approach (Dickinson and Gehrels, 2009). The method, introduced to date unfossiliferous strata in forearc or retroarc regions, is here proved to have a potential accuracy not worse than the accuracy of the U-Pb technique.

8. Provenance of eolian sediments

The aim of this section is to identify the feeder systems of dune sand in central Argentina based on: a) quantitative assessment of the similarity between the detrital modes of each river and each eolian-dune sand; b) forward mixing models based on integrated bulk-petrography and heavy-mineral data; c) multidimensional scaling (MDS) analysis of zircon-age data.

Similarity and MDS analyses show with clarity that there are fundamentally three different groups of dune fields (Fig. 7). In the northern retroarc basin (M. Grandes and M. Altos Limpios-Telteca), eolian sand is dominantly derived from the Frontal Cordillera and Precordillera, and subordinately from the Sierras Pampeanas drained by the Bermejo River. In the southern retroarc basin (M. de los Naranjos, M. de Picardo, and M. de la Varita), sand is mostly derived from the active Southern Volcanic Zone drained by the Diamante and Atuel rivers, as testified by much more abundant plagioclase, volcanic rock fragments, and numerous zircon grains yielding Pliocene-Quaternary ages. Intermediate composition characterizes the Travesía dune field and Pampean Sand Sea, where eolian sand displays petrographic, heavy-mineral, and zircon-age signatures close to Desaguadero river sand. More subtle distinctions based on detrital fingerprints can be made, allowing us to tentatively reconstruct the complex late Quaternary evolution of drainage patterns across the Andean retroarc basin and shed light on landscape changes controlled by the interplay between tectonic activity and climate.

8.1. Negros and Grandes dune fields

Dune fields in the northern part of the retroarc basin are readily distinguished by their notably greater abundance of quartz and amphibole, and scarcity of orthopyroxene (Figs. 6A and 6B). The Negros dunes occupy a closed basin within the Sierras Pampeanas and their plagioclase-rich feldspatho-quartzose composition with scarce volcanic lithics and clinopyroxene (total volcanic detritus < 15% of bulk sand) is distinct from any studied river sediment (the closest match being Bermejo sand; Fig. 5). Provenance from Famatinian arc rocks exposed in the northwestern part of the broken retroarc basin is indicated by rich amphibole-dominated tHM suites with some garnet, and by a zircon-age spectrum with sharp unimodal peak at ~480 Ma and only two ages < 230 Ma (8 Ma and 80 Ma).

In the Médanos Grandes, sand mineralogy varies gradually from east to west and from north to south, indicating mixing of two main sediment sources, a northern source chiefly represented by the Bermejo

River, and a western source represented by the San Juan River with its southern Mendoza tributary (Fig. 5). Detrital modes more closely resemble sand of the Bermejo River, which contributed most eolian sand overall: ≥ 60% to northeastern dunes (where garnet abundance and slightly higher metamorphic indices reflect 5−10% supply from basement rocks of the Sierras Pampeanas) and ≥ 40% to northwestern dunes. This provenance estimate is supported by similarity analysis based on petrographic and heavy-mineral signatures, and by MDS analyses based on U-Pb zircon age spectra that underscore a greater affinity with Bermejo sand and to a lesser extent with San Juan sand (Fig. 8). The zircon-age spectrum of the northeastern dune is closer to that of the Pie de Palo stream sand, confirming greater contribution from the Sierras Pampeanas to the northeastern part of the dune field. The northwestern dune, instead, exhibits greater similarity as San Juan river sand, confirming greater sediment contribution from the San Juan River along the western side of the dune field.

In contrast with all other eolian sands plotting in the transitional arc field of Dickinson et al. (1983), the M. Negros and M. Grandes dunes plot in the continental block and dissected arc/mixed fields, respectively (Fig. 5A). Such a provenance diagnosis is fairly accurate and consistent with sediment supply dominantly from uplifted basement blocks of the Sierras Pampeanas for the Médanos Negros, and mostly from deeper-seated tectono-stratigraphic levels of the dissected Andean continental arc for the Médanos Grandes. A lack of zircon grains significantly younger than 7 Ma was systematically observed in both dune fields and all of their fluvial feeder systems (Fig. 10), reflecting the lack of Pliocene-Quaternary magmatism in the Pampean segment of very shallow-angle Nazca-plate subduction (Ramos and Folguera, 2009). This places a maximum age constraint for the cessation of major volcanic activity in the Pampean flat-slab segment at around 7 Ma.

8.2. Altos Limpios-Telteca and Travesía dune fields

Relative to the Médanos Grandes, the Altos Limpios-Telteca and Travesía dunes are notably richer in intermediate to mafic volcanic rock fragments and pyroxene (especially orthopyroxene), are poorer in quartz, amphibole, garnet and epidote, and show distinctly higher ACI and markedly lower Cpx/Px ratio (Figs. 6A and 6B). The Altos Limpios and Telteca samples have virtually the same mineralogy, but comparison with the Travesía sample collected south of the Tunuyán River, 150 and 200 km to the SSE, highlights a subtle but steady compositional gradient. From north to south, quartz, epidote, garnet, and amphibole progressively decrease, whereas tHMC, ACI and orthopyroxene increase, and olivine appears (Fig. 5).

Similarity analysis indicates affinities of detrital modes between the Altos Limpios dune and Desaguadero, Tunuyán, or San Juan river sands, between the Telteca dune and Tunuyán or Desaguadero river sands, and between the Travesía dune and Diamante, Desaguadero or Tunuyán river sands (Fig. 6). Altos Limpios-Telteca dunes lack zircons of Pliocene-Quaternary age and yielded only a few zircons of Miocene age (4%), indicating greater affinity with San Juan sand than with Tunuyán or Desaguadero sands (Fig. 8). The relative abundance of Carboniferous-Triassic zircon grains (34-37% of ages between 300 and 230 Ma) suggests significant zircon supply from the Mendoza River (increasing from ≤ 10% in the Altos Limpios dune to ≤ 20% in the Telteca dune). The Travesía dune sample yielded 6% of Pliocene-Quaternary-aged zircons, 15% of Miocene-aged zircons, and more Jurassic-Paleogene and less Carboniferous-Triassic and Stenian zircons than Altos Limpios-Telteca dunes, which best matches Tunuyán and Desaguadero sand downstream of the Tunuyán confluence (Fig. 8).

8.3. Naranjos, Picardo, and Varita dune fields

The Naranjos, Picardo, and Varita dune fields continue the mineralogical trend observed from north to south along the Andean retroarc basin, documenting a sharp increase in volcanic detritus from the Southern Volcanic Zone (Figs. 6A and 6B). Plagioclase, intermediate to mafic volcanic rock fragments, tHMC, ACI, and orthopyroxene all increase, whereas quartz and K-feldspar contents reach a minimum (5-8% and ≤ 1% of detrital grains, respectively), felsic volcanic lithics become rare, and amphibole, ZTR minerals, epidote, garnet, and apatite relatively decrease. Sand of these dune fields most closely resembles Atuel river sand; the Naranjos dune shows affinities also with Diamante and, to a lesser extent, Tunuyán sand. Forward mixing calculations suggest that the Naranjos dune is composed of 25-30% Tunuyán sand, ~20% Diamante sand, and 50-55% Atuel sand, that the Picardo dune is composed of ~35% Diamante sand and ~65% Atuel sand, and that the Varita dune consists virtually entirely of Atuel river sand. These three dune fields show no influence of the Desaguadero River that flows along their eastern flank, indicating no westward eolian sand transport.

Detrital zircon MDS analysis confirms the affinities among these three dune fields, which are all characterized by abundant Middle Miocene to Quaternary U-Pb ages (58-63% of total zircon grains) in sharp contrast with all other dune fields (Fig. 7). Overwhelming zircon supply from the Atuel River is indicated for the Picardo and Varita dunes, whereas contribution from the Diamante River is significant for the Naranjos dune.

8.4. Pampean Sand Sea

From the San Luis Province to the Buenos Aires Province, dune sand composition remains almost indistinguishably quartzo-feldspatho-lithic to quartzo-litho-feldspathic, testifying to the substantial unity of the Pampean Sand Sea. Across the ~1000-km-wide area from the Altos Limpios-Telteca and Travesía dune fields to the Río de la Plata beaches (Fig. 6), sand displays remarkably homogeneous tHM suites (tHMC 3.0 ± 0.6), with subequal amounts of amphibole (32 ± 3%tHM), clinopyroxene (27 ± 4%tHM), and orthopyroxene (31 ± 3%tHM), a characteristic they share with sand of the Desaguadero River and its Tunuyán and Diamante tributaries. Forward-mixing calculations suggest that sand in this vast area was originally generated entirely in the Desaguadero catchment, ~55% being accounted for by the mainstem including the Bermejo, San Juan, and Mendoza branches, and 15-20% each by the Tunuyán and Diamante tributaries.

Petrographic composition changes slightly in the La Pampa Province, where ACI values tend to be higher (Table 1), and more distinctly southwards close to the La Pampa High and in the Valles Transversales (Fig. 5A). Here amphibole decreases (being least abundant in the Valle Daza dune; Fig. 5B) and a few more garnet grains occur, suggesting stronger affinity with Atuel or Colorado river sand. The compositional signatures of dune sand in the Ombucta Corridor near Bahía Blanca city point at provenance mostly from the Colorado River (~90%), with possible minor contributions from the Desaguadero River (≤ 10%).

Additional clues on sand transport pathways are provided by detrital zircon U-Pb age spectra (Fig. 9). These confirm the close affinity between Travesía and San Luis dunes but also highlight the similarity among the southernmost San Luis dune, the two northernmost La Pampa dunes, and the two dunes west of the La Pampa High. These five samples (labelled *1*, *A*, *B*, *a*, and *b* in Figs. 7 and 9) are characterized by a greater abundance of Miocene-Quaternary zircons (21-29% *vs.* 9-19% in other Pampean dunes), indicating a greater contribution from the Southern Volcanic Zone along the western side of the Pampean Sand Sea.

Further provenance information is provided by literature data (Pepper et al., 2016; Bruner et al., 2022), which highlight the similarity between zircon-age spectra of Colorado river sand with eolian sediments in the middle Colorado Valley, in the southernmost part of the Central Pampean dune field along the Depresión Diagonal (Fig. 1; Utracán-Vallimanca alignment of Martínez, 1987), and near the Atlantic coast north of Mar del Plata city (Fig. 9). Sediment supply from the Colorado River in thus indicated in the southern part of the Buenos Aires Province (Zárate and Blasi, 1993) and dominant in eolian and beach sand all along the Atlantic coast north of Bahía Blanca city (Fig. 6; Garzanti et al., 2021b).

8.5. Río de La Plata beaches and Río Salado

Río de La Plata beaches have virtually identical tHM suites as eolian dunes across the Pampean Sand Sea (Fig. 6B), revealing that they are extensively recycled from eolian Pampean sediments. Beach sand gets richer in quartz westwards, which is ascribed to mixing with pure quartzose Paraná river sand in percentages that increase progressively from only 5−10% near the estuary mouth in the east, to 20% and 30% toward Buenos Aires, eventually exceeding 90% at the western edge of the city in front of the Paraná Delta.

The relative percentages of ferromagnesian minerals are remarkably similar and homogeneous in Río de La Plata beaches east of Buenos Aires (Cpx/Px 46 ± 3%, ACI 70 ± 6%) as in eolian sand of the San Luis and Buenos Aires Provinces (Cpx/Px 47 ± 6%, ACI 74 ± 4%). Instead, they are different in fine silt of the Salado River (Cpx/Px 72%, ACI 45) and in medium-grained beach sand at the western edge of Buenos Aires city (Cpx/Px 96%, ACI 38), where higher Cpx/Px and lower ACI point to a distinct origin of recycled volcaniclastic sediment including contributions from more northern sectors of the Cordillera and broken retroarc basin.

9. Tectonic and climatic control on landscape evolution

In this section we discuss the relationships among tectonic activity, climate, and sedimentation, and specifically highlight the control exerted on drainage configurations by rock uplift on the upper plate consequent to the flat geometry of the subducting plate (Dávila and Lithgow-Bertelloni, 2015) (Table 2). The stepwise development of the Desaguadero-Colorado trunk river is related to the diachronous southward propagation of tectonic uplift generated by the migration of the site of collision between the Juan Fernández aseismic ridge and the Chilean trench from the Miocene onward (Yáñez et al., 2001; Dávila et al., 2007) (Fig. 11). A chronology of drainage change is tentatively correlated with major climatic events.

9.1. Shifting drainage in a broken retroarc basin

Landscapes and pathways of sediment distribution have changed repeatedly and considerably across the studied region in the Neogene (Goddard et al., 2020). In the Pleistocene, during deglaciation phases when large amounts of water were released by the extensive melting of the Cordilleran ice sheet, or during major pluvial events characterized by higher precipitation over sufficiently long periods, much larger volumes of sand and gravel were fed by Andean rivers into the retroarc basin and beyond toward the Atlantic Ocean coast (Iriondo and Garcia, 1993; Iriondo, 1994, 1999; Martínez and Kutschker, 2011). During drier intervening stages, instead, the available sediment volumes drastically decreased, alluvial fans and floodplains were swept by strong cold winds, and sand accumulated in the dune fields. In the dry conditions of today, after glaciers retreated notably since the middle of the nineteenth century, water and sediment fluxes are at a minimum in the Desaguadero catchment, which is now mostly disconnected from the Colorado mainstem. Wind action is strengthening in this part of the retroarc basin, lakes have dried up, and several rivers in the north have become endorheic (Piovano et al., 2009).

The Desaguadero drainage evolution faithfully reflects the tectonic evolution of the Andean broken retroarc basin and the diachronous uplift of the Sierras Pampeanas basement blocks, initiated in the late Miocene at 27°S but only at the end of the Pliocene at 33°S (Ramos et al., 2002). Its upstream Bermejo branch flows today along Neogene strike-slip and reverse faults, strictly confined between the actively uplifting Sierra de Valle Fértil and Sierra de Pie de Palo (Introcaso and Ruiz, 2001; Martínez et al., 2008). To the south, the Desaguadero course is confined by the Sierra de San Luis and, farther south, by the Sierra de Varela, a 120-km-long brachyanticline deformed and uplifted in the late Miocene (Folguera and Zárate, 2018) (Fig. 11).

Tectonic activity is held responsible for repeated drainage reconfigurations across the retroarc basin even in very recent times (Dávila et al., 2007; Vogt et al., 2010). In the Pleistocene, the Tunuyán and Mendoza rivers flowed northwards as a single river, joining the San Juan River to the west of the present confluence. River courses were still united in 1647 A.D. but already separated in 1703 A.D., when the Mendoza River started to flow eastwards first, northeastwards next, and finally again northwards (Rodríguez and Barton, 1993; Martínez et al., 2008). Farther south, the eastward propagation of Andean deformation started to affect the retroarc basin in the late Miocene, eventually leading to flexural uplift of the La Pampa High (Nivière et al., 2013; Folguera and Zárate, 2018).

The compositional signatures of eolian sands, fed from rivers sourced in a most topographically and structurally elevated tract of the Andes, reveal much about the evolution of drainage and the history of dune fields. Clear compositional affinities confirm previous hypotheses envisaging the persistent dominant supply to Pampean lowlands by the Desaguadero trunk river (Malagnino, 1988; Pampa Sur of Iriondo, 1994; Szelagowski et al., 2004). Mineralogical data indicate the possibility that the Middle Pleistocene paleo-Desaguadero turned eastwards toward Pampean lowlands after receiving the Tunuyán and Diamante tributaries but upstream of the Atuel confluence (i.e., between the Sierra de Varela in the north and the La Pampa High in the south). The southward-progressing uplift of tectonic blocks may have subsequently determined the stepwise southward shift of river courses, as indicated by the variable mineralogical and geochronological signatures of eolian sand in the bulge region. The framework petrography of the Valle Daza dune sample is closest to Desaguadero sand, whereas the tHM suite is closest to Atuel sand, indicating that sediment to this blowout dune was originally supplied by a paleo-Desaguadero trunk river that incorporated not only the Tunuyán and Diamante tributaries but also the Atuel River. Moreover, zircon-age fingerprints of dune sand along the main Utracán-Vallimanca alignment are compatible with supply by an integrated Desaguadero+Colorado paleo-river that may have flowed as an antecedent paleochannel across the southern part of Pampean lowlands toward the swampy Pampa deprimida backbulge (Fig. 7).

Southward-progressing flexural uplift thus induced the Desaguadero River to shift from eastwards to southwards, firstly incorporating the Atuel tributary and eventually joining the Colorado River. The Colorado River was subsequently diverted southwards in the broad open valley that reaches the Atlantic Ocean between Bahía Blanca city and the Ombucta dune corridor, before being displaced stepwise toward its present position farther south (Melo et al., 2003). Finally, the reunited Deaguadero+Colorado paleo-river formed a large delta (Spalletti and Isla, 2003) that prograded rapidly oceanwards during latest Pleistocene to early Holocene phases of enhanced discharge fostered by deglaciation pulses or pluvial stages (Melo et al., 2003) and nurtured northward littoral sand drift all along the coast of the Buenos Aires Province (Fig. 6). Equally dictated by tectonic regime are the present courses of the Colorado and Negro rivers, funnelled between the San Rafael block to the north and the North Patagonian Massif to the south, where they run subparallel to each other, locally only ~40 km apart.

9.2. Age constraints on drainage reorganizations

Although a very young age (< 1 Ma) yielded by a single zircon grain is admittedly unrobust, the distribution of the many tens of very young ages that we obtained is not random, and a coherent pattern emerges if our data are integrated with those obtained on different samples and with different analytical instruments and methods by Bruner et al. (2022). The integration of these two detrital-geochronology datasets may thus contain meaningful information on the timing of sediment transfer, drainage change, and duration of recycling.

Zircon ages ≤ 100 ka were obtained from sand of the Tunuyán, Diamante, and Atuel rivers draining the Southern Volcanic Zone as from the Varita dune field in the southern part of the Andean retroarc basin (27 out of 613 analysed grains), but not in the Pampean Sand Sea across the bulge and backbulge depozones (Fig. 10). The youngest U-Pb zircon ages obtained from the Pampean Sand Sea, out of the 1327 grains analysed in this study, are 192 ka (San Luis Province) and 142 ka (La Pampa Province). Bruner et al. (2022) similarly obtained youngest ages of 150 ka and 160 ka from the San Luis Province (2 out of 749 grains), but also somewhat younger ages of 80-90 ka (4 out of 1681 grains) from the southern Utracán-Vallimanca and Colorado Valley region (Fig. 10).

The lack of grains younger than 140 ka in the northern part of the Pampean Sand Sea may place a maximum age constraint for the time when the Desaguadero trunk river ceased to supply eolian sediment to this area and was diverted southwards. This event may have coincided with increasing water and sediment fluxes at the end of the penultimate (Illinoian/Riss) glacial maximum, dated as ~130 ka (MIS6/MIS5 transition; Ehlers and Gibbard, 2008; Rabassa, 2008). In turn, the lack of grains younger than 80 ka obtained from the southernmost part of the Pampean Sand Sea may place a maximum age constraint for the time when the Desaguadero, Atuel, and Colorado rivers ceased to supply sediment to this area and were diverted southwards to form a single paleo-river that fed a large delta to the south of Bahía Blanca. This event may have occurred during the last glacial period and might have coincided with abandonment of the Valles Transversales owing to reduction of stream power around the MIS 5/MIS4 transition, dated as ~70 ka (Rutter et al., 2012; Railsback et al., 2015). This tentative chronology would be broadly consistent with the reconstructed Late Pleistocene evolution of Pampean lowlands (Zárate and Tripaldi, 2012; Tripaldi and Forman, 2016), including phases of loess deposition at 140-150 ka (Kemp et al., 2004, 2006) and 70 ka (Frechen et al., 2009), and with dominant wind activity documented in the Valles Transversales since ~30 ka (Mehl et al., 2018).

9.3. Fluvial/eolian interactions in retroarc settings

The numerous sand seas found on the Earth today can be classified according to different criteria, including their compositional signatures and geographic location. These are strictly related to geodynamic setting and controlled by fluvial *versus* eolian processes of sand supply and dispersal, chiefly dependent in turn on climatic conditions. A first-order distinction is made between vast intracratonic ergs such as the Sahara, the Kalahari, or the Great Nafud in Arabia, which are mostly wind-fed and characterized by homogeneous quartzose to pure quartzose sand containing only durable minerals (Garzanti et al., 2013, 2022; Pastore et al., 2021), and dune fields adjacent to collisional orogenic belts such as those of central Asia, which are mostly river-fed and characterized by intermediate quartz content and abundant sedimentary and/or metamorphic rock fragments (Rittner et al., 2016; Garzanti et al., 2019, 2020).

A third distinct case under this respect is presented by dune fields situated in retroarc regions such as the Pampean Sand Sea of central Argentina, which is characterized by abundant to overwhelming volcanic detritus consisting of plagioclase, volcanic rock fragments, and ferromagnesian minerals with even very low quartz (< 10% of bulk sand in the Naranjos, Picardo, and Varita dunes). In each Argentine dune field, sand composition invariably displays a close correspondence with river sand generated in the adjacent highlands. Within the same dune field, as in the Médanos Grandes or M. Altos Limpios-Telteca, gradual compositional changes from west to east and from north to south reflect progressive mixing of sand supplied by rivers from different sides of the erg (Capaldi et al., 2019). The steady compositional gradient independently highlighted by framework petrography, heavy minerals, and age spectra of detrital zircons in both fluvial and eolian sands from north to south along the retroarc basin indicate that, notwithstanding a complex system of dominant seasonal winds operating through hundreds of thousand years, sand homogenization by wind reworking across the Andean piedmont and proximal retroarc basin was limited to within a range of a few tens of kilometers.

In contrast, compositional signatures are notably homogeneous in the Pampean Sand Sea occupying the distal backbulge depozone, reflecting extensive wind-reworking of Pleistocene deposits and homogenization through repeated dry climatic stages (Forman et al., 2014). Across most of the area, eolian dunes bear the same composition as sand of the Desaguadero trunk river. Composition becomes more variable only in the south, testifying to sediment contributions also by the Atuel and Colorado paleo-rivers that may have flowed close to, or antecedently across the southern Valles Transversales before the flexural uplift of the La Pampa High eventually diverted their courses farther south. Despite extensive reworking through the latest Quaternary, the composition of eolian-dune sand still largely preserves information on the original fluvial feeder system, thus bearing testimony of landscape and drainage changes through time.

10. Conclusions

A vast expanse of eolian sediment stretches across the whole of central Argentina, from the Andean piedmont to the Atlantic coast. A marked peculiarity of these deposits, relative to African and Arabian sand seas, is their quartz-poor composition dominated by volcanic rocks fragments, plagioclase, and ferromagnesian silicates. These almost purely volcaniclastic signatures, together with the presence of zircon grains yielding very young crystallization ages, modest degree of grain roundness, and occurrence of clasts as fragile as fresh pumice and glass shards, faithfully represent the characteristics of largely Andean magmatic-arc source rocks, with only trivial influence of physical abrasion or chemical weathering.

The information obtained independently from framework petrography, heavy minerals, and detrital-zircon ages in both river sands and eolian dunes accumulated in the broken retroarc basin defines a steady northward decrease in volcanic detritus. Compositional signatures thus primarily reflect presently active magmatism in the Southern Volcanic Zone and Payenia Province between 34° and 38°S, whereas the Pampean flat-slab segment between 33° and 27°S corresponds to a Pliocene-Quaternary (< 7 Ma) magmatic gap with sediment generated from deeper-seated tectono-stratigraphic levels of the continental arc, fold-thrust belt, and retroarc-basin basement blocks of the Sierras Pampeanas.

The northern Negros and Grandes dune fields are notably richer in quartz, both metamorphic and magmatic amphibole, and old (Proterozoic-Paleozoic) zircon grains, testifying to sediment supply partly from the Sierras Pampeanas. The abundance of volcanic rock fragments and orthopyroxene progressively increases southwards across the Altos Limpios-Telteca dune field, where common felsic volcanic grains and detrital zircons yielding Permian-Triassic ages indicate significant contribution from Choiyoi igneous rocks of the Frontal Cordillera. South of the Tunuyán River, the Travesía dune field records the appearance of Pliocene-Quaternary-aged zircons sourced by rivers that drain the northern edge of the Southern Volcanic Zone where amphibole-bearing andesites are common. Farther south, the Naranjos, Picardo, and Varita dune fields exhibit a further sharp increase in intermediate to mafic volcanic rock fragments, plagioclase, orthopyroxene, and < 15 Ma aged zircon grains from the Southern Volcanic Zone, whereas quartz, K-feldspar, amphibole, ZTR minerals, epidote, and garnet reach their minimum.

Across the bulge and backbulge depozones, for 1000 km from the central retroarc-basin dune fields to the beaches of the Río de la Plata Estuary, sand composition remains quartzo-feldspatho-lithic to quartzo-litho-feldspathic. Moderately rich transparent-heavy-mineral suites contain subequal amounts of mostly magmatic amphibole, clinopyroxene and orthopyroxene, and zircon grains displaying multimodal spectra with common Middle Miocene to Middle Pleistocene ages. Such a notably homogeneous mineralogy indicates that detritus was generated mostly north of 34°S and fed into the Pampean plains by a paleo-Desaguadero trunk river including the Tunuyán and Diamante tributaries.

Since the Miocene, when onset of flat subduction and passage over the Juan Fernández “hot-spot” track led to dynamic uplift of the Pampean segment of the Andean Cordillera and adjacent retroarc basin, drainage evolution has been regulated by the interplay between subduction-related tectono-magmatic processes and climate. Southward-progressing diachronous uplift of the Sierras Pampeanas induced the formation of a southward-flowing paleo-Deaguadero trunk river, which may have turned eastwards south of the Sierras Pampeanas to feed sediment into the Pampean backbulge depozone until the end of the Middle Pleistocene.

According to our tentative reconstruction, flexural uplift of the La Pampa High forced the Desaguadero, Atuel, and Colorado paleo-rivers to shift southwards in the Late Pleistocene, possibly abandoning their antecedent course along the Valles Transversales where wind activity became dominant since at least ~30 ka. Based on detrital-zircon chronostratigraphy, this event may have resulted from decreased stream power around 70 ka, whereas the previous southward diversion of the paleo-Desaguadero may have been induced by increasing water and sediment fluxes at the end of the penultimate glacial maximum around 130 ka. Such a multistep drainage reorganization culminated in the latest Pleistocene, when the Desaguadero, Atuel, and Colorado rivers eventually joined to form a large single paleo-river that fostered the progradation of a wide delta and littoral sand transport along the shores of the Buenos Aires Province. Because of the limited long-term sediment-storage capacity of the Andean broken retroarc basin, transcontinental transfer of large masses of volcanic detritus led to the outbuilding of the 400-km-wide continental terrace of the Argentine passive-margin through geological time. Stream power and sediment supply were greatly enhanced during Pleistocene to early Holocene deglaciation and pluvial stages, but inhibited during the intervening arid stages, when decreased vegetation cover and strengthened wind action led to deflation of the floodplains, eolian-sand accumulation, growth of dune fields, and loess deposition in distal areas.

Declaration of Competing Interest

The authors declare that they have no known competing financial interests or personal relationships that could have appeared to influence the work reported in this paper.

Acknowledgements

This study greatly benefitted from support by CONICET–UNLP (Centro de Investigaciones Geológicas –Universidad Nacional de la Plata), and by the help provided by Numa Sosa, Elisa Beilinson, Pablo Montilla, Liliana Tomich, and Ryan Anderson. We thank Daniel Stockli, Lisa Stockli, Margo Odlum, Andrew Kylander-Clark, and Chris Defelice for laboratory assistance and helpful discussions, and Alex Pullen and Austin Bruner for letting us incorporate their geochronological data in the present review. Alfonsina Tripaldi thanks the support of CONICET-PUE-IGEBA 22920160100030CO and PICT-2018. We warmly thank Editor Christopher Fielding for excellent handling of our manuscript and Peter DeCelles and two anonymous reviewers for careful and constructive critical comments. This study is an outcome of Progetto MIUR Dipartimenti di Eccellenza 2018–2022, Department of Earth and Environmental Sciences, University of Milano-Bicocca.

Supplementary Data

Supplementary material associated with this article includes full information on sampling sites (Table A1), together with the bulk-sand petrography (Table A2) and heavy-mineral datasets (Table A3). Appendix A contains the appendix table captions as well as additional information on forward-mixing calculations. Appendix B contains the complete technical information on U-Pb geochronological analyses of detrital zicons and the full dataset of detrital-zircon ages (Appendix B1, river sands; Appendix B2, eolian deposits). The Google-Earth™ maps of sampling sites *ArgenDunes.kmz* and *ArgenDunesDZ.kmz* are also provided. Supplementary data to this article can be found online at https://doi.org/________ or provided by the corresponding author upon request.

FIGURE AND TABLE CAPTIONS

Figure 1. Physiography of central Argentina with sampling sites (base map from Google Earth™). The La Pampa High corresponds to the flexural bulge and the Pampa deprimida to the backbulge depozone (Folguera and Zárate, 2019). **A**) Dune fields in the northern part of the broken Andean retroarc basin. **B**) Central Pampean dune field.

Figure 2. Eolian deposits of central Argentina (Iriondo and Kröhling, 1995; Zárate and Tripaldi, 2012). The magmatic gap in the Andean Cordillera between 28° and 33°S is shown (CVZ = Central Volcanic Zone). Studied dune fields (white letters): Ne, Negros; G, Grandes; AL, Altos Limpios; Te, Telteca; Tr, Travesía; Na, Naranjos; P, Picardo; V, Varita; SL, San Luis. LP, La Plata coastal province (Garzanti et al., 2021b). Sierras Pampeanas (black letters): F, Famatina; G, Guayaguas; L, San Luis; P, Pie de Palo, V, Valle Fértil,

Figure 3. Climate of Argentina. **A)** Rainfall map (after Cravero et al., 2017). Highest mountain peaks occur in the Pampean flat-slab segment of inactive magmatism: A = Cerro Aconcagua in the Andes, 6962 m a.s.l.; B = Cerro General Belgrano in the Sierra de Famatina, 6097 a.s.l.. CVZ and SVZ = Central and Southern Volcanic Zones. P = Payenia volcanic province. **B)** Eolian deposits and dominant winds after Tripaldi and Forman (2007, 2016). Wind rose for 1995-2004 near San Juan (orange circle).

Figure 4. Petrographic changes displayed by eolian dunes along the Andean retroarc basin (photos arranged in geographic order from north to south). **A**) Common quartz, perthitic K-feldspar, plagioclase, and biotite in the north. **B, C**) Volcanic detritus increasing from NE to SW in the Médanos Grandes at the expense of quartz. **D**, **E**, **F**) Predominant volcanic lithics and plagioclase in the center. **G**, **H**, **I**) Overwhelming volcanic detritus in the south. All photos with crossed polars; blue bar for scale = 100 μm.

Figure 5. Compositional trends displayed by fluvial and eolian sand along the Andean retroarc region. Quartz and amphibole progressively decrease, and volcanic detritus increase from Negros and

Grandes dunes in the north, to Altos Limpios-Telteca and Travesía dunes in the center, and to Naranjos, Picardo, and Varita dunes in the south. **A**) Main framework components (classification fields after Garzanti, 2019a). Provenance fields (from QtFL diagram of Dickinson et al., 1983): undissected (red), transitional (pink), and dissected+mixed (lilac) magmatic arc; continental block (blue); recycled orogen (yellow). **B**) Relative abundances of ferromagnesian silicates. **C**) Biplot with parameters in *A* and *B* combined. **D**) Biplot depicting sediments as mixtures of volcanic covers, sedimentary to metasedimentary detritus from deeper-seated structural levels of the continental arc, and higher-grade metamorphic detritus from the Sierras Pampeanas. Felsic volcanic lithics are largely derived from Choiyoi igneous rocks. Q = quartz; F = feldspars (P = plagioclase; K = K-feldspar); L = lithic fragments (Lvf = felsic volcanic; Lvm = intermediate and mafic volcanic; Lc = carbonate; Lsm = other sedimentary and low-rank metasedimentary; Lm = high-rank metamorphic); tHMC = transparent heavy-mineral concentration; ZTR = zircon + tourmaline + rutile; SKS = staurolite + kyanite + sillimanite; *ACI* = Amphibole Color Index.

Figure 6. Visual comparison between detrital modes of fluvial (circles with light blue outline), eolian (yellow outline), and beach sands (dark blue outline). Littoral cell of sand transport alongshore the Buenos Aires Province coast after Garzanti et al. (2021b). **A**) Quartz and sedimentary lithics increase northwards at the expense of plagioclase and volcanic rock fragments. L = lithics (metamorphic lithics include mica). **B**) Amphibole increases northwards at the expense of orthopyroxene. Note similarity of tHM suites in San Juan, Tunuyán and Desaguadero rivers, Altos Limpios-Telteca and Travesía dunes, Pampean Sand Sea, and Río de la Plata beaches (polygonal area delimited by white dotted line).

Figure 7. Similarities and differences among Argentine dune fields highlighted by KDE plots and MDS maps of U-Pb detrital-zircon ages, including data from Capaldi et al. (2019) and Bruner et al. (2022; circles with yellow outline). Four main groups are distinguished: 1) Negros, Grandes, and Altos Limpios/Telteca dunes in the northern retroarc basin, displaying a lack of Pliocene-Quaternary zircons, progressive northward decrease of Permian-Triassic zircons, and corresponding increase of

Stenian (peak ~1.1 Ga) and Cambro-Ordovician (470-490 Ma) zircons from the Sierras Pampeanas, the latter being dominant in the Negros dune and the former reaching maximum in the Grandes dunes; 2) Naranjos, Picardo, and Varita dunes in the southern retroarc basin, where most zircon grains yielded ages < 15 Ma reflecting volcanism in the Southern Volcanic Zone; 3) eolian sediments of the Colorado Valley, Depresión Diagonal, and Atlantic coast north of Mar del Plata city; 4) Travesía dune and Pampean Sand Sea (including five samples straddling the San Luis and La Pampa Provinces that contain more Miocene-Quaternary zircon grains). Inset: sample locations in the Pampean Sand Sea.

Figure 8. Provenance analysis of Andean retroarc-basin dune fields based on MDS comparison between U-Pb detrital-zircon ages in fluvial (KDE plots in blue panels) and eolian-dune sands (KDE plots in orange panels), including data from Pepper et al. (2016) and Capaldi et al. (2017, 2019, 2020). In the northern retroarc basin, zircon is fed locally by the Sierras Pampeanas (M. Negros), by both Río Bermejo and Río San Juan (M. Grandes), or mostly by Río San Juan including Río Mendoza (M. Telteca-Altos Limpios). In the southern retroarc basin, zircon is supplied by Río Desaguadero and subordinately by Río Tunuyán (M. de la Travesía), mainly by Río Diamante (M. de los Naranjos), or mainly by Río Atuel (M. de Picardo and M. de la Varita). In case of multiple samples along the same river, symbol size increases downstream (e.g., note increasing zircon supply from the Sierras Pampeanas downstream Río Bermejo).

Figure 9. Provenance analysis of the Pampean Sand Sea based on MDS comparison between U-Pb detrital-zircon ages in fluvial (KDE plots in blue panels) and eolian sediments (KDE plots in orange panels), including data from Pepper et al. (2016), Capaldi et al. (2017), and Bruner et al. (2022; circles with yellow outline). Most Pampean dunes display the same zircon-age spectrum as Desaguadero river sand, but for five samples straddling the San Luis and La Pampa Province yielding more grains of Miocene to recent ages (sample locations shown in geographic inset of Fig. 7). Distinct are eolian sediments in the Colorado Valley, Depresión Diagonal (I), and near the coast north of Mar del Plata city, which show the subordinate Cretaceous and Jurassic peaks characteristic of Colorado river sand.

Figure 10. Youngest U-Pb ages (in Ma) of detrital zircon in fluvial and eolian sediments (river sands in blue, eolian sands in orange, loess in brown, paleosol in red; data on lower Neuquén and Negro rivers after Pepper et al. 2016; data on loess and paleosol after Bruner et al. 2022). Detrital-zircon chronostratigraphy suggests cessation of volcanic activity shortly after 7 Ma in the Pampean flat-slab segment between 28°S and 33°S, a first southward shift of the Desaguadero paleo-river at end of the Middle Pleistocene and a second southward shift of the Desaguadero, Atuel, and Colorado rivers in the Late Pleistocene.

Figure 11. Contrasting drainage patterns in the overfilled Andean retroarc basin. **A**) Geological map after Gómez et al. (2019). **B**) North of the Pampean flat-slab segment, where subduction angle is steeper, the Bermejo and Pilcomayo rivers, as the Amazon River to the north, flow perpendicular to the range across the bulge zone (Repasch et al., 2020). In the Pampean flat-slab segment, instead, drainage was controlled by southward-progressing uplift of the Sierras Pampeanas and La Pampa Central blocks. Petrography, heavy minerals, and zircon ages of eolian sediments suggest that the Desaguadero River fed sediment into the backbulge depozone until the end of the Middle Pleistocene, and then shifted stepwise southward to finally join the Colorado River in the latest Pleistocene-early Holocene, forming a large delta with sediments dragged by longshore currents as far the Rio de La Plata mouth. CVZ and SVZ = Central and Southern Volcanic Zones. Highest peaks in the Cordillera and Sierra Pampeanas are indicated.

Table 1. Comparison between petrographic and heavy-mineral modes of eolian and river sands in central Argentina. GSZ = grain size. Q = quartz; KF = K-feldspar; P = plagioclase; L= lithics (Lvf = felsic volcanic; Lvm = intermediate and mafic volcanic; Lc = carbonate; Lsm = other sedimentary and low-rank metasedimentary; Lm = high-rank metamorphic); tHMC= transparent heavy-mineral concentration; ZTR= zircon + tourmaline + rutile; Ap = apatite; Ttn = titanite; Ep = epidote; Grt = garnet; SKS = staurolite + kyanite + sillimanite; Amp = amphibole; Cpx = clinopyroxene; Opx = orthopyroxene; Ol = olivine; ACI = Amphibole Color Index.

Table 2. Foreland basins, retroarc basins and foredeeps are different sedimentary basins associated with different types of orogenic belts (Doglioni, 1994; Garzanti et al., 2007). Different geodynamic setting, subduction geometry, and location on the lower plate *vs.* upper plate imply different applied forces, topographic relief, subsidence mechanisms and rates (Doglioni and Panza, 2015), and hence storage capacity and ratio between sediment retained *vs.* sediment exported long-distance away. In strongly subsiding underfilled foredeeps, axial turbidites accumulate in deep waters of both wedge-top and pro-wedge depozones (Cibin et al., 2003; Di Giulio et al., 2013). In much less rapidly subsiding overfilled foreland basins, the trunk river is confined by, and partly fed from the cratonic foreland and flows parallel to the orogen (e.g., Ganga; Garzanti, 2019b). In even less rapidly subsiding strongly overfilled retroarc basins, the bulge zone has no confining effect and drainage is transverse to the orogen (e.g., Amazon; Fig. 11).

REFERENCE LIST

Aitchison, J., Greenacre, M., 2002. Biplots of compositional data. Journal of the Royal Statistical Society: Series C (Applied Statistics) 51(4), 375-392.

Andersen, T., van Niekerk, H., Elburg, M.A., 2022. Detrital zircon in an active sedimentary recycling system: Challenging the 'source‐ to‐ sink'approach to zircon‐ based provenance analysis. Sedimentology, doi: 10.1111/sed.12996.

Andò, S., Morton, A., Garzanti, E., 2014. Metamorphic grade of source rocks revealed by chemical fingerprints of detrital amphibole and garnet. In: Scott, R.A., Smyth, H.R., Morton, A.C., Richardson, N. (Eds.), Sediment Provenance Studies in Hydrocarbon Exploration and Production. Geological Society, London, Special Publication 386(1), 351-371.

Astini, R.A., Dávila, F.M., 2004. Ordovician back arc foreland and Ocloyic thrust belt development on the western Gondwana margin as a response to Precordillera terrane accretion. Tectonics 23(4), TC4008, doi:10.1029/2003TC001620.

Astini, R.A., Benedetto, J.L., Vaccari, N.E., 1995. The early Paleozoic evolution of the Argentine Precordillera as a Laurentian rifted, drifted, and collided terrane: A geodynamic model. Geological Society of America Bulletin 107(3), 253-273.

Bahlburg, H., Vervoort, J.D., Du Frane, S.A., Bock, B., Augustsson, C, Reimann, C., 2009. Timing of crust formation and recycling in accretionary orogens: Insights learned from the western margin of South America. Earth-Science Reviews 97(1-4), 215-241.

Balgord, E.A., Carrapa, B., 2016. Basin evolution of Upper Cretaceous–Lower Cenozoic strata in the Malargüe fold‐ and‐ thrust belt: northern Neuquén Basin, Argentina. Basin Research, 28(2), 183-206.

Barazangi, M., Isacks, B.L., 1976. Spatial distribution of earthquakes and subduction of the Nazca plate beneath South America. Geology 4(11), 686-692.

Barros, V.R., Doyle, M.E., Camilloni, I.A., 2008. Precipitation trends in southeastern South America: relationship with ENSO phases and with low-level circulation. Theoretical and Applied Climatology 93(1), 19-33.

Barros, V.R., Boninsegna, J.A., Camilloni, I.A., Chidiak, M., Magrín, G.O., Rusticucci, M., 2015. Climate change in Argentina: trends, projections, impacts and adaptation. Wiley Interdisciplinary Reviews, Climate Change 6(2), 51-169.

Bense, F., Costa, C., Oriolo, S., Löbens, S., Dunkl, I., Wemmer, K., Siegesmund, S., 2017. Exhumation history and landscape evolution of the Sierra de San Luis (Sierras Pampeanas, Argentina) - new insights from low-temperature thermochronological data. Andean Geology 44(3), 275-306.

Borromeo, L., Andò, S., Bersani, D., Garzanti, E., Gentile, P., Mantovani, L., Tribaudino, M., 2022. Detrital orthopyroxene as a tracer of geodynamic setting: a Raman and SEM-EDS provenance study. Chemical Geology 596, 120809

Bruner, A., Leier, A.L., Barbeau, D.L, Pullen, A., Fidler, M.K., Stubbins, B., 2022, Detrital zircon provenance and transport pathways of Pleistocene-Holocene eolian sediment in the Pampean Plains, Argentina. Geological Society of America Bulletin, 135, doi/10.1130/B36267.1

Cabrera, A.L., 1994. Regiones fitogeográficas argentinas. Enciclopedia Argentina de Agricultura y Jardinería. Editorial Acme, Buenos Aires, tomo II, fasciculo 1, pp. 81-85.

Calmels, P., 1996. Bosquejo geomorfológico de la provincia de La Pampa. Universidad Nacional de la Pampa, Facultad de Ciencias Exactas y Naturales, Tesis Doctoral, 109 p.

Capaldi, T.N., Horton, B.K., McKenzie, N.R., Stockli, D.F., Odlum, M.L., 2017. Sediment provenance in contractional orogens: The detrital zircon record from modern rivers in the Andean fold-thrust belt and foreland basin of western Argentina. Earth and Planetary Science Letters 479, 83-97.

Capaldi, T.N., George, S.M.W., Hirtz, J.A., Horton, B.K., Stockli, D.F., 2019. Fluvial and eolian sediment mixing during changing climate conditions recorded in Holocene Andean foreland deposits from Argentina (31-33° S). Frontiers in Earth Science 7, 298, doi: 10.3389/feart.2019.00298.

Capaldi, T.N., Horton, B.K., McKenzie, N.R., Mackaman- Lofland, C., Stockli, D.F., Ortiz, G., Alvarado, P., 2020. Neogene retroarc foreland basin evolution, sediment provenance, and magmatism in response to flat slab subduction, western Argentina. Tectonics 39(7), e2019TC005958.

Capaldi, T.N., McKenzie, N.R., Horton, B.K., Mackaman-Lofland, C., Colleps, C.L., Stockli, D.F., 2021, Detrital zircon record of Phanerozoic magmatism in the southern Central Andes: Geosphere 17, 876–897.

Cembrano, J., Lara, L., 2009. The link between volcanism and tectonics in the southern volcanic zone of the Chilean Andes: a review. Tectonophysics 471(1-2), 96-113.

Charrier, R., Ramos, V.A., Tapia, F., Sagripanti, L., 2015. Tectono-stratigraphic evolution of the Andean Orogen between 31 and 37 S (Chile and Western Argentina). Geological Society, London, Special Publication 399(1), 13-61.

Chiesa, J., Basaez, A., Navio, J., Strasser, E., Ojeda, G., Lucero, N., 2011. Neogene Stratigraphy of San Luis province, Argentina. In: Salfity, J., Marquillas, R. (Ed.), Cenozoic Geology of the Central Andes of Argentina. SCS Publisher, Salta, pp. 75-89.

Cibin, U., Di Giulio, A., Martelli, L., 2003. Oligocene-Early Miocene tectonic evolution of the northern Apennines (northwestern Italy) traced through provenance of piggy-back basin fill successions. Geological Society of London, Special Publication 208, 269-287.

Clapperton, C.M., 1993. Nature of environmental changes in South America at the Last Glacial Maximum. Palaeogeography, Palaeoclimatology, Palaeoecology 101(3-4), 189-208.

Comas Cufí, M. and Thió i Fernández de Henestrosa, S., 2011. CoDaPack 2.0: a stand-alone, multi-platform compositional software.

Compagnucci, R.H., Agosta, E.A., Vargas, W.M., 2002. Climatic change and quasi-oscillations in central-west Argentina summer precipitation: main features and coherent behaviour with southern African region. Climate Dynamics 18(5) 421–435.

Cravero, S.A.C., Bianchi, C.L., Elena, H.J., Bianchi, A.R., 2017. Clima de Argentina: Mapas digitales mensuales de precipitación y precipitación menos evapotranspiración potencial. Adenda del Atlas climático digital de la República Argentina. Instituto Nacional de Tecnología Agropecuaria, Salta, 62 p.

Dahlquist, J.A., Cámera, M.M.M., Alasino, P.H., Pankhurst, R.J., Basei, M.A., Rapela, C.W., Moreno, J.A., Baldo, E.G., Galindo, C., 2021. A review of Devonian–Carboniferous magmatism in the central region of Argentina, pre-Andean margin of SW Gondwana. Earth-Science Reviews 221, 103781.

Dávila, F.M., Lithgow-Bertelloni, C., 2015. Dynamic uplift during slab flattening. Earth and Planetary Science Letters 425, 34–43.

Dávila, F.M., Astini, R.A., Jordan, T.E., Gehrels, G., Ezpeleta, M., 2007. Miocene forebulge development previous to broken foreland partitioning in the southern Central Andes, west- central Argentina. Tectonics 26(5), TC5016, doi:10.1029/2007TC002118.

DeCelles, P.G., 2012. Foreland basin systems revisited: Variations in response to tectonic settings. In Busby, C., Azor, A. (Eds.), Tectonics of sedimentary basins: Recent advances. Blackwell, pp. 405-426.

Deruelle, B., 1982. Petrology of the Plio-Quaternary volcanism of the south-central and meridional Andes. Journal of Volcanology and Geothermal Research 14(1–2), 77–124.

Dickinson, W.R., 1978. Plate tectonic evolution of sedimentary basins. In: Dickinson, W.R., Yarborough, H. (Eds.), Plate Tectonics and Hydrocarbon Accumulation. American Association of Petroleum Geologists, Continuing Education Course Note Series, 1, pp. 1-56.

Dickinson, W.R., Gehrels, G.E., 2009. Use of U–Pb ages of detrital zircons to infer maximum depositional ages of strata: a test against a Colorado Plateau Mesozoic database. Earth and Planetary Science Letters 288(1-2), 115-125.

Dickinson, W.R., Beard, L.S., Brakenridge, G.R., Erjavec, J.L., Ferguson, R.C., Inman, K.F., Knepp, R.A., Lindberg, F.A., Ryberg, P.T., 1983. Provenance of North American Phanerozoic sandstones in relation to tectonic setting. Geological Society of America Bulletin 94(2), 222-235.

Di Giulio, A., Mancin, N., Martelli, L., Sani, F., 2013. Foredeep palaeobathymetry and subsidence trends during advancing then retreating subduction: the Northern Apennine case (Oligocene- Miocene, Italy). Basin Research, 25(3), 260-284.

Di Giulio, A., Ronchi, A., Sanfilippo, A., Balgord, E.A., Carrapa, B., Ramos, V.A., 2017. Cretaceous evolution of the Andean margin between 36°S and 40°S latitude through a multi-proxy provenance analysis of Neuquén Basin strata (Argentina). Basin Research 29(3), 284–304.

Doglioni, C., 1994. Foredeeps versus subduction zones. Geology 22(3), 271-274.

Doglioni, C., Panza, G., 2015. Polarized plate tectonics. Advances in Geophysics 56, 1-167.

Dutta, P.K., Zhou, Z., dos Santos, P.R., 1993. A theoretical study of mineralogical maturation of eolian sand. In: Basu, A., Johnsson, M. (Eds.), Processes Controlling the Composition of Clastic Sediments, Geological Society of America, Special Paper 284, pp. 203–209.

Ehlers, J., Gibbard, P., 2008. Extent and chronology of Quaternary glaciation. Episodes 31(2), 211-218.

Espinoza, J.C., Garreaud, R., Poveda, G., Arias, P.A., Molina-Carpio, J., Masiokas, M., Viale, M., Scaff, L., 2020. Hydroclimate of the Andes Part I: main climatic features. Frontiers in Earth Science, 8, 64.

Etchichury, M.C., Tófalo, O.R., 2004. Mineralogía de arenas y limos en suelos, sedimentos fluviales y eólicos actuales del sector austral de la cuenca Chacoparanense: regionalización y áreas de aporte. Revista de la Asociación Geológica Argentina 59(2), 317-329.

Farías, M., Charrier, R., Carretier, S., Martinod, J., Fock, A., Campbell, D., Cáceres, J., Comte, D., 2008. Late Miocene high and rapid surface uplift and its erosional response in the Andes of central Chile (33°–35°S). Tectonics 27, TC1005, https://doi.org/10.1029/2006T C002046.

Folguera, A., Zárate, M., 2011. Neogene sedimentation in the Argentine foreland between 34°30'S and 41°S and its relation to the Andes evolution. Cenozoic Geology of the Central Andes of Argentina. SCS Publisher, Salta, pp.123-134.

Folguera, A., Zárate, M.A., 2018. La estructuración Miocena tardía del Bloque de la Pampa Central. Revista de la Asociación Geológica Argentina 75(1), 115-133.

Folguera, A., Zárate, M., 2019. Late Oligocene to Quaternary tectonic evolution of the extra-Andean basins of the Pampean plain, Argentina. Journal of South American Earth Sciences, 94,102207.

Forman, S.L., Tripaldi, A., Ciccioli, P.L., 2014. Eolian sand sheet deposition in the San Luis paleodune field, western Argentina as an indicator of a semi-arid environment through the Holocene. Palaeogeography, Palaeoclimatology, Palaeoecology 411, 122-135.

Fosdick, J.C., Carrapa, B., Ortíz, G., 2015, Faulting and erosion in the Argentine Precordillera during changes in subduction regime: reconciling bedrock cooling and detrital records. Earth and Planetary Science Letters 431, 73–83.

Fosdick, J.C., Reat, E.J., Carrapa, B., Ortíz, G., Alvarado, P.M., 2017, Retroarc basin reorganization and aridification during Paleogene uplift of the southern central Andes. Tectonics 36, 493-514, doi:10.1002/2016TC004400.

Frechen, M., Seifert, B., Sanabria, J.A., Argüello, G.L., 2009. Chronology of late Pleistocene Pampa loess from the Córdoba area in Argentina. Journal of Quaternary Science 24(7), 761-772.

Frenguelli, J., 1956. Rasgos generales de la hidrografía de la provincia de Buenos Aires. Provincia de Buenos Aires, Ministerio de Obras Publicas, Laboratorio de Ensayo de Materiales e Investigaciones Tecnológicas, Serie II, n°62, 17 p.

Gabriel, K.R., 1971. The biplot graphic display of matrices with application to principal component analysis. Biometrika 58(3), 453-467.

Garreaud, R.D., Vuille, M., Compagnucci, R., Marengo, J., Villalba, R., Grosjean, M., Kiefer, T., 2009. Present-day South American climate. Palaeogeography Palaeoclimatology Palaeoecology 281 (3-4), 180-195.

Garzanti, E., 2016. From static to dynamic provenance analysis—Sedimentary petrology upgraded. Sedimentary Geology 336, 3-13.

Garzanti, E., 2017. The maturity myth in sedimentology and provenance analysis. Journal of Sedimentary Research 87(4), 353-365.

Garzanti, E., 2019a. Petrographic classification of sand and sandstone. Earth-Science Reviews 192, 545-563.

Garzanti, E., 2019b. The Himalayan Foreland Basin from collision onset to the present: A sedimentary–petrology perspective. Geological Society of London, Special Publication 483, 65-122.

Garzanti, E., Andò, S., 2007. Heavy mineral concentration in modern sands: implications for provenance interpretation. In: Mange, M., Wright, D. (Eds.), Heavy minerals in use. Amsterdam, Elsevier, Developments in Sedimentology 58, pp.517-545.

Garzanti, E., Andò, S., 2019. Heavy Minerals for Junior Woodchucks. Minerals 9(3), 148, doi:10.3390/min9030148.

Garzanti, E., Vezzoli, G., 2003. A classification of metamorphic grains in sands based on their composition and grade. Journal of Sedimentary Research 73(5), 830-837.

Garzanti, E., Doglioni, C., Vezzoli, G., Ando, S., 2007. Orogenic belts and orogenic sediment provenance. The Journal of Geology 115(3), 315-334.

Garzanti, E., Andò, S., Vezzoli, G., 2009. Grain-size dependence of sediment composition and environmental bias in provenance studies. Earth and Planetary Science Letters 277(3-4), 422-432.

Garzanti, E., Resentini, A., Vezzoli, G., Andò, S., Malusà, M., Padoan, M., 2012. Forward compositional modelling of Alpine orogenic sediments. Sedimentary Geology 280, 149-164.

Garzanti, E., Vermeesch, P., Andò, S., Vezzoli, G., Valagussa, M., Allen, K., Khadi, K.A., Al-Juboury, I.A., 2013. Provenance and recycling of Arabian desert sand. Earth-Science Reviews 120, 1–19.

Garzanti, E., Resentini, A., Andò, S., Vezzoli, G., Vermeesch, P., 2015. Physical controls on sand composition and relative durability of detrital minerals during long-distance littoral and eolian transport (coastal Namibia). Sedimentology 62, 971-996, doi: 10.1111/sed.12169.

Garzanti E., Vermeesch, P., Al-Ramadan, K.A., Andò, S., Limonta, M., Rittner, M., Vezzoli, G., 2017. Tracing transcontinental sand transport: from Anatolia-Zagros to the Rub' al Khali Sand Sea. Journal of Sedimentary Research 87, 1196-1213.

Garzanti, E., Ghassemi, M.R., Limonta, M., Resentini, A., 2019. Provenance of Karakum Desert sand (Turkmenistan): Lithic-rich orogenic signature of central Asian dune fields. Rivista Italiana di Paleontologia e Stratigrafia 125/1, 77-89.

Garzanti, E., Liang, W., Andò, S., Clift, P.D, Resentini, A., Vermeesch, P., Vezzoli, G., 2020. Provenance of Thal Desert sand: focused erosion in the western Himalayan syntaxis and foreland-basin deposition driven by latest Quaternary climate change. Earth-Science Reviews 207, 103220, doi.org/10.1016/j.earscirev.2020.103220

Garzanti, E., Capaldi, T., Vezzoli, G., Limonta, M., Sosa, N., 2021a. Transcontinental retroarc sediment routing controlled by subduction geometry and climate change (Central and Southern Andes, Argentina). Basin Research 33(6), 3406-3437.

Garzanti, E., Limonta, M., Vezzoli, G., Sosa, N., 2021b. From Patagonia to Río de la Plata: Multistep long- distance littoral transport of Andean volcaniclastic sand along the Argentine passive margin. Sedimentology 68(7), 3357-3384.

Garzanti, E., Pastore, G., Stone, A., Vainer, S., Vermeesch, P. Resentini, A., 2022. Provenance of Kalahari Sand: Paleoweathering and recycling in a linked fluvial-aeolian system. Earth-Science Reviews 224, 103867.

Giambiagi, L.B., Ramos, V.A., Godoy, E., Alvarez, P.P., Orts, S., 2003. Cenozoic deformation and tectonic style of the Andes, between 33° and 34° south latitude. Tectonics 22(4), 1041, doi:10.1029/2001TC001354, 2003

Giambiagi, L., Mescua, J., Bechis, F., Martínez, A., Folguera, A., 2011. Pre-Andean deformation of the Precordillera southern sector, southern Central Andes. Geosphere 7(1), 219-239.

Goddard, A.L.S., Carrapa, B., 2018. Using basin thermal history to evaluate the role of Miocene–Pliocene flat- slab subduction in the southern Central Andes (27°S–30°S). Basin Research 30(3), 564-585.

Goddard, A.L.S., Larrovere, M.A., Carrapa, B., Aciar, R.H., Alvarado, P., 2018. Reconstructing the thermal and exhumation history of the Sierras Pampeanas through low-temperature thermochronology: A case study from the Sierra de Velasco. Geological Society of America Bulletin 130(11-12), 1842-1858.

Goddard, A.S., Carrapa, B., Aciar, R.H., 2020. Recognizing drainage reorganization in the stratigraphic record of the Neogene foreland basin of the Central Andes. Sedimentary Geology 405, 105704.

Gómez, J., Schobbenhaus, C., Montes, N.E., 2019. Geological Map of South America. Scale 1:5,000,000. Commission for the Geological Map of the World (CGMW), Colombian Geological Survey and Geological Survey of Brazil, Paris.

González Díaz, E.F., Fauqué, L., 1993. Geomorfología. In: Ramos, V. (Ed.), Geología y Recursos Naturales de Mendoza, Relatorio del XII Congreso Geológico Argentino y II Congreso de Exploración de Hidrocarburos, pp. 217-234.

Grimm, A.M., 2003. The El Niño impact on the summer monsoon in Brazil: regional processes versus remote influences. Journal of Climate 16(2), 263-280.

Haschke, M., Günther, A., Melnick, D., Echtler, H., Reutter, K.J., Scheuber, E., Oncken, O., 2006. Central and southern Andean tectonic evolution inferred from arc magmatism. In: Oncken, O. (Ed.), The Andes, Springer, Berlin-Heidelberg, pp. 337–353.

Heredia, N., Fernández, L.R., Gallastegui, G., Busquets, P., Colombo, F., 2002. Geological setting of the Argentine Frontal Cordillera in the flat-slab segment (30° 00′–31° 30′ S latitude). Journal of South American Earth Sciences 15(1), 79-99.

Hickey, R.L., Frey, F.A., Gerlach, D.C., Lopez- Escobar, L., 1986. Multiple sources for basaltic arc rocks from the southern volcanic zone of the Andes (34°–41°S): trace element and isotopic evidence for contributions from subducted oceanic crust, mantle, and continental crust. Journal of Geophysical Research: Solid Earth 91(B6), 5963-5983.

Horton, B.K., Fuentes, F., 2016, Sedimentary record of plate coupling and decoupling during growth of the Andes. Geology 44, 647-650.

Horton, B.K., Fuentes, F., Boll, A., Starck, D., Ramirez, S.G., Stockli, D.F., 2016. Andean stratigraphic record of the transition from backarc extension to orogenic short-ening: a case study from the northern Neuquén basin, Argentina. Journal of South American Earth Sciences 71, 17–40.

Howell, J.A., Schwarz, E., Spalletti, L.A., Veiga, G.D., 2005. The Neuquén basin: An overview. In Veiga, G.D. Spalletti, L.A., Howell, J.A., Schwarz, E. (Eds.), The Neuquén basin, Argentina: A case study in sequence stratigraphy and basin dynamics, Geological Society of London, Special Publication 252, pp. 1–14.

Hubert, J.F., 1962. A zircon-tourmaline-rutile maturity index and the interdependence of the composition of heavy mineral assemblages with the gross composition and texture of sandstones. Journal of Sedimentary Petrology 32(3), 440-450.

Imbellone, P.A., Teruggi, M.E., 1993. Paleosols in loess deposits of the Argentine Pampas. Quaternary International 17, 49-55.

Ingersoll, R.V., Bullard, T.F., Ford, R.L., Grimm, J.P., Pickle, J.D., Sares, S.W., 1984. The effect of grain size on detrital modes: a test of the Gazzi-Dickinson point-counting method. Journal of Sedimentary Petrology 54(1), 103-116.

Introcaso, A., Ruiz, F., 2001. Geophysical indicators of Neogene strike-slip faulting in the Desaguadero–Bermejo tectonic lineament (northwestern Argentina). Journal of South American Earth Sciences 14(7), 655-663.

Iriondo, M.H., 1990. Map of the South American plains—its present state. In: Rabassa, J. (Ed.), Quaternary of South America and Antarctic Peninsula. CRC Press, chapter 14, pp. 297–308.

Iriondo, M., 1994. Los climas cuaternarios de la región pampeana. Museo Provincial de Ciencias Naturales" Florentino Ameghino" 4(2), 48 p.

Iriondo, M., 1999. Climatic changes in the South American plains: records of a continent-scale oscillation. Quaternary International 57, 93-112.

Iriondo, M.H., García, N.O., 1993. Climatic variations in the Argentine plains during the last 18,000 years. Palaeogeography, Palaeoclimatology, Palaeoecology 101(3-4), 209-220.

Iriondo, M., Kröhling, D.M., 1995. El sistema eólico pampeano. In: Comunicaciones del Museo Provincial de Ciencias Naturales Florentino Ameghino (N.S.), vol. 5 (1), pp. 1-76.

Iriondo, M., Kröhling, D., 2007. Geomorfologia y sedimentologia de la cuenca superior del Río Salado (sur de Santa Fe y noroeste de Buenos Aires, Argentina). Latin American Journal of Sedimentology and Basin Analysis 14(1), 1-23.

Isla, F.I., 2014. Variaciones espaciales y temporales de la deriva litoral, SE de la Provincia de Buenos Aires, Argentina. Revista Geográfica Del Sur 5(8), 24–41.

Jordan, T.E., Zeitler, P., Ramos, V., Gleadow, A.J.W., 1989. Thermochronometric data on the development of the basement peneplain in the Sierras Pampeanas, Argentina. Journal of South American Earth Sciences 2(3), 207-222.

Kay, S.M., Godoy, E., Kurtz, A., 2005. Episodic arc migration, crustal thickening, subduction erosion, and magmatism in the south-central Andes. Geological Society of America Bulletin 117, 67-88.

Kayano, M.T., Andreoli, R.V., de Souza, R.A., 2020. Pacific and Atlantic multidecadal variability relations to the El Niño events and their effects on the South American rainfall. International Journal of Climatology 40(4), 2183-2200.

Keller, M., 1999, Argentine Precordillera, sedimentary and plate tectonic history of a Laurentian crustal fragment in South America. Geological Society of America, Special Paper 341, 1–131.

Kemp, R.A., Toms, P.S., King, M., Kröhling, D.M., 2004. The pedosedimentary evolution and chronology of Tortugas, a Late Quaternary type-site of the northern Pampa, Argentina. Quaternary International 114(1), 101-112.

Kemp, R.A., Zárate, M., Toms, P., King, M., Sanabria, J., Arguello, G., 2006. Late Quaternary paleosols, stratigraphy and landscape evolution in the Northern Pampa, Argentina. Quaternary Research 66(1), 119-132.

Kirkland, C.L., Danišík, M., Marsden, R., Piilonen, P., Barham, M., Sutherland, L., 2020. Dating young zircon: A case study from Southeast Asian megacrysts. Geochimica et Cosmochimica Acta 274, 1-19.

Kleiman, L.E., Japas, M.S., 2009. The Choiyoi volcanic province at 34°S–36°S (San Rafael, Mendoza, Argentina): Implications for the Late Palaeozoic evolution of the southwestern margin of Gondwana. Tectonophysics 473(3-4), 283-299.

Krömer, R., 1996. Los sedimentos cuaternarios del sudeste de la llanura mendocina. Implicancias paleoclimáticas. Multequina, 5, 49-55.

Kruck, W., Helms, F., Geyh, M.A., Suriano, J.M., Marengo, H.G., Pereyra, F., 2011. Late Pleistocene-Holocene history of Chaco-Pampa sediments in Argentina and Paraguay. E&G Quaternary Science Journal 60(1), 188-202.

Kruskal, J., 1964. Multidimensional scaling by optimizing goodness of fit to a nonmetric hypothesis. Psychometrika 29, 1–27.

Llambías, E.J., Sato, A.M., Suárez, A.O., Prozzi, C., 1998. The granitoids of the Sierra de San Luis. In: Pankhurst, R.J., Rapela, C.W. (Eds), The Proto-Andean Margin of Gondwana. Geological Society, London, Special Publication 142, 325-341.

Mackaman-Lofland, C., Horton, B.K., Fuentes, F., Constenius, K.N., Stockli, D.F., 2019. Mesozoic to Cenozoic retroarc basin evolution during changes in tectonic regime, southern Central Andes (31–33 S): Insights from zircon U-Pb geochronology. Journal of South American Earth Sciences 89, 299-318.

Malagnino, E.C., 1988. Evolución del sistema fluvial de la provincia de Buenos Aires desde el Pleistoceno hasta la actualidad. Actas Secundas Jornadas Geológicas Bonaerenses, Bahia Blanca, pp. 201–211.

Malagnino, E.C., 1989. Paleoformas de origen eólico y sus relaciones con los modelos de inundación de la provincia de Buenos Aires. IV Simposio de Percepción Remota, IX Reunión Plenaria SELPER. San Carlos de Bariloche, Argentina, tomo II, pp. 611-620.

Marengo, J.A., Soares, W.R., Saulo, C., Nicolini, M., 2004. Climatology of the low-level jet east of the Andes as derived from the NCEP–NCAR re-analyses: Characteristics and temporal variability. Journal of Climate 17(12), 2261-2280.

Martínez, A., Giambiagi, L., 2010. Evolución petrológica y geoquímica del magmatismo bimodal Permo-Triásico del Grupo Choiyoi en el cordón del Portillo, Mendoza, Argentina. Universidad de Oviedo, Trabajos de Geología 30, 432–451.

Martínez, J.S., 1987. La lineación Utracán-Vallimanca, provincias de La Pampa y Buenos Aires. Revista de la Asociación Geológica Argentina 42(1-2), 213-217.

Martínez, O.A., Kutschker, A., 2011. The ‘Rodados Patagónicos’ (Patagonian shingle formation) of eastern Patagonia: environmental conditions of gravel sedimentation. Biological Journal of the Linnean Society 103, 336–345.

Martínez, P.M., Perucca, L.P., Giménez, M.E., Ruíz, F., 2008. Manifestaciones geomorfológicas y geofísicas de una estructura geológica profunda al sur de la sierra de Pie de Palo, Sierras Pampeanas. Revista de la Asociación Geológica Argentina 63(2), 264-271.

Mehl, A.E., Tripaldi, A., Zárate M.A., 2018. Late Quaternary aeolian and fluvial-aeolian deposits from southwestern Pampas of Argentina, southern South America. Palaeogeography, Palaeoclimatology, Palaeoecology 511, 280-297.

Melo, W.D., Schillizzi, R., Perillo, G.M., Piccolo, M.C., 2003. Influencia del área continental pampeana en la evolución morfológica del estuario de Bahía Blanca. Latin American Journal of Sedimentology and Basin Analysis 10(1), 39-52.

Mendez, M.J., Buschiazzo, D.E., 2010. Wind erosion risk in agricultural soils under different tillage systems in the semiarid Pampas of Argentina. Soil and Tillage Research 106(2), 311-316.

Mpodozis, C., Kay, S.M., 1992. Late Paleozoic to Triassic evolution of the Gondwana margin: Evidence from Chilean Frontal Cordilleran batholiths (28°S to 31°S). Geological Society of America Bulletin 104(8), 999-1014.

Mpodozis, C., Ramos, V., 1989. The Andes of Chile and Argentina. In: Ericksen, G.E., Cañas Pinochet, M.T., Reinemund, J.A. (Eds.), Geology of the Andes and its relation to hydrocarbon and mineral resources, Houston Texas Circum-Pacific Council for Energy and Mineral Resources, Earth Science Series 11, chapter 5, pp. 59-90.

Muhs, D.R., 2004. Mineralogical maturity in dunefields of North America, Africa and Australia. Geomorphology 59, 247–269.

Mulcahy, S.R., Roeske, S.M., McClelland, W.C., Jourdan, F., Iriondo, A., Renne, P.R., Vervoort, J.D., Vujovich, G.I., 2011. Structural evolution of a composite middle to lower crustal section: The Sierra de Pie de Palo, northwest Argentina. Tectonics, 30(1), TC1005, doi:10.1029/2009TC002656.

Nivière, B., Messager, G., Carretier, S., Lacan, P., 2013. Geomorphic expression of the southern Central Andes forebulge (37°S, Argentina). Terra Nova 25(5), 361-367.

Pankhurst, R.J., Rapela, C.W., Fanning, C.M., Márquez, M., 2006. Gondwanide continental collision and the origin of Patagonia. Earth-Science Reviews 76(3-4), 235-257.

Pastore, G., Baird, T., Vermeesch, P., Resentini, A., Garzanti, E., 2021. Provenance and recycling of Sahara Desert sand. Earth-Science Reviews 216, 103606, doi.org/10.1016/j.earscirev.2021.103606

Pastran, M.G., 2012. La vegetación de los Médanos Grandes, provincia de San Juan: Análisis florístico y sinecológico. Tesis Doctoral en Biología-Probiol, Universidad Nacional de Cuyo, 128 p.

Pell, S.D., Williams, I.S., Chivas, A.R., 1997. The use of protolith zircon-age fingerprints in determining the protosource areas for some Australian dune sands. Sedimentary Geology 109(3-4), 233-260.

Pepper, M., Gehrels, G., Pullen, A., Ibanez-Mejia, M., Ward, K.M., Kapp, P., 2016. Magmatic history and crustal genesis of western South America: Constraints from U-Pb ages and Hf isotopes of detrital zircons in modern rivers. Geosphere 12(5), 1532-1555.

Peralta, Silvio H., 2003. An introduction to the geology of the Precordillera, Western Argentina. In: Peralta, S.H., Albanesi, G.L., Ortega, G. (Eds.), Ordovician and Silurian of the Precordillera, San Juan province, Argentina. Instituto Superior de Correlación Geológica, Miscelánea 10, pp.7-22.

Perillo, G.M.E., Piccolo, M.C., Parodi, E., Freije, R.H., 2001. The Bahía Blanca Estuary, Argentina. In: Seeliger, U., Kjerfve, B. (Eds.), Coastal marine ecosystems of Latin America. Springer, pp. 205–217.

Pinto, L., Alarcón, P., Morton, A., Naipauer, M., 2018. Geochemistry of heavy minerals and U-Pb detrital zircon geochronology in the Manantiales Basin: Implications for Frontal Cordillera uplift and foreland basin connectivity in the Andes of central Argentina. Palaeogeography, Palaeoclimatology, Palaeoecology 492, 104–125.

Piovano, E.L., Ariztegui, D., Córdoba, F., Cioccale, M., Sylvestre, F., 2009. Hydrological variability in South America below the Tropic of Capricorn (Pampas and Patagonia, Argentina) during the last 13.0 ka. In: Vimeux, F., Sylvestre, F., Khodri, M. (Eds.), Past Climate Variability in South America and Surrounding Regions. Springer Science & Business Media, Dordrecht, Developments in Paleoenvironmental Research 14, pp. 323-351.

Potter, P.E., 1984. South American modern beach sand and plate tectonics. Nature 311(5987), 645-648.

Prohaska, F., 1976. The Climate of Argentina, Paraguay and Uruguay. In: Schwerdtfeger, W. (Ed.), Climates of Central and South America. Elsevier, Amsterdam, World Survey of Climatology, pp. 13-112.

Rabassa, J., 2008. Late Cenozoic glaciations in Patagonia and Tierra del Fuego. Developments in Quaternary Sciences 11, 151-204.

Railsback, L.B., Gibbard, P.L., Head, M.J., Voarintsoa, N.R.G., Toucanne, S., 2015. An optimized scheme of lettered marine isotope substages for the last 1.0 million years, and the climatostratigraphic nature of isotope stages and substages. Quaternary Science Reviews 111, 94-106.

Ramos, V.A., 1988. The tectonics of the Central Andes; 30° to 33° S latitude. Geological Society of America, Special Paper 218, 31-54.

Ramos, V.A., 2004. Cuyania, an exotic block to Gondwana: review of a historical success and the present problems. Gondwana Research 7(4), 1009-1026.

Ramos, V.A., 2009. Anatomy and global context of the Andes: Main geologic features and the Andean orogenic cycle. In: Kay, S.M., Ramos, V.A., Dickinson, W.R. (Eds.), Backbone of the Americas: Shallow subduction, plateau uplift, and ridge and terrane collision. Geological Society of America, Memoir 204, pp. 31-65.

Ramos, V.A., Alemán, A., 2000. Tectonic evolution of the Andes. In: Cordani, U.G., Milani, E.J., Thomaz Filho, A., Campos, D.A. (Eds.), Tectonic evolution of South America. 31st International Geological Congress, Río de Janeiro, pp. 635-685.

Ramos, V.A., Folguera, A., 2009. Andean flat-slab subduction through time. In: Murphy, J.B., Keppie, J.D., Hynes, A.J. (Eds.), Ancient orogens and modern analogues. Geological Society, London, Special Publication 327(1), pp. 31-54.

Ramos, V.A., Folguera, A., 2011. Payenia volcanic province in the Southern Andes: An appraisal of an exceptional Quaternary tectonic setting. Journal of Volcanology and Geothermal Research 201(1-4), 53-64.

Ramos, V.A., Kay, S.M., 1991, Triassic rifting and associated basalts in the Cuyo basin, central Argentina. In: Harmon, R.S., Rapela, C.W. (Eds.), Andean Magmatism and its Tectonic Setting. Geological Society of America, Special Paper 265, pp. 79-92.

Ramos, V.A., Jordan, T.E., Allmendinger, R.W., Mpodozis, C., Kay, S.M., Cortés, J.M., Palma, M., 1986. Paleozoic terranes of the central Argentine- Chilean Andes. Tectonics 5(6), 855-880.

Ramos, V.A., Cristallini, E.O., Pérez, D.J., 2002. The Pampean flat slab of the Central Andes. Journal of South American Earth Sciences 15(1), 59-78.

Rapela, C.W., Pankhurst, R.J., Casquet, C., Fanning, C.M., Baldo, E.G., González-Casado, J.M., Galindo, C., Dahlquist, J., 2007. The Río de la Plata craton and the assembly of SW Gondwana. Earth-Science Reviews 83(1-2), 49-82.

Rapela, C.W., Pankhurst, R.J., Casquet, C., Baldo, E., Galindo, C., Fanning, C.M., Dahlquist, J.M., 2010. The Western Sierras Pampeanas: Protracted Grenville-age history (1330–1030 Ma) of intra-oceanic arcs, subduction–accretion at continental-edge and AMCG intraplate magmatism. Journal of South American Earth Sciences 29(1), 105-127.

Rapela, C.W., Verdecchia, S.O., Casquet, C., Pankhurst, R.J., Baldo, E.G., Galindo, C., Murra, J.A., Dahlquist, J.A., Fanning, C.M., 2016. Identifying Laurentian and SW Gondwana sources in the Neoproterozoic to Early Paleozoic metasedimentary rocks of the Sierras Pampeanas: Paleogeographic and tectonic implications: Gondwana Research 32, 193–212.

Rapela, C.W., Pankhurst, R.J., Casquet, C., Dahlquist, J.A., Fanning, C.M., Baldo, E.G., Galindo, C., Alasino, P.H., Ramacciotti, C.D., Verdecchia, S.O., Murra, J.A., 2018. A review of the Famatinian Ordovician magmatism in southern South America: evidence of lithosphere reworking and continental subduction in the early proto-Andean margin of Gondwana. Earth-Science Reviews 187, 259-285.

Repasch, M., Wittmann, H., Scheingross, J.S., Sachse, D., Szupiany, R., Orfeo, O., Fuchs, M., Hovius, N., 2020. Sediment transit time and floodplain storage dynamics in alluvial rivers revealed by meteoric 10Be. Journal of Geophysical Research: Earth Surface 125(7), 2019JF005419.

Resentini, A., Goren, L., Castelltort, S., Garzanti, E. (2017). Partitioning sediment flux by provenance and tracing erosion patterns in Taiwan. Journal of Geophysical Research: Earth Surface 122(7), 1430-1454.

Rittner, M., Vermeesch, P., Carter, A., Bird, A., Stevens, T., Garzanti, E., Andò, S., Vezzoli, G., Dutt, R., Xu, Z., Lu, H., 2016. The provenance of Taklamakan desert sand. Earth and Planetary Science Letters 437, 127-137.

Rocha-Campos, A.C., Basei, M.A., Nutman, A.P., Kleiman, L.E., Varela, R., Llambias, E., Canile, F.M., Da Rosa, O.D.C., 2011. 30 million years of Permian volcanism recorded in the Choiyoi igneous province (W Argentina) and their source for younger ash fall deposits in the Paraná Basin: SHRIMP U–Pb zircon geochronology evidence. Gondwana Research 19(2), 509-523.

Rodríguez, E., Barton, M., 1993. El Cuaternario de la llanura. In Geología y Recursos Naturales de Mendoza, XII Congreso Geológico Argentino y II Congreso de Exploración de Hidrocarburos. Relatorio, Mendoza, pp. 173-194.

Rubio, G., Pereyra, F.X., Taboada, M.A., 2019. Soils of the Pampean region. In: Rubio, G., Lavado, R.S., Pereyra, F.X. (Eds.), The soils of Argentina. Springer, Cham, pp. 81-100.

Rutter N., Coronato A., Helmens K., Rabassa J., Zárate M., 2012. The glacial and loess record of southern South America. In: Rutter N., Coronato A., Helmens K., Rabassa J., Zárate, M. (Eds.), Glaciations in North and South America from the Miocene to the Last Glacial Maximum. Comparisons, linkages, and uncertainties. Springer, Dordrecht, Briefs in Earth System Sciences, pp. 1-23.

Salio, P., Nicolini, M., Saulo, A.C., 2002. Chaco low- level jet events characterization during the austral summer season. Journal of Geophysical Research: Atmospheres 107(D24), 4816, doi:10.1029/2001JD001315.

Silva, V.B.S., Kousky, V.E., 2012. The South American monsoon system: climatology and variability. In: Wang, S., Gillies, R.R. (Eds.), Modern Climatology. InTech, Rijeka, pp. 123-152.

Spalletti, L.A., Isla, F.I., 2003. Características y evolución del delta del Río Colorado (“Colú-Leuvú”), provincia de Buenos Aires, República Argentina. Latin American Journal of Sedimentology and Basin Analysis 10(1), 23–37.

Stern, C.R., 2004. Active Andean volcanism: its geologic and tectonic setting. Revista Geológica de Chile 31(2), 161-206.

Stern, C.R., 2020. The role of subduction erosion in the generation of Andean and other convergent plate boundary arc magmas, the continental crust and mantle. Gondwana Research 88, 220-249.

Szelagowski, M., Zárate, M.A., Blasi, A.M., 2004. Aspectos sedimentológicos de arenas eólicas del Pleistoceno tardío-Holoceno de la Provincia de La Pampa. Latin American Journal of Sedimentology and Basin Analysis 11(2), pp.69-83.

Teruggi, M.E., 1957. The nature and origin of Argentine loess. Journal of Sedimentary Petrology 27(3), 322-332.

Tripaldi, A., 2002. Sedimentología y evolución del campo de dunas de Médanos Grandes (Provincia de San Juan, Argentina). Revista de la Asociación Argentina de Sedimentología, 9(1), 65-82.

Tripaldi, A., 2010. Campos de dunas de la planicie sanrafaelina: patrones de dunas e inferencias paleoclimáticas para el Pleistoceno tardío-Holoceno. In: Zárate, M.A., Gil, A., Neme, G. (Eds.), Paleoambientes y ocupaciones humanas del centro-oeste de Argentina durante la transición Pleistoceno-Holoceno y Holoceno. Sociedad Argentina de Antropología, pp. 65-93.

Tripaldi, A., Forman, S.L., 2007. Geomorphology and chronology of Late Quaternary dune fields of western Argentina. Palaeogeography, Palaeoclimatology, Palaeoecology 251(2), 300-320.

Tripaldi, A., Forman, S.L., 2016. Eolian depositional phases during the past 50 ka and inferred climate variability for the Pampean Sand Sea, western Pampas, Argentina. Quaternary Science Reviews 139, 77-93.

Tripaldi, A., Zárate, M.A., 2016. A review of Late Quaternary inland dune systems of South America east of the Andes. Quaternary International 410, 96-110.

Tripaldi, A., Ciccioli, P.L., Alonso, M.S., Forman, S.L., 2010. Petrography and geochemistry of late Quaternary dune fields of western Argentina: provenance of aeolian materials in southern South America. Aeolian Research 2(1), 33-48.

Tripaldi, A., Zárate, M.A., Brook, G.A., Li, G.Q., 2011. Late Quaternary paleoenvironments and paleoclimatic conditions in the distal Andean piedmont, southern Mendoza, Argentina. Quaternary Research 76(2), 253-263.

Tripaldi, A., Zárate, M.A., Forman, S.L., Badger, T., Doyle, M.E., Ciccioli, P., 2013. Geological evidence for a drought episode in the western Pampas (Argentina, South America) during the early–mid 20th century. The Holocene 23(12),1731-1746.

Tripaldi, A., Zárate, M.A., Neme, G.A., Gil, A.F., Giardina, M., Salgán, M.L., 2017. Archaeological site formation processes in northwestern Patagonia, Mendoza Province, Argentina. Geoarchaeology 32(6), 605-621.

Tripaldi, A., Mehl, A. and Zárate, M.A., 2018a. Parabolic megadunes in a subtropical Quaternary inland dune field, southwestern Pampas, Argentina. Geomorphology 321, 103-116.

Tripaldi, A., Alonso, M.S., Messineo, P., Salvo Bernárdez, S., 2018b. Composición petrográfica y proveniencia de arenas eólicas de las Dunas de la Pampa Central, Argentina: resultados preliminares. Séptimo Congreso Argentino de Cuaternario y Geomorfología, Puerto Madryn, pp. 342-343.

Valcarce, G.Z., Zapata, T., del Pino, D., Ansa, A., 2006. Structural evolution and magmatic characteristics of the Agrio fold-and-thrust belt. In: Kay, S.M., Ramos, V.A. (Eds.), Evolution of an Andean margin: A tectonic and magmatic view from the Andes to the Neuquén Basin (35°–39°S lat.). Geological Society of America, Special Paper 407, 125–146.

Vermeesch, P., 2013. Multi-sample comparison of detrital age distributions. Chemical Geology 341, 140–146.

Vermeesch, P., Garzanti, E., 2015. Making geological sense of ‘Big Data’ in sedimentary provenance analysis. Chemical Geology 409, 20–27.

Vermeesch, P., Resentini, A., Garzanti, E., 2016. An R package for statistical provenance analysis. Sedimentary Geology 336, 14–25.

Vezzoli, G., Garzanti, E., 2009. Tracking paleodrainage in Pleistocene foreland basins. The Journal of Geology 117(4), 445-454.

Vogt, H., Vogt, T., Calmels, A.P., 2010. Influence of the post-Miocene tectonic activity on the geomorphology between Andes and Pampa Deprimida in the area of Provincia de La Pampa, Argentina. Geomorphology 121, 152–166.

von Gosen, W., 1995. Polyphase structural evolution of the southwestern Argentine Precordillera. Journal of South American Earth Sciences 8(3-4), 377-404.

Weltje, G.J., 1997. End member modeling of compositional data: Numerical-statistical algorithms for solving the explicit mixing problem. Mathematical Geology 29(4), 503-549.

Yáñez, G.A., Ranero, C.R., von Huene, R., Díaz, J., 2001. Magnetic anomaly interpretation across the southern central Andes (32°–34°S): The role of the Juan Fernández Ridge in the late Tertiary evolution of the margin. Journal of Geophysical Research: Solid Earth 106(B4), 6325-6345.

Zárate, M.A., 2003. Loess of southern South America. Quaternary Science Reviews 22(18-19), 1987-2006.

Zárate, M., Blasi, A., 1993. Late Pleistocene-Holocene eolian deposits of the southern Buenos Aires Province, Argentina: a preliminary model. Quaternary International 17, 15-20.

Zárate, M.A., Tripaldi, A., 2012. The aeolian system of central Argentina. Aeolian Research 3(4), 401-417.

Zárate, M., Kemp, R., Toms, P., 2009. Late Quaternary landscape reconstruction and geochronology in the northern Pampas of Buenos Aires province, Argentina. Journal of South American Earth Sciences 27(1), 88-99.